Pathophysiology of Liver Sinusoidal Endothelial Cells

Rajkumar Cheluvappa

A thesis submitted for the degree of Doctor of Philosophy

The Centre for Education and Research on Ageing,

Concord RG Hospital ANZAC Research Institute and

The Faculty of Medicine, University of Sydney

February 2008

Declaration of candidate

The data and analyses presented in this thesis are my original work accomplished under the supervision of Prof. David G. Le Couteur and Dr. Sarah N. Hilmer, except where otherwise acknowledged.

Rajkumar Cheluvappa

Table of contents- with figures and tables

Acknowledgments

My heartfelt thanks go to my supervisors Prof. David G. Le Couteur and Dr. Sarah N. Hilmer for their exceptional support, academically and otherwise. Their prompt assistance, expert guidance, constant encouragement and optimistic goading had made my PhD work not only productive, but also very enjoyable. Their invaluable contribution to impeling my reasoning and analytical skills is much appeciated.

I place on record my gratitude to the Australian National Health and Medical Research Council (NHMRC) and the Ageing and Alzheimer's Research Foundation (AARF) which funded most of my research. The Intramural Research Program of the National Institute on Aging (NIA) of the National Institutes of Health (NIH) is to be thanked for funding the research on calorie-restricted rats. I acknowledge the support of Prof. John Thompson and Prof. Annemarie Hennessy, Dr. Sally Thomson and Mr. Scott Heffernan pertaining to the baboon colony, and the Juvenile Diabetes Research Foundation and Rebecca Cooper Foundation for financial support of the Baboon Colony.

I owe a huge debt of gratitude to Dr. Sun Young Kwun and Ms. Sue Brammah from the Department of Anatomical Pathology who rendered me invaluable assistance with their technical expertise in immunohistochemistry and electron microscopy respectively. I proffer a profound word of gratitude to Mr. Andrew Fitzhardinge and Dr. Margaret Janu, Biochemistry Department, Diagnostic Pathology Unit, Concord RG Hospital for doing the protein quantitation, liver function tests and blood biochemistry.

I would like to thank our research group's mentor Prof. Robin Fraser, Department of Pathology, Christchurch School of Medicine, University of Otago, Christchurch, New Zealand, for his able guidance, inimitable directional encouragement and consistent vivification through the years. I would also like to thank Dr. Victoria C Cogger, Centre for Education and Research on Ageing and ANZAC Research Institute, Concord RG Hospital, Sydney, Australia, for her expert guidance in specimen processing for SEM, SEM handling, and her assistance in TEM micrography and analysis.

Finally, I am grateful for all the amicable assistance and encouragement from my colleagues at the Centre for Education and Research on Ageing (CERA) and the ANZAC Research Institute, which made my academic sojourn in Sydney a pleasantly memorable one.

Dedication

This thesis is dedicated to the only one.

Abbreviations

APC: Antigen Presenting Cell

Ca^{2+}: Calcium Ion

CHL: Chylomicron

CHR: Chylomicron Remnant

CR: Calorie Restriction

CV: Central vein (Terminal Hepatic Vein)

DM: Diabetes Mellitus

Fen: Fenestration

FD: Fenestration Diameter

F/ square nm: Fenestrations/ square nm or Fenestration Frequency

FFC= Fenestration Forming Center

GIT: Gastrointestinal Tract

GSH: Glutathione (reduced glutathione)

GSSG: Glutathione (oxidized glutathione or glutathione disulphide)

HDL: High Density Lipoprotein

H_2O_2: Hydrogen Peroxide

5HT: 5-Hydroxy Tryptamine or Serotonin

KC: Kupffer Cell

LPS: Lipopolysaccharide, Endotoxin

LPL: Lipoprotein Lipase

LSEC: Liver Sinusoidal Endothelial Cell

NAC: N-Acetyl Cysteine

NADPH: Nicotinamide Adenine Dinucleotide Phosphate

P. hamadryas: *Papio hamadryas*

P. aeruginosa: *Pseudomonas aeruginosa*

P 407: Poloxamer 407

Por: Porosity

PYO: Pyocyanin

SEM: Scanning Electron Microscope or Standard Error of the Mean (contextual)

SC: Stellate Cell

SOD: Superoxide Dismutase

TEM: Transmission Electron Microscope

THV: Terminal Hepatic Vein (Central vein)

VEGF: Vascular Endothelial Growth Factor

VEGFR: Vascular Endothelial Growth Factor Receptor

VEGFR2: Vascular Endothelial Growth Factor Receptor 2

VLDL: Very Low Density Lipoproteins

Publications

(1) Cheluvappa R, Hilmer SN, Kwun SY, Jamieson HA, O'reilly JN, Muller M, Cogger VC, Le Couteur DG. The effect of old age on liver oxygenation and the hepatic expression of VEGF and VEGFR2.

Exp Gerontol. 2007 Oct;42(10):1012-1019.

(2) Cheluvappa R, Jamieson HA, Hilmer SN, Muller M, Le Couteur DG. The effect of Pseudomonas aeruginosa virulence factor, pyocyanin, on the liver sinusoidal endothelial cell.

J Gastroenterol Hepatol. 2007 Aug;22(8):1350-1351.

(3) Cheluvappa R, Hilmer SN, Kwun SY, Cogger VC, Le Couteur DG. Effects of old age on hepatocyte oxygenation.

Ann N Y Acad Sci. 2007 Oct;1114:88-92.

(4) Cheluvappa R, Cogger VC, Kwun SY, O'Reilly JN, Le Couteur DG, Hilmer SN. Liver sinusoidal endothelial cells and acute non-oxidative hepatic injury induced by Pseudomonas aeruginosa pyocyanin.

Int J Exp Pathol. 2008.

(5) Cheluvappa R, Shimmon R, Dawson M, Hilmer SN, Le Couteur DG. The interaction of *Pseudomonas aeruginosa* pyocyanin with reduced glutathione.

(Submitted).

(6) Jamieson HA, Cogger VC, Twigg SM, McLennan SV, Warren A, Cheluvappa R, Hilmer SN, Fraser R, de Cabo R, Le Couteur DG. Alterations in liver sinusoidal endothelium in a baboon model of type 1 diabetes.

Diabetologia. 2007 Sep;50(9):1969-1976.

(7) Jamieson HA, Hilmer SN, Cogger VC, Warren A, Cheluvappa R, Abernethy DR, Everitt AV, Fraser R, de Cabo R, Le Couteur DG. Caloric restriction reduces age-related pseudocapillarization of the hepatic sinusoid.
Exp Gerontol. 2007 Apr;42(4):374-378.

Conference presentations

(1) Cheluvappa R, Muller M, Le Couteur DG. Glutathione conjugation of pyocyanin may be a crucial determinant in limiting airway pathology in Pseudomonas aeruginosa infections "From Cell to Society 4" 4th College of Health Sciences Research Conference at Wednesday 3rd & Thursday 4th November 2004. Peppers Farimont Resort, Leura, Blue Mountains. November 2004.

http://www.pg.chs.usyd.edu.au/conf04/submit/minipost/by-chelu.pdf

(2) Cheluvappa R, Muller M, LeCouteur DG. Glutathione Induced Modification Of Pyocyanin May Be Crucial In Limiting Pathology In Pseudomonal Lung Infections ASCEPT-APSA Combined Conference, Melbourne Hilton, Melbourne, VIC, Australia. December 2005.

http://www.ascept.org/asm/finalprogram.pdf Page 21

(3) Cheluvappa R, Hilmer SN, Kwun SY, Le Couteur DG. Old Age is Associated with Hepatocyte Hypoxia. 3rd International Conference on Healthy Ageing & Longevity, Melbourne Convention Centre, VIC, Australia. October 2006. Programme developed by the International Research Centre for Healthy Ageing and Longevity (IRCHAL). Co-sponsored by the World Health Organization (WHO). Endorsed by United Nations Focal Point on Ageing and the Australian Federal Government. October 2006.

http://ichal06.longevity-international.com/images/Final%20Programme.pdf Page 4

(4) Cheluvappa R, Hilmer SN, Cogger VC, Le Couteur DG. Liver sinusoidal endothelial cells and acute Pseudomonas aeruginosa pyocyanin-induced hepatic

injury. SEAWP - ASCEPT Combined Conference, Adelaide Hilton, 233 Victoria Sq, Adelaide, SA 5000, December 2007

http://www.meetingsfirst.com.au/meetings/SEAWP2007/Images/program.pdf

Thesis overview

1. Introduction: Pathophysiology of liver sinusoidal endothelial cells and their fenestrations
2. Liver sinusoidal endothelial cells and acute hepatic injury induced by *Pseudomonas aeruginosa* pyocyanin
3. The effect of old age on liver oxygenation, sinusoidal fenestrations and expression of VEGF and VEGFR2
4. Scanning electron microscopic analysis of two models of altered liver sinusoidal porosity: Diabetes mellitus 1 and Calorie-restriction
5. Conclusions
6. References
7. Protocols and criteria sheets

Chapter 1

Introduction: Pathophysiology of liver sinusoidal endothelial cells and their fenestrations

1. Pathophysiology of liver sinusoidal endothelial cells and their fenestrations

1.1. Introduction

Owing to its strategic position in the liver sinusoid, pathologic and morphologic alterations of the Liver Sinusoidal Endothelial Cell (LSEC) have far-reaching repercussions for the whole liver and systemic metabolism. LSECs are perforated with fenestrations, which are pores that facilitate the transfer of lipoproteins and macromolecules between blood and hepatocytes. Loss of LSEC porosity is termed defenestration, which can result from loss of fenestrations and/ or decreases in fenestration diameter. Gram negative bacterial endotoxin (Lipopolysaccharide, LPS) has marked effects on LSEC morphology, including induction LSEC defenestration. Sepsis is associated with hyperlipidemia, and proposed mechanisms include inhibition of tissue lipoprotein lipase and increased triglyceride production by the liver. The LSEC has an increasingly recognized role in hyperlipidemia. Conditions associated with reduced numbers of fenestrations such as ageing and bacterial infections are associated with impaired lipoprotein and chylomicron remnant uptake by the liver and consequent hyperlipidemia. Given the role of the LSEC in liver allograft rejection and hyperlipidemia, changes in the LSEC induced by LPS may have significant clinical implications.

This literature review summarizes the key concept of the liver sieve including the morphology and dynamics of LSEC fenestrations and its significance in

pathophysiology. This review also includes details of the immune function of the liver with a focus on the LSEC and its response to gram negative bacterial toxins, especially LPS. Another gram negative bacterium *Pseudomonas aeruginosa*, its toxin pyocyanin, and its relevance to liver infections have also been discussed. This review also encompasses age-related liver sinusoidal changes, which include LSEC defenestration, and may impede the transfer of small-lipoproteins and oxygen across the sinusoidal endothelium.

1.2. The liver acinus and liver sinusoidal cells

In humans, the liver is functionally divided into right (including caudate and quadrate lobes) and left lobes and further subdivided into 8 segments by divisions of the right, middle and left hepatic veins, each segment receiving its own portal pedicle (Fig. 1.1).

Figure 1.1. Segmental anatomy of the liver showing the eight hepatic segments

II-IV the left hemiliver; V-VIII the right hemiliver (Kumar and Clark, 2005).

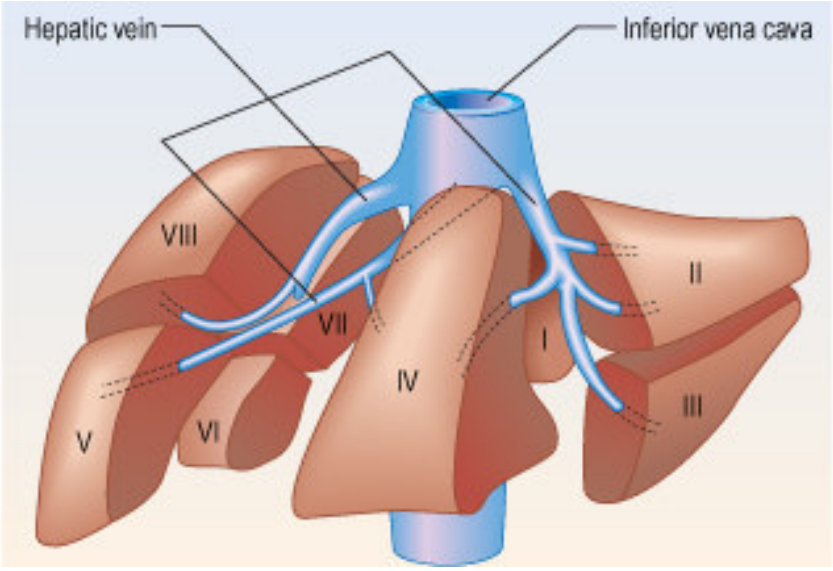

The liver is supplied by the hepatic artery (25% of the total blood flow and 50% of oxygen delivery) and the portal vein (75% of the total blood flow and 50% of oxygen) (Kumar and Clark, 2005).

The acinus is the functional unit of the liver (Fig. 1.2). Each acinus consists of parenchyma composed of hepatocytes supplied by the smallest portal tracts containing portal vein radicles, hepatic arterioles and bile ductules. Hepatocytes make up approximately 60% of all hepatic cells and 80% of total hepatic volume. The portal tract for each acinus is called the portal triad. The hepatic sinusoids which carry blood from the hepatic portal vein and the hepatic artery emanate from the portal triad and radiate outwards. The hepatocytes are drained by the central veins, also addressed as the terminal hepatic veins. The hepatocytes in the surrounding the portal triads (periportal area, zone 1) are well supplied with oxygenated blood and are generally more resistant to hypoxia and ischaemic injury than the hepatocytes surrounding the central veins (pericentral area, zone 3).

Four types of cells constitute the hepatic sinusoid, namely Liver Sinusoidal Endothelial Cells (LSECs), Kupffer cells (KCs), stellate cells (SCs), and pit cells, each with specific morphology and function. LSECs make up approximately 20% of the hepatic cells, KCs 15%, and SCs 5%. Depending on the disease process, each cell type can undergo morphologic or quantitative changes (Fraser et al, 1986; Wisse et al, 1996).

Figure 1.2. Diagram of an acinus

Zones 1, 2 and 3 are defined according to their relationship to the portal triads and central veins. Zone 1, which is periportal, is best oxygenated. Zone 3 is supplied by blood remote from afferent vessels and is in the microcirculatory periphery of the acinus. The pericentral area (star shaped green area around THV) is formed by the most peripheral parts of zone 3 of several adjacent acini and is the least well oxygenated. THV, Terminal Hepatic Venule or Central Vein; PT, Portal Triad (Kumar and Clark, 2005).

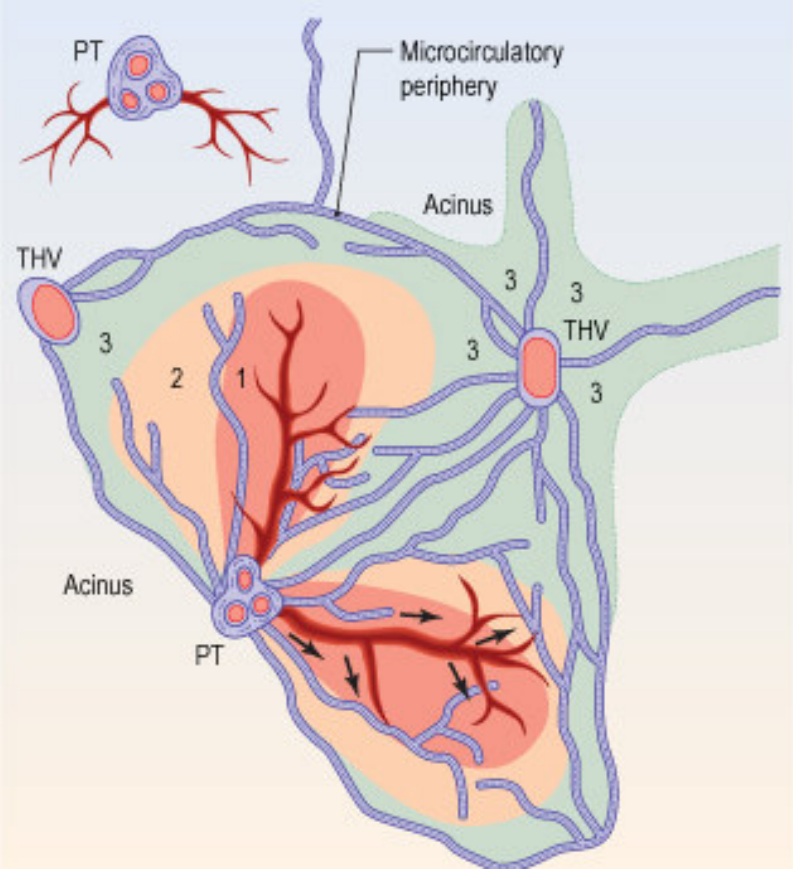

LSECs constitute the liver sinusoidal capillary wall. They lack basement membrane and possess pores termed fenestrations (Bouwens et al, 1992; Wisse et al, 1996). KCs phagocytose and degrade gastrointestinal antigens, bacteria and toxins which are carried by the portal vein to the liver (Bouwens, 1988; Wake et al, 1989). They also assist in tissue repair, clearance of senescent and damaged erythrocytes, T and B lymphocyte interactions and in antigen presentation (Kmiec, 2001). Stellate cells (Ito cells) store retinoids (Kmiec, 2001; Rockey, 1997) in their resting state and contain the intermediate filament, desmin. During hepatic injury, they undergo a radical transformation into a myofibroblast type cell that produces copious quantities of collagen types I, III and IV (Rockey, 1997). Pit cells are situated in liver sinusoidal walls, in portal tracts and in granuloma-like cellular aggregates (Bouwens et al, 1990). It is speculated that they are hepatic large granular lymphocytes or natural killer cells (Bouwens, 1988; Luo et al, 2000).

1.3. LSECs contribute to the liver sieve apparatus

LSECs constitute the lining or wall of the hepatic sinusoid. They lack basement membrane (Bouwens et al, 1992; Wisse et al, 1996) and possess fenestrations with diameters ranging from 100 to 200 nm (Wisse et al, 1996; Wisse et al, 1985). LSEC fenestrations are visible on electron microscopy as circular or oval perforations arranged in sieve plates within the thin extensions of the cytoplasm (Henriksen et al, 1984). Both fenestrations and sieve plates are structurally delineated by cytoskeleton elements (Braet(b) et al, 1995). The subendothelial space that lies between the sinusoids and hepatocytes is called the space of Disse, which contains a low-density matrix of basement membrane constituents and stellate cells. The LSECs, which contain fenestrations arranged in sieve plates, and the subendothelial space of Disse, containing extracellular matrix, together constitute the liver sieve. Since LSECs have fenestrations and lack basement membrane, molecules from the sinusoidal lumen can translocate directly through the fenestrations, to the low-density matrix of the space of Disse, to make contact with hepatocyte microvilli, and *vice versa* (Fraser et al, 1995; Wisse et al, 1996). Blood constituents that are too large to pass through fenestrations, such as erythrocytes and chylomicrons are excluded from the space of Disse, while smaller molecules, such as Chylomicron Remnants (CHR) are able to pass directly through the fenestrations (Wisse, 1970).

LSEC porosity is determined by fenestration frequency (F/um^2) and fenestration diameter (FD). The total area covered by the fenestrations has been estimated to account for approximately 10% of the LSEC surface area (Wisse, 1970). The natural porosity of the hepatic sinusoids increases from the portal triad (zone 1) towards the

central vein (zone 3) owing to a slight increase in fenestration frequency (Horn et al, 1986; Wisse et al, 1983) and perhaps also an increase in fenestration diameter (Vidal-Vanaclocha and Barbera-Guillem, 1985; Wisse et al, 1983). Vidal-Vanaclocha and co-workers observed approximately double the number of sieve plates and the number of fenestrations per sieve plate in the pericentral sinusoids than in the periportal sinusoids (Vidal-Vanaclocha and Barbera-Guillem, 1985). They classified fenestrations into two types, clustered pores, which are more prevalent in the pericentral sinusoids, and free pores, which are more prevalent in the periportal sinusoids (Vidal-Vanaclocha and Barbera-Guillem, 1985).

Utilizing "endothelial massage", erythrocytes and leukocytes may flush plasma through the fenestrations in the endothelium (Wisse et al, 1985). Permeation selectivity of different molecules is regulated by the fenestration sizes, the molecule sizes, and the transport kinetics of the molecules relative to steric and frictional properties of the fenestrations. Therefore, passage of small sized particles like albumin (7 nm diameter), is probably not size-limited in the normal liver. However, passage of larger molecules like IgM antibodies (10- 20 nm diameter) may be size-limited.

Fenestration diameters and frequency patterns vary from species to species. Utilizing fenestration diameter and fenestration frequency as parameters, these patterns have been reviewed (Table. 1.1), adapted from(Cogger and Le Couteur, 2008).

Table 1.1. Inter-species variations in fenestration parameters

Adapted from (Cogger and Le Couteur, 2008)

Species	Porosity (area %)	Diameter (nm)	Frequency (per μm^2)	Citation
Rat (zone 1)	6.0±0.2	111±1	9.1±0.3	(Wisse et al, 1983)
Rat (zone 3)	7.9±0.3	105±0.2	13.3±0.5	(Wisse et al, 1983)
Rat	4.1±2.3	73±1	2.7±1.1	(Le Couteur et al, 2001)
Rat	12.0±2.1	110±7	12.4±3.6	(Fraser et al, 1986)
Mice	4.1±2.2	74±4		(Warren et al, 2005)
Rabbit	5.2±0.9	60±5	17.3±3.8	(Fraser et al, 1986)
Rabbit	4.0±1.5	69±8	12.7±2.5	(Fraser et al, 1986)
Chicken	3.6±1.6	99±15	3.9±0.9	(Fraser et al, 1986)
Chicken	2.2±0.6	90±18	2.9±0.3	(Fraser et al, 1986)
Rainbow trout		123		(McCuskey et al, 1986)
Gold Fish		50-200		(Nopanitaya et al, 1979)
Dog	6.7	118±2	7.2	(McCuskey et al, 1986)
Sheep		60±2		(Wright et al, 1983)
Baboon	2.6±0.2	50±1	12.1±0.8	(Jamieson et al, 2007)
Baboon	4.2±0.5	58±1	9.4±0.9	(Cogger et al, 2003)
Baboon	1.8	82	3.3	(Mak and Lieber, 1984)
Human (zone 1)	7.6		19	(Horn et al, 1986)
Human (zone 3)	9.1		23.5	(Horn et al, 1986)
Human (zone 1)	3.4±0.2	170±12	9.8±1.8	(Madarame et al, 1991)
Human (zone 3)	4.0±0.4	160±10	11.2±2.6	(Madarame et al, 1991)

Fenestrations have been reported in all of the very wide range of species studied. Some of the many reports in different species are presented in Table.1.1, showing that fenestrations are widespread, and quite similar in size and distribution, in animals and humans. Porosity is the % of the surface area of the sinusoid covered with fenestrations. The frequency of fenestration refers to the number of fenestrations per unit area.

Alterations in fenestration diameter or fenestration frequency can affect exchange of plasma across the sinusoidal lumen and the space of Disse, influencing liver function

(Henriksen et al, 1984). Loss of LSEC porosity is termed defenestration and can be due to reduction in fenestration frequency and/ or fenestration diameter. In specific pathological processes, defenestration occurs along with endothelial thickening and deposition of excessive extracellular matrix in the subendothelial space of Disse. These changes, called capillarization in cirrhosis and pseudocapillarization in ageing, pose an impediment to the transfer of many substrates from the sinusoidal lumen to the hepatocytes, through the space of Disse.

Figure 1.3. Transmission electron micrograph of the liver from a young adult rat

Transmission electron micrograph of the perfused liver (Magnification 17000×) of a young adult rat aged 6 months showing the liver sieve apparatus (Le Couteur et al, 2002); (*, Fenestration; S, Sinusoidal Space; E, Endothelium; D, Space of Disse; H, Hepatocyte).

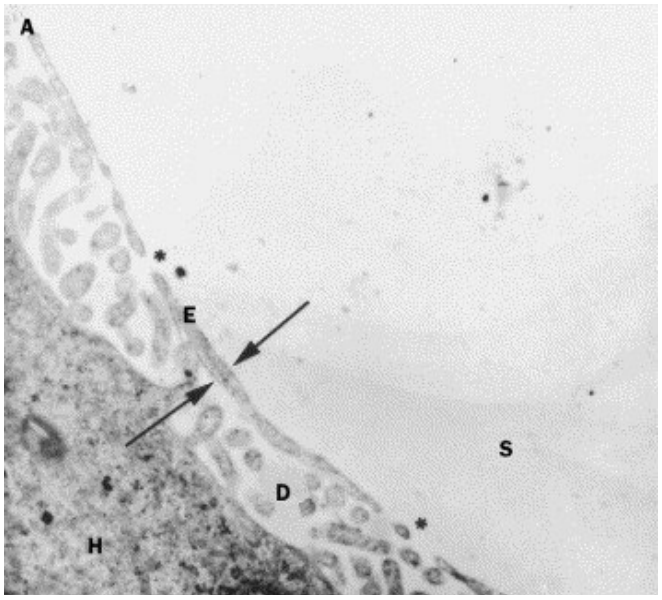

1.4. LSEC fenestration morphology and the role of the cytoskeleton in fenestration formation and regulation

LSEC fenestrations (* in Fig 1.3) are inducible structures and the cytoskeleton is involved in their formation (Braet(a) et al, 1995; Steffan et al, 1987). Each fenestration is circumscribed by a filamentous, Fenestration Associated Cytoskeleton Ring (FACR). The average filament thickness of the FACR averages around 16 nm (Braet(b) et al, 1995). The sieve plates, which enclose fenestrations, are encircled by microtubules. The sieve plates and the fenestrations are linked to the cell cytoskeletal tree. Agents that alter the sieve plate structure and porosity induce cytoskeletal changes and *vice versa* (Braet(a) et al, 1995). Routinely used actin-disruptor agents like cytochalasin B and other actin-disruptor agents including marine-sponge-derived macrolides like latrunculin A, jasplakinolides (jaspamides), swinholide A, misakinolide A, each with its distinct specific actin-disrupting property, have also been used to study LSEC cytoskeletal changes and fenestration dynamics (Braet et al, 1996; Braet et al, 2003; Braet et al, 1998; Braet et al, 2002; Braet(a) et al, 1995; Spector et al, 1999). The findings of these studies are summarized in Table. 1.2.

Table 1.2. Use of actin-disrupting agents to elucidate LSEC fenestration dynamics

	Treatment Agent	Por	Fen Diameter	Fen Freq	Cytoskeletal Changes	Other Changes	Citations
1	Antimycin A	↓↓↓	↓↓↓	↑	Actin disassembly	↓ATP + Sieve plate protrusion	(Braet et al, 2003)
2	Cytochalasin B	↑↑↑	None, Variable	↑↑	Actin disassembly + ↑Polymerization	FFCs not connected to fenestrations	(Braet et al, 1996; Braet(a) et al, 1995; Spector et al, 1999; Steffan et al, 1987)
3	Latrunculin A		↓	↑↑	Actin disassembly + ↑Polymerization	FFCs not connected to fenestrations	(Braet et al, 1996; Spector et al, 1999)
4	Misakinolide A		↓	↑↑	Actin disassembly + ↑Polymerization	FFCs connected to fenestrations	(Braet et al, 1998; Spector et al, 1999)
5	Swinholide A		↓	↑↑	Actin disassembly + ↑Polymerization	FFCs not connected to fenestrations	(Braet et al, 1998; Spector et al, 1999)
6	Jasplakinolide		↓	↑	Actin disassembly + F- actin bundle loss + ↑ F- actin dots	FFCs not connected to fenestrations	(Braet et al, 1998; Spector et al, 1999)
7	Hydrohalichondramide		↓	↑↑	Actin disassembly + ↑Polymerization	FFCs not connected to fenestrations	(Braet et al, 2002; Spector et al, 1999)
8	Dihydrohalichondramide		↓	↑↑	Actin disassembly + ↑Polymerization	FFCs connected to fenestrations	(Braet et al, 2002; Spector et al, 1999)

Por- Porosity; Fen Diameter- Fenestration Diameter; Fen Freq- Fenestration Frequency; FFC- Fenestration Forming Center.

1.5. Effect of endobiotics, xenobiotics and patho-physiologic processes on LSEC fenestration

Some endogenous and exogenous agents and pathophysiologic conditions that alter LSEC fenestrations are summarized in Table 1.3.

1.5.1. Autonomic regulation and cellular mediators

Hormones of the autonomic nervous system have effects on LSEC fenestration dimensions. Acetylcholine dilates LSEC fenestrations, while noradrenaline constricts them (Tsukada et al, 1986; Wisse et al, 1980). Serotonin (5 HT) increases intracellular calcium, leading to myosin light chain phosphorylation and constriction of fenestrations (Braet(a) et al, 1995; Gatmaitan et al, 1996). This indicates that fenestration contraction is active process mediated *via* LSEC Ca^{2+}.

Ca^{2+} and adenosine triphosphate (ATP) have been shown to constrict fenestrations, thereby reducing porosity (Braet et al, 2003; Gatmaitan et al, 1996; Oda et al, 1993). Additionally, the Ca^{2+}-calmodulin-actomyosin system has been implicated in the structural regulation of LSEC fenestrations (Oda et al, 1993).

1.5.2. Alcohol or nicotine exposure

Acute and medium-term exposure to alcohol in rats *in vivo* or in isolated LSECs *in vitro* is associated with increased LSEC fenestration diameter, frequency and porosity (Braet(a) et al, 1995; Charels et al, 1986; Fraser et al, 1980; Mori et al, 1991; Sarphie et al, 1997). In contrast, with chronic long-term alcohol intake, humans (Horn et al, 1987) and mice (Sarphie et al, 1997) display LSEC defenestration. It has therefore been speculated that increased transmission of larger chylomicrons across the LSECs with acute and medium term alcohol consumption may be a crucial step in the pathogenesis of alcoholic hepatic steatosis (Fraser et al, 1980). Alcoholic liver disease can have three overlapping sequential phases, namely alcoholic hepatic steatosis, alcoholic hepatitis, and alcoholic cirrhosis. It is possible that following short-term/medium-term alcohol consumption after the alcoholic steatosis/hepatitis phase where the LSEC porosity is increased, and prior to the cirrhotic phase of alcoholic liver disease where the LSEC porosity is decreased, LSEC defenestration commences. LSEC defenestration has been shown to occur early in the pathogenesis of cirrhosis in patients suffering from chronic alcohol abuse (Horn et al, 1987), accompanied by hyperlipoproteinemia (Clark et al, 1988). LSEC defenestration also occurs in animal models of cirrhosis (Le Couteur et al, 2005; Nopanitaya et al, 1976).

Nicotine, fed to rats at a weight adjusted dose equivalent to that of a human smoking 50 to 100 cigarettes per day for 6 weeks, decreased LSEC porosity to about 40% that of control animals and induced hypercholesterolemia (Fraser et al, 1988).

1.5.3. Exposure to agents present occasionally in the environment

The hepatic carcinogen dimethylnitrosamine, which is found in processed meat, induces defenestration (Fraser et al, 1995). The detergent poloxamer-407 induces loss of LSEC porosity by decreasing the fenestration frequency with no changes in ATP or mitochondrial function, and with marked associated hyperlipidemia (Cogger et al, 2006).

1.5.4. Pathophysiologic processes

Cirrhosis and ageing are also associated with marked structural changes in the sinusoidal endothelium and space of Disse that influences bulk plasma transfer into the space of Disse, through the LSECs (Le Couteur et al, 2005). Capillarization associated with cirrhosis differs from ageing-associated pseudo-capillarization by having additional features of bridging fibrosis or nodular regeneration, periportal or pericentral fibrosis, loss of hepatocyte microvilli, and only minor deposits of collagen in the space of Disse. These changes impede the transfer of many substrates including chylomicron remnants, albumin, protein-bound drugs and other macromolecules to the hepatocytes *via* the space of Disse (Le Couteur et al, 2002).

Paracetamol overdose dilates fenestrations and causes the generation of large gaps (Walker et al, 1983). The hepatic carcinogen dimethylnitrosamine, which is found in processed meat, induces defenestration (Fraser et al, 1995). Post-hepatic inferior vena cava occlusion dilates fenestration diameter to drastic proportions, while decreasing

the fenestration frequency (Nopanitaya et al, 1976). Artificial high perfusion pressure through the hepatic portal vein simulating portal hypertension dilates fenestrations and also results in the trapping of large chylomicrons (Fraser et al, 1980). This particular study also suggests a possible mechanism in the hepatic steatosis seen in the "nutmeg liver" of chronic venous congestion.

Though diabetes mellitus is associated with extensive vascular pathology, very little is known about its long-term effects on the liver sinusoid and its fenestrations. Possible ultrastructural liver sinusoidal changes are important because of the role of LSEC fenestrations on the hepatic disposition of lipoproteins. The vascular complications of diabetes are well established and are clinically significant (Singleton et al, 2003). In old age, there is a substantial loss of fenestrations in the LSEC (Cogger et al, 2003; Le Couteur et al, 2001; McLean et al, 2003; Warren et al, 2005), which impairs lipoprotein transfer to the hepatocyte (Hilmer et al, 2005). Clearly, there are potential parallels between age-related dyslipidemia and diabetes mellitus-related dyslipidemia (Adiels et al, 2006; Battula et al, 2000; Mamo et al, 1993). It will be interesting to determine whether diabetes mellitus influences liver sinusoidal fenestrations because of potential mechanistic implications for diabetic dyslipidemia.

Alterations in fenestration number, frequency, distribution, and diameter by hormones, xenobiotics, hepatotoxins, and diseases have important ramifications for hepatic microcirculation, substrate handling, drug metabolism, and overall function. Chylomicrons (100- 1000 nm diameter) are too large to pass through the fenestrations (Naito and Wisse, 1978). Only partially catabolised chylomicrons (chylomicron remnants) attain individual dimensions small enough to pass through the fenestrations

into the space of Disse (Fraser et al, 1978; Le Couteur et al, 2002). In defenestration seen in cirrhosis (Clark et al, 1988; Fraser et al, 1995; Le Couteur et al, 2005), normal ageing (Cogger et al, 2003; Hilmer et al, 2005; Le Couteur et al, 2005; McLean et al, 2003) or treatment with the commonly used detergent poloxamer-407 (Cogger et al, 2006), distribution of chylomicron remnants was excluded from the space of Disse (Cogger et al, 2006).

Table 1.3. Effect of commonly exposed agents and pathogenic processes on LSEC fenestrations

	Treatment Agent	Por %	Fen Diameter	Fen Freq	Other Changes	Citations
AUTONOMIC AND VASOACTIVE-AGENT REGULATION						
1	Acetylcholine		↑			(Tsukada et al, 1986; Wisse et al, 1980)
2	Noradrenaline		↓			(Tsukada et al, 1986; Wisse et al, 1980)
3	5HT	↓	↓		↑Cell Ca^{2+} ↑ cAMP Changes blocked by Ca^{2+} chelation or Ca^{2+} channel blocker	(Braet(a) et al, 1995; Gatmaitan et al, 1996)
4	Endothelin 1		↓			(Oda et al, 1997)
5	ET_A-R antagonist (BQ123)		↓	↓		(Watanabe et al, 2007)
6	Prostaglandin E1		↑			(Oda et al, 1997)
7	Pantethine	↑	↑	↑		(Fraser et al, 1989)
ALCOHOL OR NICOTINE EXPOSURE						
8	Ethanol	↑	↑	↑		(Braet(a) et al, 1995; Charels et al, 1986; Fraser et al, 1980; Mori et al, 1991; Sarphie et al, 1997)
9	Ethanol (Chronic)	↓		↓	Hepatic Steatosis	(Horn et al, 1987; Sarphie et al, 1997)
10	Nicotine	↓	↓	-	Hypercholesterolemia	(Fraser et al, 1988)
EXPOSURE TO AGENTS PRESENT OCCASIONALLY IN THE ENVIRONMENT						
11	Dimethylnitrosamine (Processed meat)	↓				(Fraser et al, 1995)
12	Poloxamer 407 (Various products)	↓		↓	No ATP changes No Mitochondrial dysfunction	(Cogger et al, 2006)
PATHOLOGICAL PROCESSES						
13	Ageing	↓		↓	↓ Mass ↓ Blood flow ↑ Endothelial thickening, Pseudocapillarization	(Cogger et al, 2003; Hilmer et al, 2005; Le Couteur et al, 2005; McLean et al, 2003)
14	Cirrhosis	↓		↓	Cirrhotic nodules, ↑ Endothelial thickening, Capillarization	(Clark et al, 1988; Fraser et al, 1995; Le Couteur et al, 2005; Nopanitaya et al, 1976)
15	Posthepatic Inferior Vena Cava occlusion	↑	↓	↑↑↑		(Nopanitaya et al, 1976)
16	Portal hypertension	↑		↑		(Fraser et al, 1980)
17	Paracetamol overdose		↑			(Walker et al, 1983)

1.6. The Ageing Liver

1.6.1. Effect of ageing on liver, sinusoidal and LSEC morphology

Age-induced liver sinusoidal endothelial changes (pseudocapillarization) include increases in endothelial thickness, extra-cellular matrix deposition in the space of Disse and decreases in LSEC porosity and fenestration frequency (defenestration) (Table. 1.4). These changes were evident across a range of animal models inclusive of rats (Le Couteur et al, 2001), humans (McLean et al, 2003), mice (Warren et al, 2005), and baboons (Cogger et al, 2003). In the afore-cited studies, the ultramicroscopic changes were accompanied by increased von Willebrands factor (capillary marker) expression in all species, but increased collagen and laminin expression only in humans and rats. Since old age is the pivotal risk factor for most diseases including liver disease, studies of the effects of disease on the liver should take these age-related changes into consideration.

Table 1.4. Effects of ageing on the porosity and thickness of the liver sinusoidal endothelium

	Young	Old	Fractional Change	Citation
ENDOTHELIAL POROSITY % (SEM)				
Mouse	4.1±2.2	2.2±3.5	0.53	(Warren et al, 2005)
Rat	4.1±2.3	2.5±1.2	0.61	(Le Couteur et al, 2001)
Baboon	4.2±0.5	2.4±0.4	0.57	(Cogger et al, 2003)
Human	Not done			
FENESTRATION DIAMETER (nm) (SEM)				
Mouse	74±4	58±12	0.78	(Warren et al, 2005)
Rat	73±1	60±1	0.82	(Le Couteur et al, 2001)
Baboon	58±1	70±2	1.20	(Cogger et al, 2003)
Human	Not done			
ENDOTHELIAL THICKNESS (nm) (TEM)				
Mouse	154±4	245±8	1.59	(Warren et al, 2005)
Rat	230±50	320±80	1.39	(Le Couteur et al, 2001)
Baboon	130±8	186±9	1.43	(Cogger et al, 2003)
Human	165±17	289±9	1.75	(McLean et al, 2003)

The effects of old age on porosity %, fenestration diameter (nm) and thickness (nm) of the hepatic sinusoidal endothelium across four species. Porosity and fenestration diameter were elucidated using scanning electron microscopy (SEM) and endothelial thickness using transmisson electron microscope (TEM). Adapted from (Warren et al, 2005).

1.6.2. Functional implications of morphologic changes in the ageing liver.

Research into the ageing process of the liver is of paramount importance because of the significant decrease in xenobiotic detoxification by the liver in old age (Le Couteur and McLean, 1998), and because the liver is the main site for metabolism of many substrates associated with age-related problems such as vascular disease, neurotoxicity and adverse drug reactions (Le Couteur et al, 2002; Le Couteur and McLean, 1998; Le Couteur et al, 2002).

Old age is associated with reduced clearance of highly atherogenic chylomicron-remnants from the liver (Krasinski et al, 1990; Weintraub et al, 1996). Experimentally it has been demonstrated that age-related pseudocapillarization substantially impedes small-lipoprotein transfer across the sinusoidal endothelium (Hilmer et al, 2005). Though normal hepatic sinusoidal endothelium provides insignificant resistance to oxygen transfer (Kassissia et al, 1992), there is a significant diffusion barrier to oxygen diffusion posed by the blood vessels in cirrhosis (Froomes et al, 2003; McLean and Morgan, 1991) and in normal capillaries in other organs (Cho et al, 2001; Rose and Goresky, 1985). It is thus of interest to determine whether age-related pseudocapillarization constitutes an oxygen diffusion barrier (Fig. 1.4B) similar to that seen in cirrhosis (Le Couteur and McLean, 1998).

Phase 1 hepatic drug metabolism, encompassing oxidation, reduction or hydrolysis of drugs, is diminished in old age (Herrlinger and Klotz, 2001; Kinirons and O'Mahony, 2004). These age-related changes could be caused by one or more of the following: decreased liver perfusion (Schmucker, 2001), possible oxygen-diffusion barrier secondary to age-associated liver pseudocapillarization of the liver sinusoidal

endothelial cell (Le Couteur et al, 2001), mitochondrial oxidative stress (Sastre et al, 2003) or mitochondrial dysfunction (Sastre et al, 1996). The differences between *in vivo* and *in vitro* assessments of phase I drug metabolism in old age (Herrlinger and Klotz, 2001; Kinirons and O'Mahony, 2004), could possibly reflect intrahepatocytic hypoxia because oxygen is an essential cofactor for cytochrome P450 enzymes (Le Couteur and McLean, 1998). Livers from aged rats have decreased high-energy phosphate metabolite pools than those from young rats, suggestive of hypoxia (Le Couteur et al, 2001) . Livers from aged mice have less total ATP than those from young mice (Selzner et al, 2007), However, this was associated with diminished oxygen consumption and ATP production by isolated mitochondria, which is suggestive of mitochondrial dysfunction rather than hypoxia (Selzner et al, 2007). There is also an upregulation of several genes and proteins that respond to hypoxia in old age (Kang et al, 2005).

These age-related changes in liver high-energy phosphate metabolites and oxygenation could be caused by decreased oxygen delivery to hepatocytes secondary to either reduced liver perfusion (Schmucker, 2001), or an oxygen-diffusion barrier secondary to age-associated “pseudocapillarization” of the liver sinusoidal endothelial cell (LSEC) (Le Couteur et al, 2001). Augmenting the latter possibility is a study that experimentally induced partial pseudocapillarization *via* ATP depletion (Braet et al, 2003). Alternatively, the reduction in ATP might also be secondary to age-related mitochondrial oxidative stress (Sastre et al, 2003) or mitochondrial dysfunction (Sastre et al, 1996).

Figure 1.4. Transmission electron micrograph of livers from young *versus* aged rats

Transmission electron micrograph of the liver of a young rat showing a normal liver sieve (A) and an old rat showing pseudocapillarization with LSEC defenestration, endothelial thickening and basement membrane deposition (B) (Hilmer et al, 2005). A conceptual illustration is also depicted in this figure (C) (Le Couteur et al, 2002). The sinusoidal endothelium is thin and perforated with fenestrae, which permit the passage of substrates such as smaller lipoproteins, while excluding larger substrates such as chylomicrons. In old age, the endothelium is defenestrated and thickened, with deposition of collagen and basal lamina. These changes (pseudocapillarization) will impede the transfer of substrates between sinusoidal blood and hepatocytes. (S= Sinusoidal Space, A= Chylomicron, E= Endothelium, B= Basement membrane, D= Space of Disse, H= Hepatocyte)

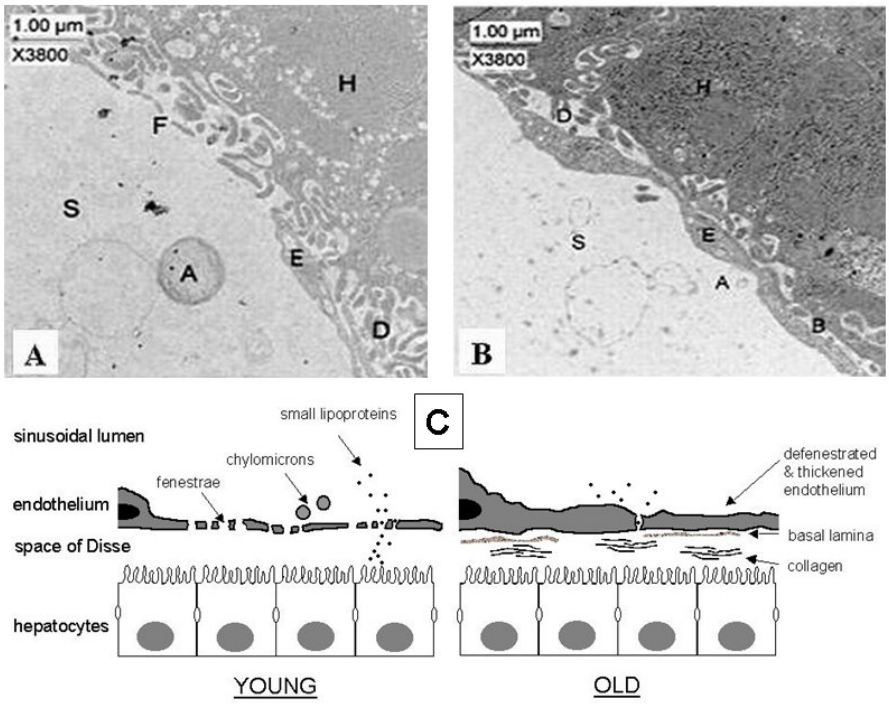

1.6.3. Stategies to delay ageing- calorie restriction

The outcomes of age-related impairment in liver function are well recognized (Le Couteur et al, 2005; Schmucker, 2005). One mechanism for this change is age-related alterations in the ultrastructure of the liver sinusoidal endothelium (Le Couteur et al, 2005). The loss of fenestrations in old age, which is part of pseudocapillariation, impedes the transfer of some lipoproteins from the blood to the hepatocytes, which provides a mechanism for age-related postprandial hypertriglyceridemia and impaired chylomicron remnant clearance (Hilmer et al, 2005; Huet and Villeneuve, 2005).

Caloric restriction (CR) increases longevity and the pathophysiological processes which are delayed by CR are considered to be an integral part of the ageing process (Ingram et al, 2004; Masoro, 2005; Sinclair, 2005). Reduction in the intake of calories delays the onset of age-related diseases and increase maximum lifespan by between 20% and 40% in many species (Everitt et al, 2005). CR improves lipoprotein profiles and delays the onset of vascular disease in animal models (Zhu et al, 2004), with similar effects observed in short term studies in humans (Heilbronn et al, 2006).

It is plausible that one mechanism for the effects of CR on lipoprotein metabolism and susceptibility to vascular disease may pertain to its effects on the liver sinusoidal endothelium and its fenestrations (Le Couteur et al, 2001). The liver sinusoidal endothelium is exquisitely sensitive to oxidative stress (Cogger et al, 2001; Cogger et al, 2004) and other toxic insults (McCuskey, 2006). Thus, it is possible that its ultrastructure may be influenced profoundly by the dietary load, which includes oxidants and toxins delivered to the liver *via* the portal vein. Since age-related hepatic

pseudocapillarization may contribute to the pathogenesis of dyslipidemia and since CR is a powerful model for the study of ageing as it extends lifespan, it will be interesting to determine whether pseudocapillarization is preventable and hence unravel a possible novel target for the prevention of age-related dyslipidemias.

1.7. Immunological functions of the liver: Focus on hepatic immune response to gram negative bacterial toxins

1.7.1. Introduction

The liver contains many immunologically active cells including KCs, LSECs and neutrophils and lymphocytes, and perhaps the hepatocytes themselves (Kmiec, 2001; Knolle and Gerken, 2000). The liver acts as a filter or a 'sieve' for bacteria and antigens carried to it *via* the portal tract from the gastrointestinal tract (GIT). These antigens are phagocytosed and degraded by KCs, which are modified macrophages attached to the endothelium (Wake et al, 1989). The near lack of lymphoid tissue implies that antigens are degraded without the production of antibody (Kmiec, 2001; Knolle and Gerken, 2000). The antigens are thus precluded from reaching other antibody-producing sites in the body, thereby preventing adverse systemic hypersensitivity. The liver favors the induction of tolerance rather than the induction of immunity (Kmiec, 2001; Knolle and Gerken, 2000). Different liver cell types may contribute in a myriad of ways to induce liver antigenic tolerance. These may include control of antigen presentation (immune ignorance), clonal deletion and immune deviation. Naive T cells are activated by LSECs, but do not differentiate into effector T cells. These T cells demonstrate a functional phenotype and cytokine induction profile typical of tolerance induction (Knolle et al, 1999). Dendritic cells (DCs), LSECs, KCs and hepatocytes also contribute to tolerance induction by deletion of T cells through induction of apoptosis (Knolle and Gerken, 2000).

1.7.2. Kupffer cells

The liver filters bacteria and antigens that come from the gastrointestinal tract *via* the portal vein. These antigens are phagocytosed and degraded by KCs, which are predominantly located in the periportal area. The KCs assist in tissue repair, T and B lymphocyte interaction, and cytotoxic activity in disease processes (Schumann et al, 2000). KCs have specific membrane receptors for ligands, and are activated by several factors such as infection (Scoazec and Feldmann, 1990). They secrete interleukins, tumor necrosis factor-α (TNF-α), collagenase and lysosomal hydrolases. KCs are Antigen Presenting Cells (APCs), which modulate immune responses, oral tolerance development to bacterial superantigens, and suppression of T-cell activation by antigen-presenting LSECs, prostanoids and TNF-α (Knolle and Gerken, 2000; Schumann et al, 2000). They play a pivotal role in the clearance of senescent and damaged erythrocytes. KCs are also involved in neutrophil adhesion and migration in the hepatic sinusoids during liver injury. This is mediated through TNF-α production in KCs and Inter Cellular Adhesion Molecule-1 (ICAM-1) expression in LSECs (Jaeschke, 1997; Sakamoto et al, 2002).

During acute hepatic insult, KCs secrete enzymes and cytokines that damage hepatocytes, and are active in the remodeling of Extracellular Matrix (ECM). Following LPS stimulation, KCs release IL-6, IL-8 and TNF-α, which induce liver parenchymal damage. These cytokines also stimulate LSECs, stellate cells and natural killer cells to release pro-inflammatory cytokines, thus exacerbating the damage (Kmiec, 2001).

Exposure of KCs to LPS can lead to intensive inflammatory mediator production, and subsequently, liver injury. KCs are involved in the initial hepatic insult, followed by neutrophils in the latter phase of hepatic injury (Jaeschke and Farhood, 1991; Jaeschke et al, 1996), both of them utilizing reactive oxygen species (ROS) to effect the injury (Jaeschke, 2002; Jaeschke and Farhood, 1991; Jaeschke et al, 2002).

Alcohol increases gastrointestinal tract permeability, liberating LPS from gut bacteria into the blood stream, which stimulates KCs. KCs and gastrointestinal tract-derived LPS are crucial in the pathogenesis of alcohol induced hepatotoxicity (Enomoto et al, 2000). Long-term alcohol exposure changes KC sensitivity to LPS (Enomoto et al, 2001).

TNF-alpha plays a critical role in the pathogenesis of hepatic injury in response to LPS. Leukotriene D4 and ROS induction seem to precede TNF-α action in the induction of LPS-induced hepatitis in the murine endotoxin/ galactosamine TNF-α model (Tiegs and Wendel, 1988; Tiegs et al, 1989). Thus, TNF-α is a crucial mediator secreted by KCs in LPS induced LSEC apoptosis (Takei et al, 1995). Granulocyte-colony stimulating factor (G-CSF) is a negative feedback signal for macrophage-derived TNF-α production after LPS induced hepatotoxicity (Gorgen et al, 1992). Thalidomide prevents KC mediated LPS-induced liver injury *via* suppression of TNF-α secretion from KCs (Enomoto et al, 2003).

P. aeruginosa exotoxin A induces liver damage not only by inhibition of protein synthesis but also by indirectly stimulating TNF-α secretion by KCs (Schumann et al,

1998). In order to induce rapid hepatocyte necrosis and apoptosis, *P. aeruginosa* Exotoxin A requires the presence of T cells to stimulate KCs to secrete TNF-α (Schumann et al, 1998; Schumann et al, 2000).

In hepatic reperfusion injury, KCs are the predominant cause of initial hepatic damage, which is mediated through ROS (Jaeschke and Farhood, 1991). However, neutrophils mediate the pathogenesis of later progression phase of hepatic ischaemia/reperfusion injury (Jaeschke and Farhood, 1991; Jaeschke et al, 1990).

1.7.3. Neutrophils

In endotoxin mediated liver injury, KCs are involved in the initial insult, followed by neutrophils in the latter phase of hepatic injury (Jaeschke et al, 1996), both using ROS to effect the damage (Jaeschke, 2002; Jaeschke et al, 2002; Liu et al, 1995). Though the significance of the prominent presence of neutrophils in liver parenchyma during alcoholic hepatitis is not clear, the presence of neutrophil degranulation and chemotactic agent release point to the crucial role of neutrophils in the pathogenesis alcoholic hepatitis. In addition, apoptosis-induced transmigration of neutrophils during alcoholic hepatitis is certain owing to colocalization between neutrophils and apoptotic hepatocytes (Jaeschke, 2002). Neutrophils play a crucial role in the pathogenesis of the later progressive phase of hepatic ischaemia/reperfusion injury (Jaeschke et al, 1990).

1.7.4. Lymphocytes

Mucosal lymphocytes migrate towards the site of hepatic insult. LSECs regulate the recruitment of specific lymphocyte subtypes (Klugewitz et al, 2002). LSECs suppress IFN- γ producing cell expansion. Alternatively, they prime IL-4-expressing Th2 cells, creating immune suppression in the liver. Antigen presentation in the liver therefore promotes modulation of immunity (Klugewitz et al, 2002). Adhesion molecule expression and chemokines initiate lymphocyte adhesion. Many adhesion molecules and chemokines are necessary for lymphocyte endothelial binding as enumerated elsewhere (Lalor and Adams, 1999; Lalor et al, 2002). Circulation of sustained high concentrations of TNF-α, which depends on the presence of T cells, is peculiar feature of synergistic *P. aeruginosa* Exotoxin A with LPS-induced hepatotoxicity (Schumann et al, 2000). LPS suppresses Ag-specific immune responses by CD4+ T cells by antigen-presenting LSECs (Knolle et al, 1999).

1.7.5. LSECS: Overall contribution to liver immunology

LSECs are crucial to antigen processing, scavenging and tolerance induction to GIT and systemic antigens. LSECs constitutively express all molecules necessary for antigen presentation (CD40, CD54, CD80, CD86, MHC-I and MHC-II) and function as MHC-I and MHC-II restricted antigen-presenting cells (APC) (Kmiec, 2001; Knolle and Gerken, 2000; Knolle et al, 1999; Scoazec and Feldmann, 1991). LSECs exhibit antigenic resemblance to dendritic cells by expressing CD4, the mannose

receptor and CD 11C (Knolle et al, 1999; Knolle et al, 1998; Magnusson and Berg, 1989; Scoazec and Feldmann, 1990). LSECs are very good antigen presenting cells and have been shown to induce proliferation of, co-stimulate, and upregulate cytokine production in CD4+ T Cells (Knolle et al, 1998; Lohse et al, 1996)..

LSECs regulate the recruitment of specific lymphocyte subtypes. CD4 and CD8 T cells that simultaneously interact with LSECs have a tolerant phenotype (Knolle and Limmer, 2003). They suppress IFN- γ producing cells and promote IL-4-expressing helper T cell subset 2 (Th2) cells cells, creating immune suppression in the liver (Klugewitz et al, 2002). LSEC primed CD4+ T cells differentiate into regulatory T cells, whereas myelocytic APC primed T cells differentiate into helper T cell subset 1 (Th1) cells (Limmer and Knolle, 2001). Therefore, LSEC primed CD4+ T cells play a crucial role in tolerance induction in the liver. The CD4+ T cells priming activity of LSECs can be negatively regulated by prostaglandin E2 (PGE2) and interleukin-10 (Knolle et al, 1998). LSECs also play a role in the development of tolerance by CD8 T cells towards orally adminsistered antigens (Limmer et al, 2005). LSECs are also important in tolerance induction in liver transplantation. In one study, the rejection of donor livers correlated closely with the presence of anti-LSEC antibodies, increased activation of T cells and decreased TGF-β (Sumitran-Holgersson et al, 2004).

In addition to the antigen processing, LSECs scavenge antigens such as LPS and advanced glycation end products (Knolle and Limmer, 2003; Shnyra et al, 1993; Shnyra and Lindberg, 1995; Smedsrod et al, 1990). Scavenging is distinctly different from antigen processing. LSECs endocytose glycoproteins, extracellular matrix

components, immune complexes, transferrin and ceruloplasmin, thereby clearing antigens from the vasculature (Svistounov and Smedsrod, 2004).

LSECs may assist immune surveillance *via* T cell activation, which in turn is influenced by the milieu encompassing bacteria and LPS. LSECs express CD14, the LPS-Binding protein receptor (Gong et al, 2002; Scoazec and Feldmann, 1991). LSECs may also assist immune surveillance by releasing immunosuppressive mediators such as interleukin-10, prostaglandin E2 and transforming growth factor-β (TGF-β) (Knolle and Gerken, 2000; Knolle et al, 1998; Sumitran-Holgersson et al, 2004). LSECs secrete several vasoactive substances and eicosanoids such as cytokines, prostanoids, leukotrienes, endothelin-1 and nitric oxide (Knolle and Gerken, 2000).

1.7.6. LSECS and lipopolysaccharide

Lipopolysaccharide (LPS or bacterial endotoxin) is a secreted by most gram-negative bacteria including *P. aeruginosa*. LPS is present in normal portal blood at high physiological concentrations of 10 pg/ml to 1 ng/ml (Knolle and Gerken, 2000). One study done on samples collected from 21 patients with cirrhosis using a limulus-based chromogenic assay, estimated the portal venous LPS concentrations to be 142 ± 167 pg per ml in contrast to the peripheral venous LPS concentration of 82 ± 150 pg per ml ($P<0.001$) (Lumsden et al, 1988). In another study done using limulus lysate assay on samples from 34 elective abdominal surgery patients, 97% of the patients had LPS in their portal blood demonstrating that LPS is present normally in portal blood and is

not necessarily pathogenic (Jacob et al, 1977). In this study, systemic endotoxemia was observed in 3 of the 4 patients who also had liver disease, and none of the patients without liver disease. Therefore, pathological concentrations of LPS seem to be present in systemic blood only during gram-negative bacterial sepsis or during liver disease (Jacob et al, 1977; Yamamoto et al, 1994).

When LSECs are incubated with physiological concentrations of LPS, specific immune responses by CD4+ cells are down-regulated (Knolle et al, 1999). LPS also induces LSEC scavenger and endocytotic functions (Shnyra et al, 1993) and subsequently antigen presentation to lymphocytes (Knolle et al, 1998; Lohse et al, 1996). LPS can also induce LSEC apoptosis *via* TNF secreted by KCs (Takei et al, 1995).

LPS defenestrates LSECs (Fraser et al, 1995). One intravenous dose of LPS (2 mg/kg body weight) in Dark-Agouti rats reduced LSEC porosity significantly, the changes being spontaneously reversed after 14 days. With the same LPS dose, Sprague-Dawley rats showed similar but irreversible changes at-least 3 days after LPS challenge (Dobbs et al, 1994). Intravenously injected LPS (2.5 mg/kg body weight) in F344 rats resulted in LSEC enlargement, sieve plate disruption and gap formation 6 hours after LPS challenge (Seto et al, 1998). KCs seem to modulate LPS-induced LSEC defenestration and impaired hyaluronan scavenging (Sarphie et al, 1996). Takei and co-workers reported that co-incubation of LSECs with LPS-stimulated KCs induces significant apoptosis in LSECs that are in contact with KCs, and that anti-TNF-α antibody prevents this (Takei et al, 1995).

Alcohol abuse may promote the uptake of LPS from alcohol lysed gut bacteria or from direct injury to the intestinal wall (Enomoto et al, 2000) . LPS could possibly induce liver damage, starting with the LSEC (Dobbs et al, 1994) or secondary to Kupffer cell and neutrophil (Enomoto et al, 2000; Jaeschke et al, 1996) activation. This could be a pivotal pathogenic factor in alcoholic cirrhosis.

1.7.7. LSECS and Pseudomonas aeruginosa

P. aeruginosa is a common nosocomial bacterial pathogen associated with a high incidence of morbidity and mortality in acute cases (Gouvea et al, 2004). Post-operative pseudomonal infections, including *P. aeruginosa* infections after liver transplantation (Gouvea et al, 2004; Iinuma et al, 2004; Korvick et al, 1991; Singh et al, 2004) can result in sepsis (Hart et al, 2003; Hart et al, 2003), bacteremia (Iinuma et al, 2004; Singh et al, 2004), hepatic damage (Muhlen et al, 2004; Schumann et al, 2000) and fatal multiple-organ failure (Hart et al, 2003; Hart et al, 2003). The few studies which describe the *P. aeruginosa* as one of the commonest multi-antibiotic resistant nosocomial organisms, especially in post-surgical and post-liver transplant scenarios, are tabulated in Table. 1.4 below.

Table 1.5. Incidence of P. aeruginosa in post-surgical and post-liver transplant infections

Study Dates	Patient Cohort	Cohort Size	Pathogen Parameter Examined	Cohort % with Parameter Present	Incidence of Pseudomonal Infections	Pathology Specifics	Citations
2000-2003	Liver transplant	30	Bacteremia	30%	44% of bacteremia	100 % with bacteremia died	(Doria and Marino, 2005)
1999-2003	Liver transplant	103	Bacterial pneumonia	32%	17% of pneumonia	50% with pneumonia had acute rejection	(Ma et al, 2005)
1989-2003	Liver transplant	233	Bacteremia	52%	Topmost		(Singh et al, 2004)
2001-2002	Living donor liver transplant	113	Surgical site infection	37%	33 % of Gram negative bacterial infections	26% with surgical site infection died	(Iinuma et al, 2004)
1999-2002	Liver transplant	99	Multiple antibiotic resistance	57%	23% of all bacterial infections	63% of all infections by multi-antibiotic resistant bacteria	(Gouvea et al, 2004)
1998-2001	Liver transplant	401	Pneumonia	5%	>57% of pneumonia		(Aduen et al, 2005)
1990-1999	Liver transplant	165	Multiple antibiotic resistance	31%	50% of multi-antibiotic resistant bacteria	Higher mortality	(Singh et al, 2001)
1995-1998	Liver transplant in ICU	90	Pulmonary infiltration	40%	27% of pneumonia	38% with infiltrates had pneumonia	(Singh et al, 1999)
1990-1995	Liver-lung-heart transplant in Cystic Fibrosis	10	Double organ transplants		100%	100% Multi-antibiotic resistant	(Couetil et al, 1995)
1990-1993	Liver transplant	284	Aerobic gram –ve bacteria	45%	Most frequently isolated from blood		(Wade et al, 1998)
1988-1991	Liver transplant	185	Bacteremia & fungemia	29%	10% of bacteremias & fungemias	95% of all infections nosocomial	(Moreno et al, 1994)
1985-1991	Kidney transplant	568	Bacteremia & fungemia	11%	19% Bacteremias & fungemias	70% of all infections nosocomial	(Moreno et al, 1994)
1981-1984	Liver transplant	129	Early death> 24 hours	37%	53% of deaths due to bacterial sepsis	Bacterial sepsis in 81% of deaths	(Cuervas-Mons et al, 1986)

Pyocyanin, a redox active, pro-inflammatory, pro-apoptotic, cytotoxic and immunomodulating phenazine dye is secreted in copious quantities by *Pseudomonas aeruginosa*. Though systemic, portal or hepatic concentrations of pyocyanin have not been estimated in Pseudomonal sepsis, it is well known that it is produced in large amounts (up to 130 μM) in respiratory secretions from cystic fibrosis and bronchiectasis patients with *P. aeruginosa* infections (Pitt, 1986; Wilson et al, 1987; Wilson et al, 1988).

Pyocyanin has been shown to exert its *in vivo* cytotoxicity by impairing the cellular redox status and depleting intracellular GSH and thiols in endothelial cells (Muller, 2002) and transformed epithelial cells (O'Malley et al, 2004) *via* superoxide and H_2O_2 generation (Muller, 2002; O'Malley et al, 2004), or through direct oxidation of GSH (O'Malley et al, 2004). Pyocyanin may possibly induce induce sinusoidal H_2O_2, which may then enter the cell, inducing modifications in the cellular actin cytoskeleton leading to altered LSEC morphology.

1.7.8. Hepatic immune response to gram negative bacterial toxins

The liver is the first organ which encounters pathogens or pathogen products from the gut. Alcohol-induced gut permeability dependent mechanisms liberate LPS from gastrointestinal gram negative bacteria (Enomoto et al, 2000). Alcohol decreases the usual endotoxemia- induced increased glucose production and uptake *via* inhibition of hepatic glucose production and peripheral glucose utilization (Molina et al, 1989). Burns sensitize KCs to LPS *via* gut-derived LPS dependent mechanisms (Enomoto et al, 2004). Gram negative bacterial sepsis or liver disease can lead to the presence of

high concentrations of systemic and portal LPS (Jacob et al, 1977). As documented in the 1.7.2. section on Kupffer cells, exposure of KCs to LPS leads to intensive inflammatory mediator production, adhesion molecule expression, neutrophil chemotaxis and activation, and subsequent LSEC and hepatocyte injury. These findings suggest that LPS-induced structural changes in the liver sinusoid are mediated by LPS-induced Kupffer cell activation. Exposure of LSECs to LPS induces defenestration (Fraser et al, 1995) and the LSEC functions of scavenging (Shnyra and Lindberg, 1995), endocytosis (Shnyra and Lindberg, 1995) and antigen presentation to lymphocytes (Knolle et al, 1998; Lohse et al, 1996). LPS induces LSEC apoptosis *via* TNF secreted by KCs (Takei et al, 1995). LPS alters the membrane fluidity of hepatocytes (Salgia et al, 1993). LPS may influence hepatocyte-macrophage communications (Ogle et al, 1995) and in humans lead to a transient increase in liver insulin-like growth factor (IGF) in addition to transient increases in cortisol and pituitary growth hormone, similar to changes seen in acute trauma (Lang et al, 1997). In the isolated perfused rat liver model, LPS induces cholestasis without significant hepatic damage which suggests a possible role for extrahepatic mechanisms for induction of liver damage (Gaeta and Wisse, 1983).

Leukotriene D4 and ROS induction seem to precede TNF-α action in the induction of LPS-induced hepatitis (Tiegs and Wendel, 1988; Tiegs et al, 1989). Granulocyte-colony stimulating factor (G-CSF) is a negative feedback signal for macrophage-derived TNF-α production after LPS induced hepatotoxicity (Gorgen et al, 1992). Superoxide generation in the hepatic sinusoid in response to LPS challenge is likely to be a factor involved in liver damage (Yokoyama et al, 1998). LPS is a potent stimulator of hepatocyte fibronectin which suggests that hepatocytes may also be

directly involved in liver fibrosis (Jia et al, 1998). In one murine model study, co-administration of non-hepatotoxic doses of the commonly used H2-blocker ranitidine and LPS activated the clotting system *via* over expression of plasminogen-activator inhibitor-1 (PAI-1), with fibrin deposition in the liver and hepatocyte damage (Luyendyk et al, 2004; Luyendyk et al, 2004). Thrombin is a promoter (Copple et al, 2003) and a distal mediator (Moulin et al, 1996) of LPS induced hepatotoxicity. LPS induces decreased LSEC thrombomodulin which results in sinusoidal microthrombus formation and exacerbation of hepatic injury (Kume et al, 2003). Platelets (Pearson et al, 1995) and the coagulation cascade (Hewett and Roth, 1995) contribute to LPS induced hepatic injury. KCs play an important role in LPS induced sinusoidal thrombogenesis, fibrin degradation and deposition (Takeuchi et al, 1994). LPS also synergizes with monocrotaline (Yee et al, 2003), aflatoxin B1(Luyendyk et al, 2003), polychlorinated biphenyls (Brown et al, 1996) and a range of liver toxins like carbon tetrachloride, ethanol, cadmium, halothane and allyl alcohol (Roth et al, 1997) in causing hepatic injury.

Most antioxidant mechanisms are upregulated by LSECs in response to LPS including H_2O_2-detoxifying capacity (Spolarics et al, 1996), LSEC GSH efflux mechanisms (Jaeschke, 1992), glucose transporter 1 (GLUT1), glucose-6-phosphate dehydrogenase (G6PD) (Spolarics and Navarro, 1994), superoxide dismutases (SODs), and glutathione peroxidase (GPx) (Spolarics, 1998). In cirrhosis, there is augmented LPS uptake by the liver and increased biliary excretion of LPS (Ueno, 1990).

P. aeruginosa exotoxin A induces liver damage by protein synthesis inhibition, activation of KCs to produce TNF-α, and perforin-dependent, Fas-independent, apoptotic pathways (Schumann et al, 1998). To induce substantial hepatocyte damage, *P. aeruginosa* exotoxin A requires the presence of T cells to stimulate KCs to secrete TNF-α (Schumann et al, 1998; Schumann et al, 2000). For *P. aeruginosa* exotoxin A to synergize with LPS to induce severe hepatotoxicity, T cells are required to produce circulation of sustained high concentrations of TNF-α (Schumann et al, 2000).

P. aeruginosa pyocyanin exerts LSEC cytotoxicity by impairing the cellular redox status *via* generation of H_2O_2, which probably depletes intracellular GSH and thiols in endothelial cells (Muller, 2002) and may cause defenestration and its consequences.

1.8. Hypertriglyceridemia of sepsis, bacteremia and gram-negative bacterial toxemia

Sepsis is associated with free radical induction (Rose et al, 1994), altered redox balance (Hart et al, 2003; Hart et al, 2003; Pedersen et al, 1989), cellular NADH/ ATP reduction (Hart et al, 2003), cellular cytoskeletal modifications and decreased hepatic energy metabolism (Hart et al, 2003; Hart et al, 2003; Spitzer et al, 1989; Spitzer et al, 1988). Strikingly similar changes can also be induced by gram negative bacterial toxins, either LPS (Bannerman and Goldblum, 1999; Jaeschke, 1992; Liu et al, 1995; Spolarics, 1996; Yokoyama et al, 1998) or pyocyanin (Britigan et al, 1992; Harman and Macbrinn, 1963; Hassett et al, 1992; Landau et al, 1963; Mahajan-Miklos et al, 1999; Muller, 2002; Muller and Sorrell, 1997; O'Malley et al, 2004; Ran et al, 2003; Stewart-Tull and Armstrong, 1972) alone. Conditions including the presence of free radicals and cytoskeletal modifying agents are particularly conducive to LSEC defenestration.

It is possible that LSEC defenestration induced by bacterial toxins such as LPS or pyocyanin may impede hepatic uptake of chylomicron remnants and increase their circulation time, leading to the hyperlipidemia of sepsis reported often in literature (Harris et al, 2000; Scholl et al, 1984). The currently accepted hypothesis for pathogenesis of sepsis associated hypertriglyceridemia is that sepsis stimulates catecholamine release which stimulates release of free fatty acids (FFAs) from adipose tissue. The FFAs are taken up by the liver which then releases them as triglycerides in lipoproteins (Harris et al, 2000; Spitzer et al, 1988). Alternatively, sepsis stimulated TNF-α and IL-1 may suppress lipoprotein lipase (LPL) synthesis,

which decreases the rate of triglyceride clearance, leading to hypertriglyceridemia (Harris et al, 2000; Spitzer et al, 1988). Both LPS injection and *E. coli* bacteremia in rats result in hypertriglyceridemia and decreased LPL activity. Experimental sepsis stimulates liver putrescine and spermidine synthesis in addition to ornithine decarboxylase activation, responses that can also be simulated by LPS and pro-inflammatory cytokines (Tiao et al, 1995). Therefore it is clear that not only sepsis, but also recurrent gram negative infections, bacteremia and toxemia can lead to hypertriglyceridemia.

During endotoxemia states, one third of LPS binds to high-density lipoproteins (HDL) and is taken up into peripheral tissues. The remaining two thirds are taken up more rapidly by predominantly in reticuloendothelial organs with copious phagocytes, APCs and cells with scavenger function (Munford and Dietschy, 1985; Munford et al, 1981). The tissues by which LPS is taken up and the proportion of LPS taken up depends upon LPS-HDL binding parameters (Munford et al, 1981). Increased serum HDL and its LPS-binding capacity may serve to protect against LPS induced damage in chronic alcohol exposure (Kitano et al, 1996; Kitano et al, 1996).

It has been shown that triglyceride-rich lipoproteins including very low density lipoproteins (VLDL) and chylomicrons bind LPS. They form lipoprotein-LPS complexes or chylomicron-LPS complexes, modulate the host immune responses and therefore impede LPS-induced toxicity (Harris et al, 2000). Chylomicron-LPS complexes inhibit nitric oxide release by hepatocytes much better than either of them alone, suggesting that chylomicron bound LPS inhibits hepatocyte NF-κB and prevents liver damage (Kumwenda et al, 2002). Lipoproteins have also been shown to

protect animals from lethal polymicrobial gram-negative bacterial sepsis. Therefore it is possible that hypertriglyceridemia could be an innate immune response to gram negative sepsis (Read et al, 1995). Alternatively, it could also be a possible mechanism to perpetuate LPS-induced toxicity owing to prolonged systemic LPS persistence.

In this thesis, an additional mechanism is proposed which could account for the hypertriglyceridemia of sepsis. LSEC defenestration in gram negative bacterial (including pseudomonal) sepsis induced by toxins such as LPS (Fraser et al, 1995) may exclude lipoproteins and chylomicron remnants from the liver. This could lead to retention of lipoproteins and chylomicron remnants in the peripheral vasculature leading to hyperlipidemia (Fig. 1.5).

Figure 1.5. Hypothesised pathogenesis of hyperlipidemia related to pseudomonal sepsis

LSEC defenestration in bacterial/ pseudomonal sepsis owing to toxins like pyocyanin or LPS may exclude chylomicron remnants from the liver. This could lead to retention of lipoproteins in the peripheral vasculature leading to Pseudomonal sepsis-related hyperlipidemia.

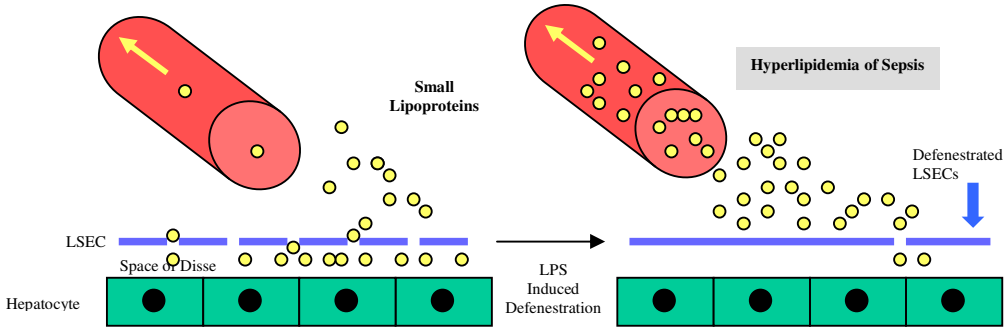

1.9. Conclusions and hypotheses

LPS- or pyocyanin-induced LSEC defenestration may impede hepatic chylomicron remnant uptake, increasing the circulation time of chylomicron remnants (Cogger et al, 2006; Hilmer et al, 2005) leading to the hyperlipidemia (Fig. 1.5) seen frequently in sepsis (Harris et al, 2000; Scholl et al, 1984). The effect of pyocyanin or LPS on LSEC fenestrations is likely to be different between young and old animals as healthy old animals exhibit decreased porosity and fenestration density (Le Couteur et al, 2001). Differences in LSEC fenestration status may at least partly account for the increased mortality that has been reported in sepsis in older patients.

Contraction of fenestrations is associated with Ca^{2+} influx (Gatmaitan et al, 1996). Endotoxemia alters Ca^{2+} homeostasis, with minute Ca^{2+} flux alterations (Deaciuc and Spitzer, 1987). These changes, possibly due to catecholamine mediated Ca^{2+} influx, are reversible by Ca^{2+} channel blockers (Sayeed and Maitra, 1987). Under induced endotoxemia, Ca^{2+} channel blockers limit hepatocyte injury and inhibit LPS-induced KC inducible nitric oxide synthase expression (Mustafa and Olson, 1999). LPS induced membrane fluidity of hepatocytes can be prevented by Ca^{2+} channel blockers (Salgia et al, 1993). Ca^{2+} channel blockers may also curb the sepsis induced acute phase response by preventing sepsis-related hepatic Ca^{2+} changes (Rose et al, 1994) that lead to reorganization of fenestrations, and so modulate the metabolic response.

Pyocyanin or LPS can trigger oxidant stress. This can lead to an increased sinusoidal efflux of GSH and its extracellular oxidation. GSH is depleted in LPS mediated hepatic injury (Jaeschke, 1992). Animal models have shown that antioxidants such as

GSH (Liu et al, 1994) and adequate nutrition (Wojnar et al, 1995) are protective in septic shock. Superoxide generation in the hepatic sinusoid in response to LPS challenge is likely to be a factor involved in liver damage (Yokoyama et al, 1998). Superoxide dismutase (SOD), which dismutates superoxide to H_2O_2 has been shown to offer protection against LPS induced liver injury (Rose et al, 1994). Modifying the response of LSEC porosity to LPS and *P. aeruginosa* pyocyanin with calcium channel blockers, anti-TNF-α antibody, G-CSF, VEGF, HGF, GSH, N-acetyl cysteine (NAC), SOD, and catalase could offer novel therapeutic targets in acute sepsis, especially sepsis caused by *P. aeruginosa*.

It has been clearly demonstared that fenestrations can be regulated with a variety of pharmacological agents (Arias, 1990; Braet and Wisse, 2002). Table 1.2 and table 1.3 clearly summarize these. Morphological changes in liver sinusoidal fenestrations seem to have systemic implications particularly for lipoprotein metabolism (Fraser et al, 1986), clearance of medications (Le Couteur et al, 2005) and immunity (Warren et al, 2006), as well as hepatoprotective effects (Deleve, 2007). Thus the targeting of fenestration modulation *via* development of appropriate pharmacological agents to treat pathophysiological states such as dyslipidemias in ageing (Le Couteur et al, 2007; Le Couteur et al, 2002) and diabetes mellitus is a viable therapeutic option.

VEGF activates endothelial cell division, angiogenesis and vascular permeability. It generates fenestrations and caveolae in a number of different endothelial cells including tumour (Roberts and Palade, 1997), renal (Chen et al, 2002) and adrenocortical (Esser et al, 1998) endothelial cells. In the liver, hepatocytes produce VEGF which acts on liver endothelial cells *via* the receptors: VEGFR1 (Flt-1) and

VEGFR2 (KDR/Flk-1) of which VEGFR2 is the most important (Ferrara, 2002; Funyu et al, 2001; LeCouter et al, 2003). In isolated liver endothelial cells, VEGF increases porosity about twofold, mostly through its effects on the number of fenestrations (Funyu et al, 2001; Yokomori et al, 2003). Conversely, transgenic inhibition of VEGF receptors altered the hepatic endothelium of early postnatal mice, including loss of endothelial lining in many sinusoids (Gerber et al, 1999) and was associated with defenestration and hyperlipidemia (Carpenter et al, 2005). VEGF is considered to be the major cytokine involved in the regulation of fenestrations (Chen et al, 2002). Therefore amongst the currently available fenestration modulating agent possibilities (Table. 1.2 and Table. 1.3), VEGF can be considered as a forerunner pertaining to therapeutic options to modulate fenestrations in pathophysiological states.

In this thesis, the following major hypotheses are explored:

1. Pyocyanin induces defenestration of the LSEC both *in vitro* and *in vivo*
2. The effects of pyocyanin on the LSEC are mediated by oxidative stress
3. Defenestration induced by old age and poloxamer 407 causes intrahepatocytic hypoxia and upregulation of hypoxia-related responses
4. Defenestration of the LSEC seen in old age can be exacerbated by diabetes mellitus and prevented or ameliorated by caloric restriction commencing early in life

Chapter 2

Liver sinusoidal endothelial cells and acute hepatic injury induced by *Pseudomonas aeruginosa* pyocyanin

2. Liver sinusoidal endothelial cells and acute hepatic injury induced by *Pseudomonas aeruginosa* pyocyanin

2.1. Introduction

Pseudomonas aeruginosa is an increasingly important cause of sepsis and death in organ transplant recipients, particularly those receiving liver transplants (Aduen et al, 2005; Singh et al, 2004; Wagener and Yu, 1992). *P. aeruginosa* has a special affinity for tissue vasculature, typically surrounding blood vessels circumferentially (perivascular cuffing) during infection (Schaber et al, 2007; Soave et al, 1978) or congregating in postcapillary venules (Fetzer et al, 1967). *P. aeruginosa* induces apoptosis in the endothelial cell line, ECV304 (Takahashi et al, 1990; Valente et al, 2000). *P. aeruginosa* produces a number of virulence factors including pyocyanin, a phenazine dye with broad range of activities including: redox activity (Britigan et al, 1997; Hassan and Fridovich, 1980), immunomodulation (Muhlradt et al, 1986; Muller et al, 1989), pro-inflammatory effects (Lau et al, 2004), ROS-generation (Muller, 2002), succinic dehydrogenase enzyme-inactivation (Harman and Macbrinn, 1963), cytotoxicity (Britigan et al, 1997; Lau et al, 2004), pro-apoptotic effects (Usher et al, 2002), and induction of senescence (Muller, 2006).

There are several reasons to suspect that pyocyanin might have important effects on the LSEC. Pyocyanin has been shown to induce oxidative stress and morphological changes in endothelial cells (Britigan et al, 1992). Within the liver, the sinusoidal endothelial cell (LSEC) is very sensitive to both oxidative stress (Cogger et al, 2001)

and the effects of bacterial lipopolysaccharide (LPS) (Dobbs et al, 1994; Seto et al, 1998). However the effects of pyocyanin have not been described. LSECs are perforated with fenestrations, pores with diameters ranging from 30 to 300 nm, that facilitate the transfer of lipoproteins, particularly triglyceride-rich chylomicron remnants, between blood and hepatocytes (Fraser et al, 1995). Given the role of the LSEC in liver allograft rejection (Sumitran-Holgersson et al, 2004) and hyperlipidemia (Fraser et al, 1995; Le Couteur et al, 2005), changes in the LSEC induced by pyocyanin may have significant clinical implications. Therefore, the effects of pseudomonal pyocyanin on the structure of isolated LSECs were investigated and whether such effects are mediated by oxidative stress.

Another possible mechanism for possible LSEC changes is the alteration of caveolin-1 expression. LPS, which induces defenestration in LSECs (Dobbs et al, 1994), also induces the overexpression of caveolin-1 (Kamoun et al, 2006), which is a key component of fenestrations (Ogi et al, 2003). Similarly, pyocyanin could possibly influence fenestrations through its interactions with proteins such as F-actin or caveolin-1 that maintain fenestrations (Braet et al, 2003; Ogi et al, 2003).

The LSEC has a key role in the maintenance of liver function and its viability following ischemia-reperfusion and transplantation. The rejection of donor livers is associated with demonstrable LSEC antibodies (Sumitran-Holgersson et al, 2004). LSEC apoptosis correlates with preservation-perfusion related dysfunction of donor rat livers (Zhu et al, 2006) and LSEC apoptosis without concomitant hepatocellular injury occurs in preservation injury during liver transplantation (Gao et al, 1998). Rat livers subjected to cold ischemia-warm reperfusion injury undergo LSEC alterations

without accompanying hepatocellular changes (Huet et al, 2004). LSEC responses to ischemia-reperfusion injury in donor rat livers influence the outcome of transplantation (Shimizu et al, 2001; Sun et al, 2001). For such reasons, changes induced in the LSEC are likely to have significant clinical outcomes in terms of liver transplantation.

Therefore it was postulated that the effects of pyocyanin on the LSEC are a key component of the toxicity of pseudomonal sepsis. Better knowledge of the pathogenesis of the changes in LSECs induced by pyocyanin may partially explain the mechanisms of liver allograft rejection (Sumitran-Holgersson et al, 2004) and hyperlipidemia of sepsis (Fraser et al, 1995; Harris et al, 2000; Spitzer et al, 1988). Since *P. aeruginosa* is a major cause of sepsis and death following liver transplantation and the LSEC is critical for graft survival, the effects of *P. aeruginosa* pyocyanin on LSECs were investigated using electron microscopy, immunohistochemistry and biochemistry.

2.2. Materials and methods

2.2.1. Synthesis of pyocyanin

Pyocyanin was chemically synthesized by the photolysis of phenazine methosulfate (Knight et al, 1979) and purified (Muller and Sorrell, 1992) as described earlier. Briefly, phenazine methosulfate (P-9625-5g, Sigma-Aldrich Pt Ltd, Sydney, Australia) was made up in 0.01 M tris-HCl buffer (pH 7.4) in a round-bottomed Pyrex flask and exposed to fluorescent tube light (Phillips TLD 18 W/54) for 2.5 hours. The resulting solution was extracted with chloroform and vacuum dried to a powdery residue. The residue was dissolved in chloroform and acidified with an equal volume of 0.1 M HCl. The red acidic form of pyocyanin was converted into the blue form using 0.5 M NaOH. This blue form of pyocyanin, now in the aqueous phase was extracted with chloroform and this cycle repeated 3 times. At the end of the last cycle, the blue form of pyocyanin was extracted with chloroform; vacuum dried, and hexane washed. The residue was dissolved in a small quantity of chloroform and sufficient hexane added to precipitate the pyocyanin. This pyocyanin was trapped using a type EH 0.5 μm filter, reconstituted in chloroform and purified by thin-layer chromatography (HPTLC Pre-coated Silica Gel 60 Plates; Merck Ltd) using an equimolar chloroform methanol mixture solvent. The purity of pyocyanin was ascertained and it's concentration quantitated by utilizing its known absorption spectrum and extinction coefficient values as elucidated earlier (Watson et al, 1986). The pyocyanin thus purified was stored in methanol at -70°C and protected from light owing to its photosensitivity. Before use, the methanol solvent was completely removed in a stream of nitrogen gas to leave behind a dried pyocyanin residue. When

completely dry, the pyocyanin was reconstituted in tissue culture medium or saline and immediately used.

2.2.2. Animal protocols, LSEC isolation and pyocyanin treatment and enzyme pre-treatment

Animal studies were approved by the Sydney Southwest Area Health Service Animal Welfare Committee. All rats were specific pathogen free males obtained from the Animal Research Centre (Perth, Australia). Each rat used was anesthetized with ketamine and xylazine (50 and 5 mg/kg, respectively, Troy Laboratories, Smithfield, Australia) by intraperitoneal injection.

LSECs were harvested from livers of Sprague-Dawley rats (aged 2-3 months, 250-350 g) according to methodology described previously (Cogger et al, 2004). Briefly, livers were perfused with 0.05 % collagenase and LSECs centrifuged with a 2-step Percoll gradient. After centrifugation and selective adherence to remove Kupffer cells, LSECs were suspended in RPMI-1640 medium (0.02 % L-glutamine, 2% fetal bovine serum, 100 U/mL penicillin, 100 μg/mL streptomycin). The resulting cells were plated onto collagen-coated Thermanox cover slips (Nalge Nunc Int, Rochester, NY) at a density of 1.60×10^6 /ml at 37°C in RPMI-1640 media with 2% FCS (GIBCO®, Invitrogen Pty Limited, Australia) and antibiotics (100 U/ml penicillin, 100 μg/ml streptomycin). A series of dose-response experiments in triplicate were performed to assess the effects of pyocyanin at the following concentrations: 0, 10, 20, 50 and 100 μM. These concentrations were chosen because pyocyanin has been detected *in vivo* at

concentrations of 1-130 μM (Wilson et al, 1988). For the experiments involving anti-oxidant enzymes, pyocyanin was added to LSECs at a concentration of 10 μM then incubated at 37°C for 1 hour prior to sampling. In selected experiments, immediately before adding pyocyanin, superoxide dismutase (SOD) (from bovine erythrocytes; Sigma-Aldrich, St. Louis, MO, USA; S-2515; at a concentration of 30 U/mL) and/or catalase (from bovine liver; Sigma-Aldrich, St. Louis, MO, USA; C-40; at a concentration of 3000 U/mL) were added. For ten to thirty scanning electron microscopic fields to be studies for each treatment group, experiments were performed in triplicate or duplicate.

The *in vivo* experiments were performed in male Fisher F344 rats (aged 2-3 months, approximately 200 g). A midline laparotomy incision was made in anesthetised animals and saline (n = 5) or pyocyanin (n = 7) was injected into the portal vein. Pyocyanin, when injected portally, was calculated to give a final systemic concentration of 11.9 μM. Total blood volume was calculated for each rat using the following formula (Lee and Blaufox, 1985), $Blood\ Volume\ (ml) = 0.06 \times BodyWeight\ (g) + 0.77$. The laparotomy was closed and respiratory rate monitored. After 30 minutes, the incision was re-opened. Blood was collected from the inferior vena cava for biochemical analysis, and the liver was removed and processed for scanning electron microscopy and immunohistochemistry as described previously (Cogger et al, 2006; Cogger et al, 2004). Two lobes were snap-frozen in liquid nitrogen for biochemical analyses.

2.2.3. Electron microscopy

Scanning electron microscopy of LSECs and liver tissue blocks was performed as described previously (Cogger et al, 2006; Cogger et al, 2004) with a Jeol JSM-6380LV scanning electron microscope (Jeol, Akishima-Shi, Japan). All scanning electron micrographs were analysed using ImageJ (http://rsb.info.nih.gov/ij/) to determine endothelial porosity, average fenestration diameter, fenestration density and the presence of gaps. Endothelial porosity is the area of the endothelial surface covered with fenestrations is calculated by dividing the sum total of the individual area of each fenestration in a given field divided by the total area of that particular field examined. Endothelial porosity is expressed as a percentage and is dependent on 2 parameters, the fenestration diameter and the fenestration density. Fenestration density is the number of fenestrations in a specific field measured. Fenestration density is expressed as the number of fenestrations/ μm^2. Fenestration diameter is expressed in nanometers (nm).

For electron microscopic processing of isolated LSECs, LSECs were fixed with 3 % glutaraldehyde in 0.1 M Na-Cacodylate buffer with 0.1 M sucrose at room temperature for 1 hour, post-fixed with filtered 1% tannic acid in 0.15 mol/L Na-cacodylate at pH 7.4 for 1 hour and post- fixed yet again with 1% osmium tetroxide in 0.1 mol/L Na-cacodylate at pH 7.4 for 1 hour. They were dehydrated in a graded ethanol series, dried with hexamethyldisilazane, and sputter coated with 10 nm of gold. The samples were examined with a Jeol JSM-6380LV scanning electron microscope (Jeol, Akishima-Shi, Japan). For analysis of isolated LSECs, three representative micrographs from each of four cellular fields per cover-slip were taken

at 15000× magnification. The number of fenestrations analyzed for each treatment were: control 1860, pyocyanin 10 μM 1084, pyocyanin 10 μM + SOD 1521, pyocyanin 10 μM + catalase 1079, and pyocyanin 10 μM + SOD + catalase 2858.

Processing of liver tissue blocks for scanning electron microscopy was performed as follows. Liver tissue blocks measuring approximately 1 mm^3 each were fixed with 3% glutaraldehyde and 2.5 % paraformaldehyde in 0.1 M Na-cacodylate buffer with 0.1 M sucrose and 2 mmol/ L $CaCl_2$ and postfixed with 1% osmium tetroxide in 0.1 M Na-cacodylate at pH 7.4. They were dehydrated using a graded ethanol series, dried with hexamethyldisilazane, and sputter coated with 20 nm of platinum. A total of 12 representative fields from at least 3 liver blocks per animal were photographed at 25000× magnification.

Transmission electron microscopy of liver tissue sections was performed as described previously (Cogger et al, 2004). Briefly, two technically eligible blocks per liver were examined. Sections from each block were chosen at random for ultrastructural measurement. Twenty representative micrographs per animal were taken at 19000× and 10 at 4600× with a Philips CM10 Transmission Electron Microscope fitted with a Megaview III camera and Analysis® software (Olympus). The 19000× micrographs were analysed with Image J to measure endothelial thickness, gap frequency, and fenestration frequency. Fenestrations were defined as pores < 300 nm in diameter and gaps were defined as pores > 300 nm. The 4600× micrographs were analysed with Image J to measure collagen bundle, Kupffer cell activation and hepatocyte mitochondria.

2.2.4. Light microscopy and immunohistochemistry

Liver specimens were fixed in 4% paraformaldehyde buffered saline and embedded in paraffin for light microscopy and immunohistochemistry. 4 μm sections were stained with haematoxylin and eosin for light microscopy. Immunohistochemistry was used to detect the differences in staining intensity, distribution and pattern of caveolin-1, which is present on the plasma membrane of LSEC fenestrations (Ogi et al, 2003); 3-nitrotyrosine, which marks tyrosine nitration occurring during oxidative stress; and malondialdehyde, which indicates lipid peroxidation occurring during oxidative stress. Immunohistochemical staining was performed using an indirect polymer immunoperoxidase method. Four μm sections of fixed liver tissue were deparaffinized in xylene (3×3 min) and taken to absolute ethanol (3×2 min). Endogenous peroxidase was blocked by incubating slides in 3% H_2O_2 in absolute methanol for 10 min at room temperature. After hydrating the sections, the slides utilized for nitrotyrosine and caveolin-1 immunohistochemistry were heated at 125°C for 4 min in a Decloaking Chamber (Biocare Medical) with epitope retrieval buffer and then cooled. This was followed by incubation with goat serum for 20 min. Without washing, the primary antibodies were applied and incubated overnight. The primary antibodies used were rabbit anti-human caveolin-1 antibody (N-20, Cruz Biotechnology, Santa Cruz, CA, USA), mouse monoclonal anti-nitrotyrosine antibody (ab7048, Abcam), and rabbit polyclonal anti-malondialdehyde antibody (ab6463, Abcam). The epitope retrieval buffers used were citrate buffer (0.01 M, pH 6.0) for caveolin-1 and tris buffer (0.05 M Tris-EDTA, pH 8.0) for 3-nitrotyrosine immunohistochemistry. No pre-treatment was needed for tissues for malondialdehyde immunohistochemistry. During the immunostaining all slides were washed in washing buffer (0.001 M Tris, pH 7.6)

containing Tween 20. After the primary incubation, the secondary antibody, affinity purified goat anti-mouse or anti-rabbit immunoglobulin linked polymeric horseradish peroxidase (AP340P-50ML/ AP342P-50ML, Chemicon International, Inc. Australia Pty Ltd.) was applied for 30 min. After buffer wash, the sections were treated with diaminobenzidine (DAB) chromogenic substrate solution for 5 min and slides were washed in water. The slides were then immersed in 1% aqueous $CuSO_4$ solution for further intensification of staining and counterstained with haematoxylin, dehydrated and mounted. The slides were graded consensually by three blinded observers according to staining distribution (periportal, zone 2, pericentral) and intensity of staining (0, +, ++, +++), and semi-quantitatively assessed.

2.2.5. ATP assay

ATP was measured by the luciferin-luciferase method with a luminometer as per the manufacturer's instructions (G7570, CellTiter-Glo™ Luminescent Cell Viability Assay kit, Promega, Madison, WI, USA). The luciferase enzyme requires ATP in order to generate light. As active cells produce ATP, after an equal volume of CellTiter-Glo™ reagent is added to the LSECs, luminescence is measured. The light signal produced is proportional to the amount of ATP present. The final ATP concentrations were calculated from a calibration curve constructed at the same time by means of standard ATP dissolved in the given buffer. Results were normalized to each well containing LSECs at density of 1.60×10^6 /ml.

2.2.6. Glutathione assay and blood biochemistry

Glutathione levels were assessed in order to determine the existence or absence of oxidative stress on pyocyanin treated liver specimens. Liver samples were homogenised in ice-cold 10 % 5-sulfosalicylic acid. Samples were centrifuged and supernatants removed for analysis. Total glutathione (GSH + GSSG) and glutathione disulfide (GSSG) levels were assayed according to the recycling method of Griffith (Griffith, 1980). GSSG analysis entailed removal of GSH by addition of 2 µl of 2-vinylpyridine per 100 µl of supernatant prior to the recycling reaction.

Protein quantitation, blood biochemistry and liver function tests were done by the Biochemistry Department, Diagnostic Pathology Unit, Concord RG Hospital, using the automated Roche Diagnostics Modular Analytics Serum Work Area (F.Hoffmann-La Roche Ltd). Briefly, the principles utilized in these assays are enclosed in brackets as follows: Total Protein (Biuret/ Endpoint with Blank), Albumin (BCG-Citrate buffer), ALT and AST (IFCC Modified), ALP (AMP Buffer- IFCC), LDH (IFCC Modified), Creatinine (Alkaline Picrate- Rate- Blank, Compensate), CK (IFCC/ Imidazole Buffer), $Na^+/K^+/Cl^-$ (Iron Specific Electrode- Indirect), HCO_3^- (Enymatic), and Ca^{++} (Cresol.Complex- No Dialysis).

2.2.7. Western Blot analysis for pyocyanin interaction with caveolin-1

To determine whether pyocyanin irreversibly binds to caveolin-1 and alters protein size, caveolin-1 electromobility was examined using Western Blot. Twenty

micrograms of cell lysate from SK-HEP-1 cells, an immortal endothelial cell-line (Heffelfinger et al, 1992), treated with pyocyanin; and controls were separated by SDS-PAGE. Lanes were run with 100 μM pyocyanin or 2 μM pyocyanin in the presence of lysate; or with 100 μM pyocyanin alone. Lysate, when loaded, was always 20 μg/ well. After transfer onto nitrocellulose membrane (Amersham Biosciences, Australia) the blot was blocked, incubated with primary antibodies to caveolin-1 (Santa Cruz Biotechnology, Santa Cruz, CA, USA), washed and incubated with a rabbit anti-goat IgG secondary antibody conjugated to horseradish peroxidase (Amersham Biosciences, Australia). Proteins were visualized using chemiluminescence.

2.2.8. Statistical analysis

Statistical analysis was performed using SigmaStat Statistics Software (SPSS Inc, Chicago, IL). Data are presented as the mean ± standard error of the mean. For isolated LSEC morphometry statistical significance levels ($P < 0.05$) were determined by one-way analysis of variance (ANOVA) with Student-Newman-Keuls method for post hoc pairwise multiple comparisons. For fenestration morphometry of intact sinusoids in the *in vivo* liver studies, the Mann–Whitney test were used to compare groups and considered significant when $P < 0.05$.

2.3 Results

2.3.1. Effect of pyocyanin on porosity of isolated LSECs

Treatment of LSECs with pyocyanin concentrations ranging from 0 to100 μM induced a dose-dependent decrease in LSEC porosity (Fig. 2.1) as measured by scanning electron micrograph morphometry.

Figure 2.1. Pyocyanin dose and porosity of LSECs

Porosity (%) of isolated LSECs decreased as concentration of pyocyanin increased from 0 to100 μM.

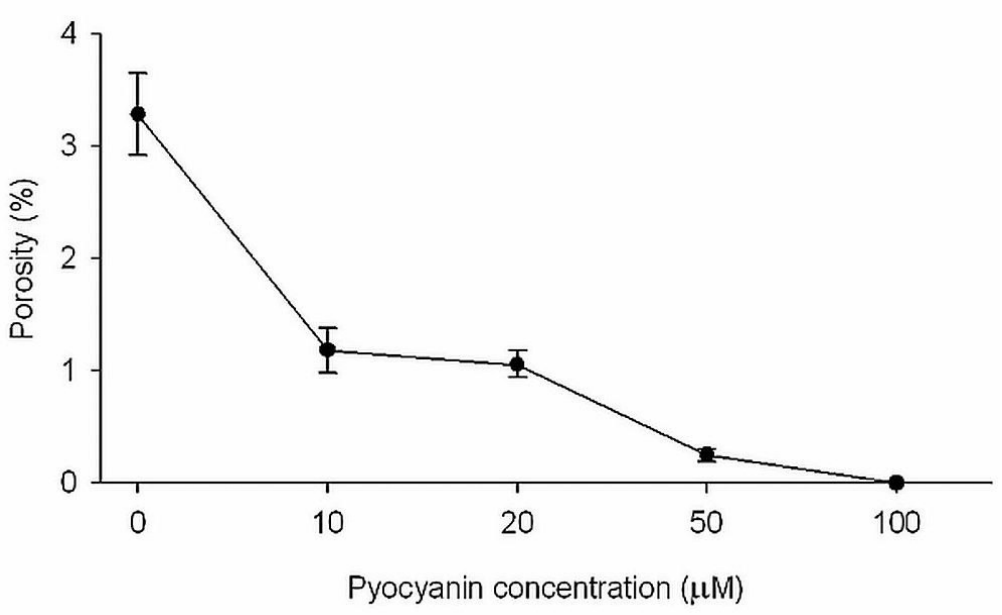

2.3.2. Effect of pyocyanin on porosity and fenestrations of isolated LSECs

Treatment with pyocyanin (10 μM) was associated with a significant reduction in LSEC porosity from 3.3 ± 1.8 % to 1.2 ± 1.0 % ($P < 0.001$) with a loss of sieve plate organization (Fig. 2.2). This was prevented by the addition of catalase, but superoxide dismutase did not have any statistically significant effect (Fig. 2.3). The effects of pyocyanin appeared to be mediated by changes in the frequency of the fenestrations. Catalase appeared to improve porosity mostly by its effects on the diameter of the fenestrations (Fig. 2.2).

2.3.3. Effect of pyocyanin on morphology of isolated LSECs

All changes in cell morphology were dose-dependent (Table. 2.1). Cell membrane blebbing, cytoplasmic retraction and cell membrane retraction were extensive at 50 μM, occasionally present at 10 and 20 μM but not seen at 1 and 5 μM.

Figure 2.2. Scanning electron microscopy of control-, pyocyanin and anti-oxidant enzyme-treated rat LSECs

Scanning electron microscopy (Magnification 15000 ×) of isolated rat LSECs under control incubation conditions (A); after treatment with 10 μM pyocyanin (B); pyocyanin and superoxide dismutase (C); and pyocyanin and catalase (D). Fenestrations (→) are grouped into sieve plates in A and D.

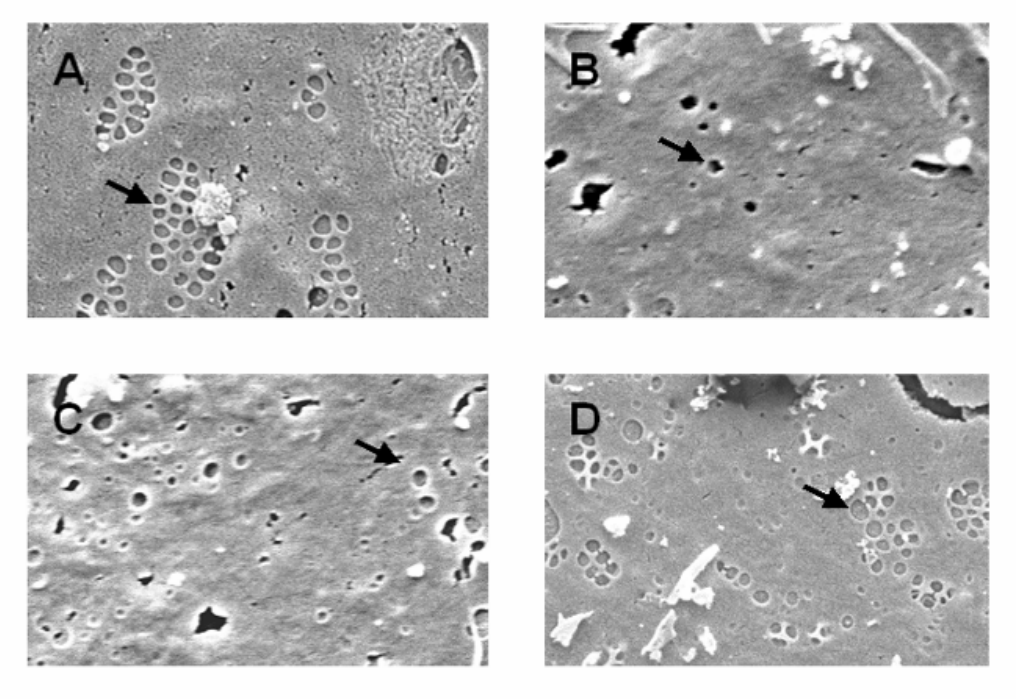

Figure 2.3. Quantification of the porosity, frequency and diameter of fenestrations in the LSECs

There was a reduction in fenestrations after treatment with 10 μM pyocyanin, which was reversed by catalase but not superoxide dismutase (* $P < 0.05$ compared to control).

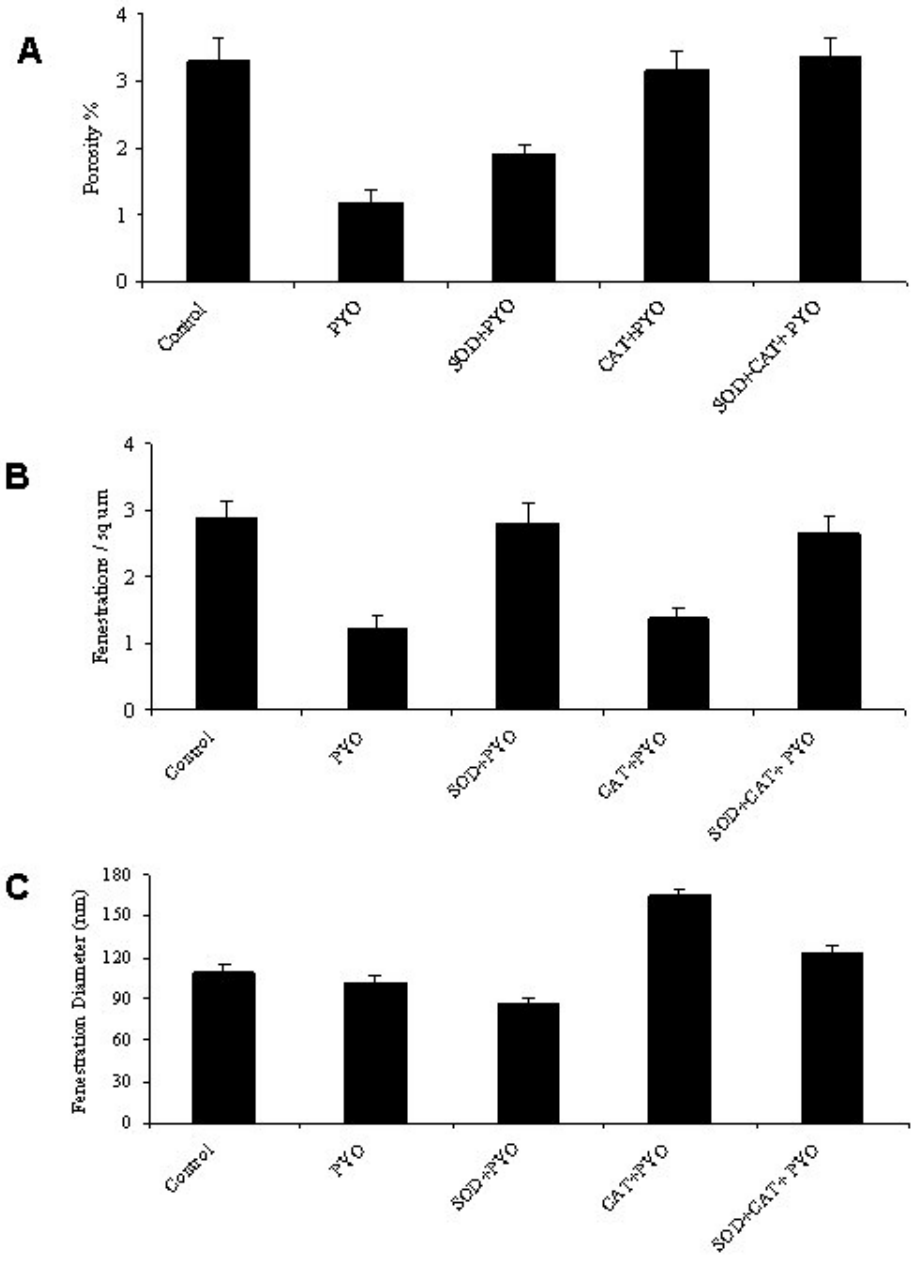

Table 2.1. Pyocyanin dose and LSEC morphology

	Pyocyanin Concentration (μM)						
	0	**1**	**5**	**10**	**20**	**50**	**100**
Sieve plate obliteration	-	-	-	+	+	+++	-
LSEC membrane retraction	-	-	-	+	+	+++	-
Cytoplasmic contraction		-	-	+	+	+++	-
Perinuclear plasma membrane blebbing	-	-	-	-	-	++	-
Cellular disintegration	-	-	-	-	-	+	++

Cell membrane blebbing, cytoplasmic retraction and cell membrane retraction were extensive at 50 μM, occasionally present at 10 and 20 μM but not seen at 1 and 5 μM.

2.3.4. Effects of pyocyanin on ATP content of isolated LSECs

ATP decreases in several cellular systems have been reported with pyocyanin treatment. These changes were also evident in a one-off experiment. Antioxidant enzymes (SOD and catalase) seemed to have a minimum ameliorating effect on pyocyanin-induced ATP decrease (Fig. 2.4).

Figure 2.4. Confirmation of cellular ATP fluctuations with pyocyanin treatment

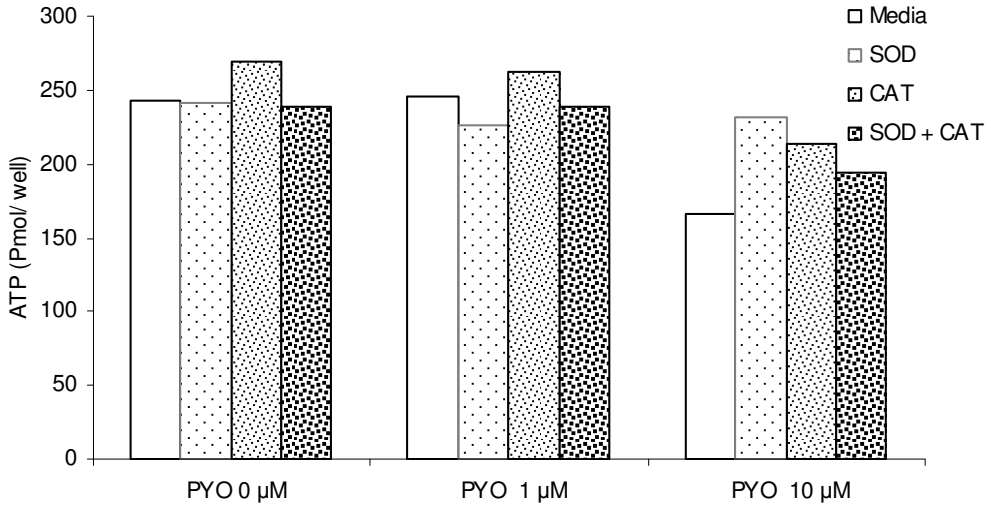

ATP decreases were also evident in a one-off experiment not equilibrated with protein. SOD and catalase seemed to have a minimum ameliorating effect on pyocyanin-induced ATP decrease.

2.3.5. Scanning electron microscopy of liver sinusoids

Scanning electron micrograph analysis of liver sinusoids (Fig. 2.5A, 2.5B) revealed a decrease in porosity of liver sinusoids with pyocyanin treatment, with significant contributions from both fenestration diameter and fenestration frequency (number of fenestrations per square µm) (Table. 2.2). Pyocyanin treatment was associated with smaller fenestration diameters than those seen in control liver sinusoids (Fig. 2.5C). The number of gaps (diameter > 300 nm) was slightly raised with pyocyanin treatment, although statistically insignificant (Fig. 2.5C).

2.3.6. Transmission electron microscopy of liver sinusoids and the space of Disse

Transmission electron micrograph analysis revealed normal hepatocyte architecture in both control and pyocyanin-treatment groups (Fig. 2.6). The hepatocellular nuclei, mitochondria and endoplasmic reticulum were well-preserved and had normal morphology. Pyocyanin treatment was associated with a statistically significant decrease in endothelial thickness from 175.8 ± 5.8 to 156.5 ± 4.0 nm (Fig. 2.6C, 2.6D, Table 2.2). No changes in hepatocellular mitochondrial count, collagen bundle count, and Kupffer cell count were observable (data not shown).

Figure 2.5. Scanning electron microscopy of liver sinusoids from control and pyocyanin-treated rats

The fenestrations of the control liver sinusoid (A) are larger in diameter and higher in frequency (number of fenestrations per square μm) than those of the Pyocyanin treated liver (B). The arrow-head indicates a single fenestration and the full arrow, a sieve-plate circumscribing many fenestrations. Original magnification 25000x, scale bar = 1 μm. C is a histogram of fenestration diameters measured on scanning electron micrographs, showing a lower proportion of smaller fenestrations in pyocyanin treated liver endothelium than in control livers. There was a non-significant trend towards an increased number of gaps (> 300 nm) with pyocyanin treatment.

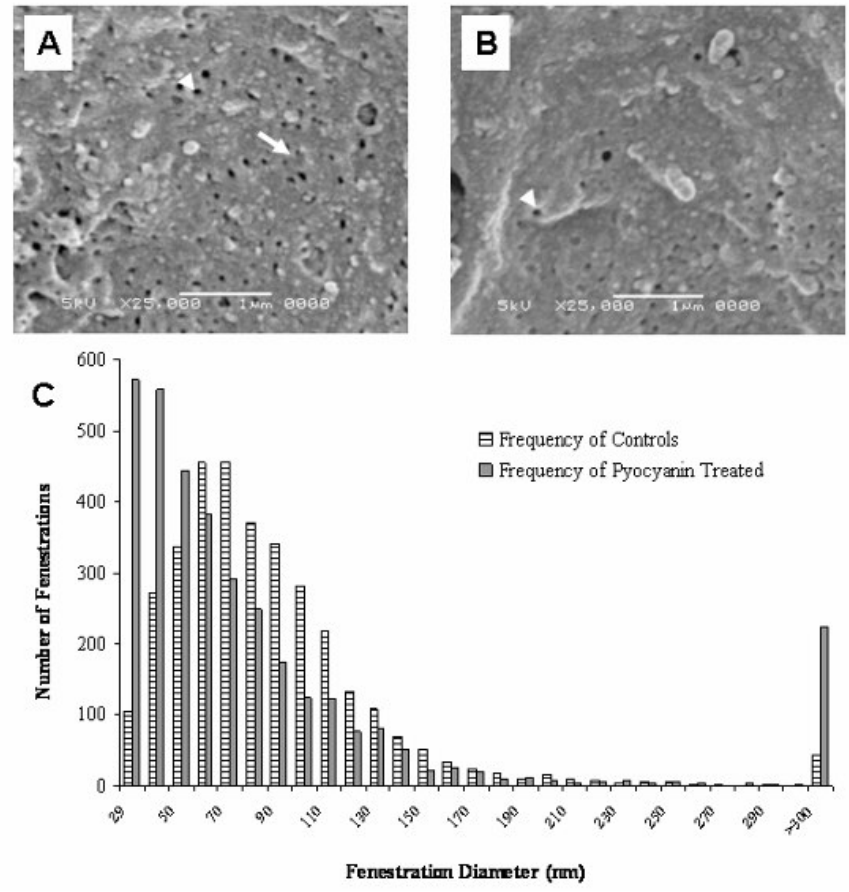

Figure 2.6. Transmission electron microscopy of livers from control and pyocyanin-treated rats

Organelle size and number were unaffected by pyocyanin treatment with normal morphology of mitochondria (M) observed in control and pyocyanin treated rats: A Control liver sinusoid, B Pyocyanin treated liver sinusoid. S; sinusoidal lumen, scale bar = 2 μm, original magnification 4600x. At original magnification 19000x, a decrease in the thickness of the endothelium (E) was seen in the pyocyanin treatment group. The space of Disse (D), hepatocytes (H) and hepatocellular endoplasmic reticulum (ER) appeared normal in both groups: C Control liver sinusoid, D Pyocyanin treated liver sinusoid. F; fenestrations, scale bar = 1 μm.

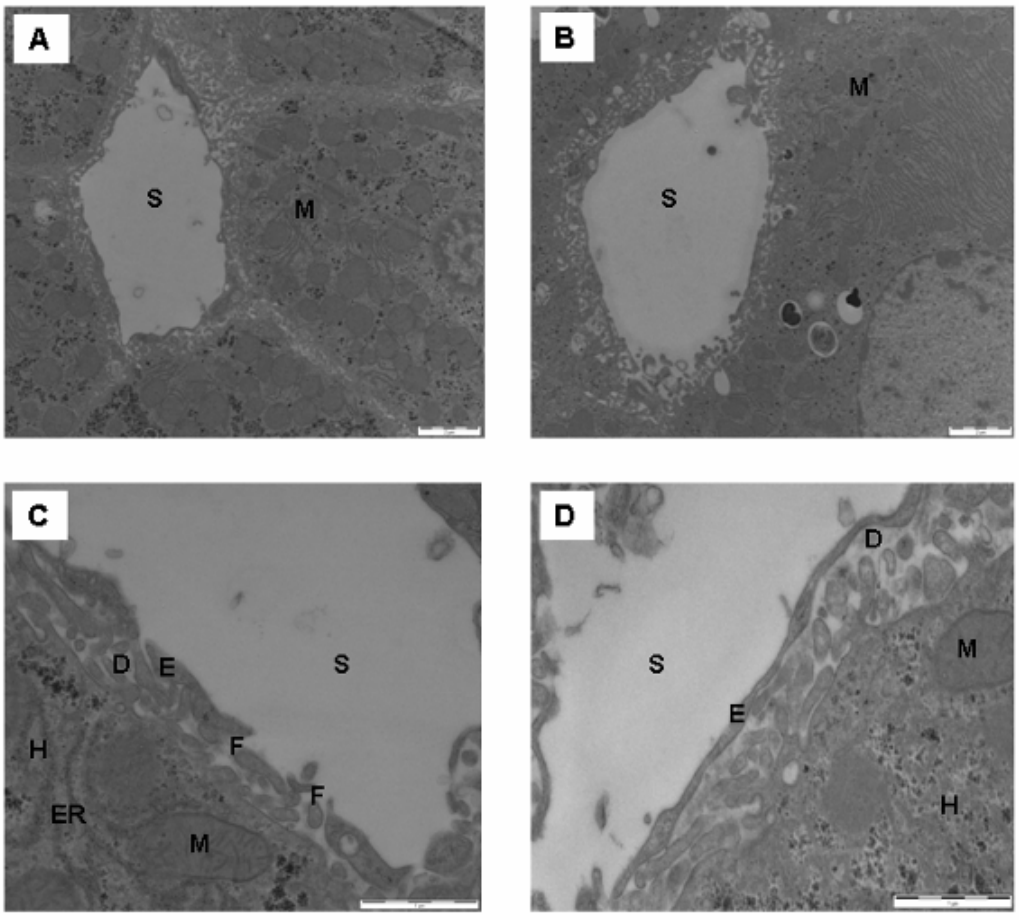

Table 2.2. Electron micrograph morphometry of the liver endothelium and peri-sinusoidal hepatocytes from rat livers with and without pyocyanin treatment in vivo

	No Treatment (*n*= 5)	**Pyocyanin Treatment (*n*= 7)**	***P* Value**
SCANNING ELECTRON MICROSCOPY			
Porosity %	3.4 ± 0.2	1.3 ± 0.1	< 0.001
No. of Fenestrations/ μm^2	5.5 ± 0.3	2.4 ± 0.1	< 0.001
Fenestration Diameter (nm)	80.4 ± 0.6	71.0 ± 0.8	< 0.001
TRANSMISSION ELECTRON MICROSCOPY			
Endothelial Thickness (nm)	175.8 ± 5.8	156.5 ± 4.0	< 0.01

With pyocyanin treatment, scanning electron micrograph analysis revealed a decrease in porosity, fenestration diameter and fenestration frequency of liver sinusoids. With pyocyanin treatment, transmission electron micrograph analysis revealed a decrease in endothelial thickness.

2.3.7. Light microscopy and immunohistochemistry of livers

Light microscopy (Fig. 2.7A, 2.7B), 3-nitrotyrosine immunohistochemistry (Fig. 2.7C, 2.7D) and malondialdehyde immunohistochemistry (Fig. 2.7E, 2.7F) of livers revealed no observable changes with pyocyanin treatment.

2.3.8. Investigation of relationship of caveolin-1 to pyocyanin-induced endothelial changes

Caveolin-1 immunohistochemistry (Fig. 2.7G, 2.7H) of livers revealed no observable changes with pyocyanin treatment. During Western Blot analysis for caveolin-1 (Fig. 2.8), pyocyanin treatment of SK-HEP-1 cells did not alter caveolin-1 mobility.

Figure 2.7. Light microscopy and immunohistochemistry of livers from control and pyocyanin groups

Light microscopy of liver sections stained with eosin and haematoxylin staining A Control liver, B Pyocyanin treated liver), malondialdehyde immunohistochemistry (C Control liver, D Pyocyanin treated liver), 3-nitrotyrosine immunohistochemistry (E Control liver, F Pyocyanin treated liver) and caveolin-1 immunohistochemistry (G Control liver, H Pyocyanin treated liver) revealed no changes across the hepatic lobule with pyocyanin treatment. Immunohistochemical stains appear brown, original magnification 100x.

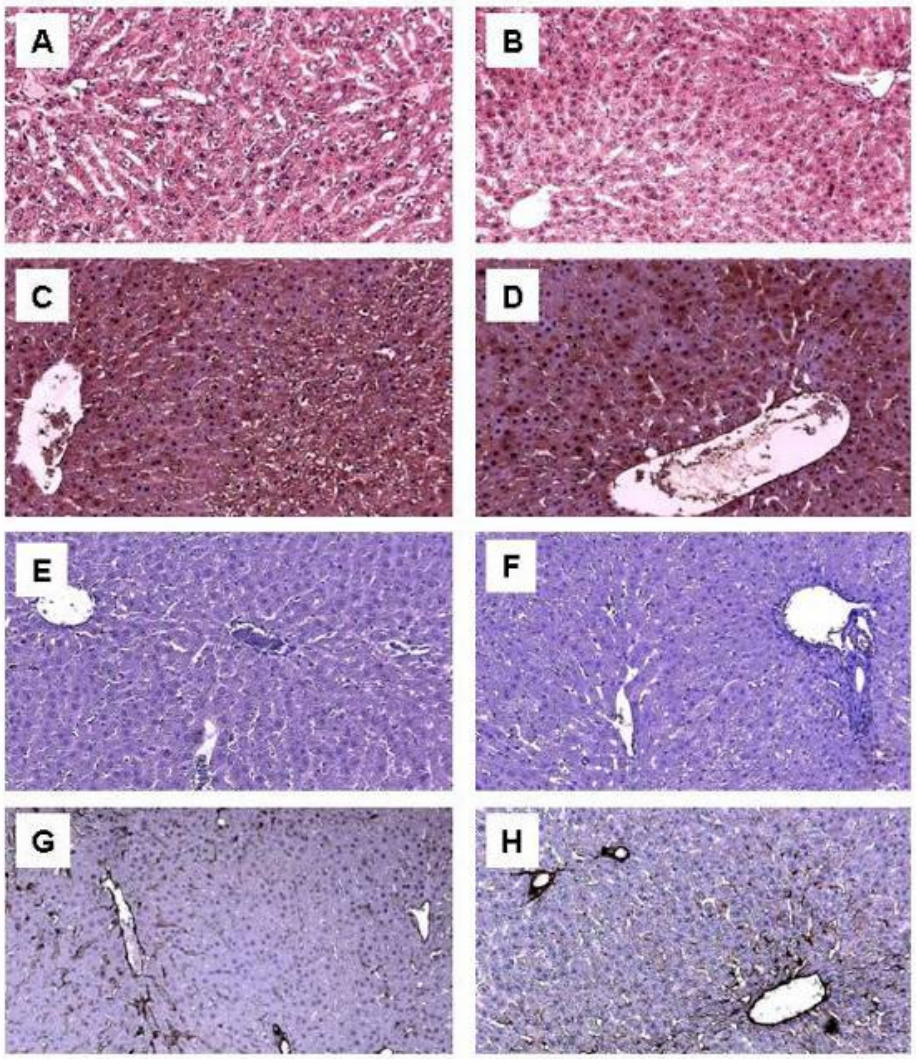

Figure 2.8. Western blot analysis for caveolin-1

SDS page gel run with 20 µl of SK-HEP-1 cells-lysate with 2 µM pyocyanin (Lane A), 100 µM pyocyanin (Lane B) or no pyocyanin (Lane D & E); or with 100 µM (Lane C) pyocyanin alone and stained for caveolin-1. Lysate, when loaded, was always 20 µg/ well (Lane A, B, D & E). Band migration was unaltered for SK-HEP-1 cell lysate with and without pyocyanin treatment.

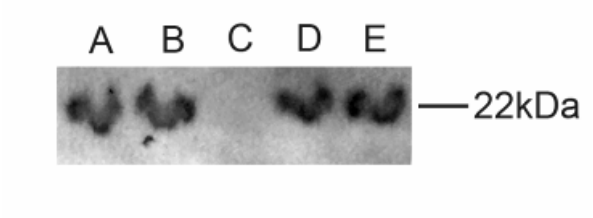

2.3.9. Blood glutathione and biochemistry

The GSSG to GSSG + GSH ratio was 60 ± 15 % of that seen in controls and was statistically insignificant. Serum biochemistry including liver function tests (total protein, albumin, ALT, AST, ALP) and analysis of markers of cytolysis (LDH, CK, creatinine, K+) showed no significant change with pyocyanin treatment (Table 2.3).

Table 2.3. Liver function tests and markers of cytolysis with and without in vivo pyocyanin

	No Treatment (n= 5)	**Pyocyanin (n= 7)**
ELECTROLYTES		
Na^+ (mmol/ L)	134.5 ± 0.6	134.6 ± 0.4
Ca^{++} (mmol/ L)	2.5 ± 0.0	2.7 ± 0.1
Cl^- (mmol/ L)	96.5 ± 0.6	95.6 ± 0.5
$HCO3^-$ (mmol/ L)	28.5 ± 1.0	26 ± 0.9
LIVER FUNCTION TESTS		
ALP (U/L)	186.6 ± 16.7	174.2 ± 12.2
ALT(U/L)	69.0 ± 13.7	71.5 ± 8.4
AST(U/L)	90.6 ± 14.3	120.2 ± 33.4
Protein (g/L)	52.0 ± 1.2	54.4 ± 1.0
Albumin (g/L)	33.2 ± 0.8	34.4 ± 0.8
MARKERS OF CYTOLYSIS		
LDH (U/L)	264.3 ± 24.8	747 ± 227.8
CK Total (U/L)	832.4 ± 128.0	1642.7 ± 348.2
Creatinine (mmol/ L)	28.4 ± 1.0	30.2 ± 1.9
K^+ (mmol/ L)	6.4 ± 0.2	5.9 ± 0.2

Serum electrolytes, liver function tests and markers of cytolysis showed no statistically significant changes with pyocyanin treatment.

2.4. Discussion

This study demonstrates that pyocyanin treatment over a wide range of concentrations is associated with a substantial loss of LSEC porosity. Pyocyanin also induces significant acute changes in the *in vivo* liver sinusoidal endothelium without evidence that these changes are mediated by reactive oxygen and nitrogen species. These LSEC changes were not accompanied by evidence of structural or biochemical hepatocellular changes.

Many toxins have been shown to induce LSEC injury. In particular, oxidative stress has been shown to have dramatic effects on the morphology of the LSEC. We found that H_2O_2 (0.7 mM) delivered *via* the portal vein in the perfused liver had effects that were largely confined to the perisinusoidal areas (Cogger et al, 2001) and that *tert*-butyl hydroperoxide injected into the portal vein *in vivo* and in isolated LSECs caused disruption of the liver sieve plates (Cogger et al, 2004). Regards pyocyanin, Britigan and coworkers used spin trapping to show that pyocyanin induced oxidative injury *via* the hydroxyl free radical in pulmonary artery endothelial cells (Britigan et al, 1992; Miller et al, 1996).

Pyocyanin-induced H_2O_2 production by human umbilical vein endothelial cells with marked depletion of intracellular glutathione, and these changes were preventable by catalase (Muller, 2002). In this study exploring the effects of pyocyanin on isolated LSECs, catalase which inactivates hydrogen peroxide to water, prevented pyocyanin-induced morphological changes in the LSECs, specifically defenestration. In this study in intact livers *in vivo*, portally injected pyocyanin (blood concentration of 11.9

μM for 30 min) induced a dose-dependent loss of porosity in isolated LSECs. Furthermore, portally injected pyocyanin *in vivo* led to a significant reduction in porosity of the endothelium showing that this effect is seen both *in vivo* and *in vitro*. In addition, a decrease in endothelial thickness with pyocyanin was noted, a change that has not been reported with any other toxic injury to the LSEC.

It is important to note that the ultramicroscopic LSEC changes were present without any morphological hepatocellular alterations including mitochondrial morphology and frequency or any other signs of hepatocyte injury or oxidative stress. This indicates that the LSEC is initial site of injury induced by pyocyanin, and indeed may even have a role in protecting hepatocytes from endo- and xenobiotics. There were no changes in malondialdehyde and 3-nitrotyrosine immunohistochemistry. A decrease in 3-nitrotyrosine immunohistochemical staining was expected because of previous reports incriminating pyocyanin in the inhibition of nitric oxide production (Warren et al, 1990) *via* guanylyl cyclase inhibition (Hussain et al, 1997), but no differences accruing with pyocyanin treatment were observed in this study. Likewise, although an increase in malondialdehyde immunohistochemistry was expected owing to the possibility of increased membrane-lipid peroxidation *via* H_2O_2 production with pyocyanin treatment (Muller, 2002), no differences were oberved. This is in contradistinction to the studies in isolated LSECs where an increase in markers of oxidative stress was found. It is plausible that *in vivo*, hepatocyte-derived antioxidants prevented any overall changes in markers of oxidative stress but not sufficient to prevent defenestration of the LSEC. Alternatively, it is possible that pyocyanin induces defenestration through mechanisms independent of oxidative stress.

To explore this possibility, caveolin-1, a membrane protein involved in the maintenance of fenestrations, was studied (Braet et al, 2003; Ogi et al, 2003). It has been demonstrated that LSEC defenestration, which occurs in models of pathological liver states such as cirrhosis (Nopanitaya et al, 1976) and type 1 diabetic liver (Jamieson et al, 2007), is accompanied by caveolin-1 overexpression. Similarly, LPS which induces defenestration in LSECs (Dobbs et al, 1994), also induces the overexpression of caveolin-1 (Kamoun et al, 2006) (Table 2.4). However, there were no caveolin-1 immunohistochemical changes with the liver endothelial defenestration induced by pyocyanin. The possibility of pyocyanin binding to caveolin-1 or altering the properties of caveolin-1 was also investigated. Again, there was no alteration in caveolin-1 using an immunoblot method. These results exclude the possibility that pyocyanin induces defenestration *via* any major effects on caveolin-1. Therefore it is possible that pyocyanin induces defenestration through mechanisms independent of oxidative stress or interaction with caveolin-1. As pyocyanin has been shown to influence the expression and secretion of numerous cytokines (Leidal et al, 2001; Muhlradt et al, 1986), further investigations into the expression and activity of these cytokines may serve to partly or fully unravel the appropriate mechanism (Table 2.4).

The observation that pyocyanin influences endothelial morphology may have significant clinical implications. LSECs are important in tolerance induction in liver transplantation and rejection of donor livers correlates closely with the presence of LSEC antibodies (Sumitran-Holgersson et al, 2004). Furthermore, LSEC responses to ischemia-reperfusion injury in the donor organ influences outcome of liver transplantation (Shimizu et al, 2001; Sun et al, 2001). Thus damage to the LSEC induced by pyocyanin could impact graft outcome and prognosis following

pseudomonal sepsis. It has also been reported that hyperlipidemia is an important response to sepsis. The mechanism for sepsis-associated hyperlipidemia is multifactorial, but impaired catabolism of lipoproteins is a contributory factor (Harris et al, 2000; Spitzer et al, 1988). LSECs, which are perforated with fenestrations that facilitate the transfer of lipoproteins between blood and hepatocytes, have an increasingly recognized role in hyperlipidemia (Fraser et al, 1995). Conditions associated with reduced numbers of fenestrations such as ageing (Hilmer et al, 2005) and treatment with the surfactant poloxamer 407 (Cogger et al, 2006) are associated with impaired lipoprotein uptake by the liver and hypertriglyceridemia. The results here with pyocyanin support the concept that hyperlipidemia associated with sepsis might in part be a result of LSEC defenestration. Pseudomonal sepsis may cause the release of toxins like pyocyanin and LPS which may lead to endothelial changes including loss of LSEC porosity, subsequently excluding lipoproteins from the liver, leading to lipoprotein retention in the peripheral vasculature. This mechanism may account for sepsis-related hyperlipidemia (Fig. 2.9). In the current study, the 30 min of pyocyanin exposure would not have been sufficient to cause profound changes in blood lipoprotein levels.

In conclusion, the *P. aeruginosa* toxin, pyocyanin caused loss of fenestrations over a range of concentrations in isolated LSECs as well as the *in vivo* liver endothelium. This has potential implications for mechanisms for liver transplantation and for hyperlipidemia associated with sepsis. The ultrastructural LSEC changes in the absence of hepatocellular injury indicate that the LSEC is a prime target for pyocyanin and support the sentinel role of the LSEC in hepatoprotectivity. Pyocyanin-

induced LSEC changes seen *in vivo* in the absence of free radical or oxidative stress injury points to a novel mechanism for the pathogenesis of *P. aeruginosa* pyocyanin.

Figure 2.9. Possible pathogenetic mechanism of pseudomonal sepsis-related hyperlipidemia

LSEC defenestration in bacterial/ pseudomonal sepsis owing to toxins like pyocyanin or LPS may exclude lipoproteins from the liver leading to lipoprotein retention in the peripheral vasculature accounting for bacterial/ pseudomonal sepsis-related hyperlipidemia.

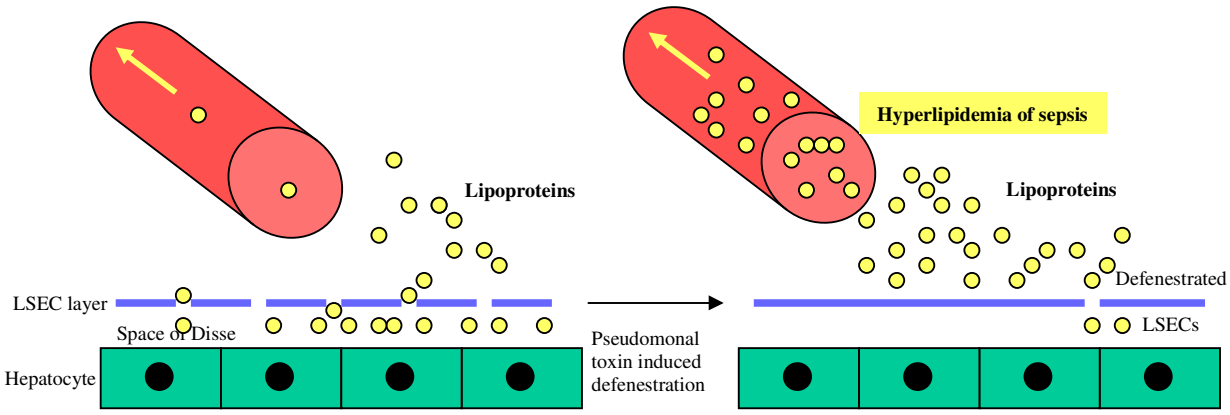

Table 2.4 . Possible defenestration mechanisms of pseudomonal agents

	Pseudomonal agent inducing defenestration	Location of LSECs in study	Possible mechanism	Mechanisms excluded	Citations
1	Pyocyanin	Isolated LSECs *in vitro*	ROS	-	This study
2	Pyocyanin	Intact *in vivo* liver sinusoids (this study only)	Cytokines? Vasoactive mediators?	ROS, caveolin-1	This study, (Leidal et al, 2001; Muhlradt et al, 1986)
3	LPS (*E. coli* LPS-structurally similar to pseudomonal LPS)	Isolated LSECs *in vitro* and intact *in vivo* liver sinusoids	Caveolin-1? Vasoactive mediators?		(Dobbs et al, 1994; Kamoun et al, 2006)

Possible mechanisms behind pseudomonal agent-induced defenestration

Chapter 3

The effect of old age on liver oxygenation, sinusoidal fenestrations and expression of VEGF and VEGFR2

3. The effect of old age on liver oxygenation, sinusoidal fenestrations and the expression of VEGF and VEGFR2

3.1 Introduction

It has been well established that phase 1 hepatic drug metabolism, which involves oxidation, reduction or hydrolysis, is diminished in old age (Herrlinger and Klotz, 2001; Kinirons and O'Mahony, 2004). These age-related changes could be caused by decreased liver perfusion (Schmucker, 2001), oxygen-diffusion barrier secondary to age-associated liver pseudocapillarization of the liver sinusoidal endothelial cell (Le Couteur et al, 2001), mitochondrial oxidative stress (Sastre et al, 2003) or mitochondrial dysfunction (Sastre et al, 1996). In the oxygen diffusion barrier hypothesis, it was proposed that the disparity between *in vivo* and *in vitro* measures of phase I drug metabolism in old age (Herrlinger and Klotz, 2001; Kinirons and O'Mahony, 2004), could reflect intrahepatocytic hypoxia because oxygen is an essential cofactor for cytochrome P450 enzymes (Le Couteur and McLean, 1998). Using ^{31}P-nuclear magnetic-resonance studies on freeze-clamped samples, it was reported that aged rat livers have decreased ATP and high-energy phosphate metabolite pools, suggestive of hypoxia (Le Couteur et al, 2001). Others have shown that livers from old mice have less total ATP (Selzner et al, 2007). However, this was associated with diminished oxygen consumption and ATP production by isolated mitochondria, which is suggestive of mitochondrial dysfunction rather than hypoxia (Selzner et al, 2007). Apart from changes in ATP levels, it has also been reported that there is upregulation of several genes and proteins that respond to hypoxia in old age.

Using Western Blotting and RT-PCR it was shown that the hypoxia marker Hypoxia Inducible Factor-1α (HIF-1α) and hypoxia-responsive products such as Heme Oxygenase-1 (HO-1), Vascular Endothelial Growth Factor (VEGF), Erythropoietin, and inducible nitric oxide synthase (iNOS) were increased in aged rat liver (Kang et al, 2005). Age-related changes in hepatic ATP and oxygenation could be caused by decreased oxygen delivery to hepatocytes secondary to either reduced liver perfusion (Schmucker, 2001), or an oxygen-diffusion barrier secondary to age-associated "pseudocapillarization" of the liver sinusoidal endothelial cell (LSEC) (Le Couteur et al, 2001). On other hand, the reduction in ATP might also be secondary to age-related mitochondrial oxidative stress (Sastre et al, 2003) or mitochondrial dysfunction (Sastre et al, 1996).

Alterations in liver oxygen and ATP will have specific implications for age-related changes in the LSECs. Morphological age-related changes in the hepatic sinusoid include endothelial thickening, defenestration, basement membrane formation and sporadic collagen disposition in the space of Disse, collectively called age-related 'pseudocapillarization' (Le Couteur et al, 2005). Pseudocapillarization impedes transfer of substrates such as lipoproteins from the sinusoidal lumen to the hepatocyte (Hilmer et al, 2005). Although the normal hepatic sinusoidal endothelium provides an insignificant resistance to oxygen transfer (Kassissia et al, 1992; Le Couteur et al, 1999), there is a significant diffusion barrier to oxygen diffusion posed by the blood vessels in cirrhosis (Froomes et al, 2003; McLean and Morgan, 1991) and in normal capillaries in other organs (Cho et al, 2001; Rose and Goresky, 1985). It was therefore hypothesized that age-related pseudocapillarization might also constitute an oxygen diffusion barrier analogous to that seen in cirrhosis (Le Couteur and McLean, 1998).

Age-related changes in the LSEC ('pseudocapillarization') have been partially induced by ATP depletion (Braet et al, 2003).

Furthermore, age-related changes in hepatic oxygen-dependent metabolism and oxygenation might contribute to age-related pseudocapillarization of the LSEC. Depletion of ATP has been shown to induce marked defenestration of isolated LSECs (Braet et al, 2003). Hypoxia also induces VEGF and VEGF receptors. VEGF is a potent stimulus for the generation of fenestrations in isolated LSECs (Funyu et al, 2001) and the VEGFR2 knockout mouse is defenestrated (Carpenter et al, 2005). The effects of old age on LSEC ATP levels and liver VEGF and VEGFR2 expression are not established but may have implications for the pathogenesis of ageing change in the hepatic sinusoid.

Therefore, here it was investigated whether ageing is associated with *in vivo* hypoxia in the aged rat liver. Immunohistochemistry with pimonidazole, and ATP levels in isolated LSECs were used to determine the presence of hypoxia in the hepatocytes and LSECs, respectively. 2-Nitroimidazoles including pimonidazole have been reliably used as *in vivo* hypoxia markers in a number of systems (Arteel et al, 1998). Nitroimidazole-adduct formation, which is increased in regions with low oxygen tension, is determined by immunohistochemistry. Staining is substantially increased when the intracellular oxygen tension falls below 10 mm Hg (Gross et al, 1995). Here, pimonidazole immunohistochemistry was performed on four young (4-month old) and six old (2-year old) rats in an attempt to directly visualize and compare the distribution and intensity of hypoxic areas in young and old rat livers. The ubiquitous synthetic surfactant poloxamer 407 was also used to induce defenestration of the

LSEC in livers of young rats (Cogger et al, 2006) in order to determine whether structural changes in the LSEC can induce hypoxia and thus test the concept of an oxygen diffusion barrier. Poloxamer 407 induces defenestration of the LSEC, probably by coating the LSEC cell membrane (Cogger et al, 2006). Finally, the effects of age on the expression of VEGF and VEGFR2 were studied because these respond to hypoxia (Ferrara, 2004; Ferrara et al, 2003) and also because any changes in their expression may shed light on the pathogenesis of pseudocapillarization of the LSEC.

3.2 Materials and methods

3.2.1. Animal protocols

The studies had approval by the Sydney Southwest Area Health Service Animal Welfare Committee. Rats were anesthetized with Ketamine and Xylazine (50 and 5 mg/kg respectively, Troy Laboratories, Smithfield, Australia) by intraperitoneal injection. Blood was collected from the inferior vena cava and the liver removed and processed for scanning electron microscopy and immunohistochemistry as described previously (Cogger et al, 2001). For the pimonidazole studies to determine the effect of ageing on hepatic oxygenation, specific pathogen free male Fisher F344 rats were obtained from the National Institute of Aging, Bethesda, Maryland, USA. Young (4 months, 315-346 g; n = 4) and old (24 months, 322-440 g; n = 6) rats were used. Pimonidazole (HP1-1000, Chemicon) was administered by intraperitoneal injection at a dose of 120 mg/ kg body weight two hours prior to harvesting the livers. For the poloxamer 407 study, male Sprague-Dawley rats (3-4 months, 381-477 g) obtained from the Animal Research Centre (Perth, Australia) were used. In this study, poloxamer 407 (gifted by BASF Australia Ltd, Sydney, Australia; 1 g/ kg body weight, n = 5) was administered in the test rats by intraperitoneal injection 24 hours prior harvesting the livers.

3.2.2. Immunohistochemistry

Immunohistochemical staining was performed using an indirect polymer immunoperoxidase method. Liver specimens were fixed in 4% phosphate buffered formalin and embedded in paraffin. Four micrometer sections were deparaffinized in xylene (3 × 3 min) and taken to absolute ethanol (3 × 2 min). Endogenous peroxidase was blocked by incubating slides in 3% H_2O_2 in absolute methanol for 10 min at room temperature. After hydrating the sections, the slides were heated at 125°C for 4 min in a pressure cooker (Decloaking Chamber, Biocare Medical) with epitope retrieval buffer and then cooled. This was followed by treatment with goat serum for 5 min. The primary antibody was applied and incubated overnight. The primary antibodies used were Hypoxyprobe Mab-1 (HP1-1000, Chemicon) for pimonidazole immunohistochemistry, mouse monoclonal VEGF antibody (ab1316, Abcam), and rabbit polyclonal VEGFR2 antibody (ab2349, Abcam). The epitope retrieval buffers used were citrate buffer (0.01 M, pH 6.0) for pimonidazole and VEGF immunohistochemistry, and Tris buffer (0.05 M Tris-EDTA, pH 8.0) for VEGFR2 immunohistochemistry. The slides were washed in Tris wash buffer (0.01 M Tris-EDTA, pH 7.6). Then the secondary antibody, goat anti-mouse immunoglobulin polymer conjugated with horseradish peroxidase (TL-060-HL, LabVision, DKSH Australia Pty Ltd.) was applied for 30 min. After buffer wash, the sections were treated with diaminobenzidine (DAB) substrate for 5 min treated with 1% $CuSO_4$, counterstained with haematoxylin, dehydrated and mounted. Sixteen random photographs per blinded slide were taken, graded by four observers blinded to the identity of the slides, according to staining distribution (periportal, zone 2, pericentral) and intensity of staining (0, +, ++, +++). Subsequently, after reaching a consensus, the

resultant grading was semi-quantitatively assessed by using Chi-square analysis for intensity differentiation.

3.2.3. Scanning electron microscopy

Scanning electron microscopy was performed as described previously (Cogger et al, 2001; Le Couteur et al, 2001; McLean et al, 2003). Briefly, liver specimen blocks 1 mm^3 each were fixed with 3 % glutaraldehyde in 0.1 M Na-Cacodylate buffer with 0.1 M sucrose and post- fixed with 1% osmium tetroxide in 0.1 mol/L Na-cacodylate at pH 7.4. They were dehydrated using a graded ethanol series, dried with hexamethyldisilazane, and sputter coated with 15- 20 nm of platinum. These were examined with a Jeol JSM-6380LV scanning electron microscope (Jeol, Akishima-Shi, Japan). A total of 12 representative fields from at-least 3 liver blocks per animal were photographed at 25000× magnification. Using the photographs thus obtained the software program ImageJ (http://rsb.info.nih.gov/ij/) was used to determine endothelial porosity, average fenestration diameter, and fenestration density. Endothelial porosity, the percentage area of the endothelial surface covered with fenestrations is dependent on 2 parameters, the fenestration diameter and the fenestration density which is the sum total of the individual area of each fenestration in a given field divided by the total area of the field examined, expressed as a percentage.

3.2.4. LSEC isolation

The method for the isolation of LSECs has been described (Braet et al, 1994; Smedsrod et al, 1985). The livers of young and old male F344 rats were perfused with collagenase A (Sigma) and the cell suspension centrifuged at 100 × g for 5 min. The supernatant, containing a mixture of sinusoidal liver cells, was layered on a 2-step Percoll gradient (25–50%) and centrifuged for 20 min at 900 × g. The intermediate zone was enriched in LSECs. LSEC purity was enhanced by selective adherence of Kupffer cells onto untreated plastic Petri dishes for 5 min. For SEM, LSECs were cultivated in 24-multiwell plates on collagen coated Thermanox cover slips in serum-free culture medium consisting of RPMI-1640 with 2 mmol/l L-glutamine, 100 U/ml penicillin, and 100 g/ml streptomycin.

3.2.5. ATP and protein assays

For the determination of cellular ATP, LSECs were plated at 0.8×10^6 cell/ml (100 µl/well) into clear bottom, opaque wall 96-well tissue culture plates and cultured for 16 h (37^oC/5% CO_2) in RPMI-1640 with fetal bovine serum (5%), L-glutamine (2 mmol/L), penicillin (100 U/mL) and streptomycin (100 g/ml). ATP was assayed using a CellTiter-Glo luminescent cell viability assay kit (Promega, Sydney) with an ATP standard curve. The luminescent signal was detected using a FluorStar Optima plate reader equipped with a luminescence probe. To determine cellular protein content, cells were washed twice with PBS to remove serum and protein quantified using the bicinchoninic acid protein determination kit (Sigma, Sydney).

3.2.6. Statistics

SigmaStat Statistics Software (SPSS Inc, Chicago, IL) was used for statistical analysis. Data are presented as mean ± standard deviation. The Chi-squared test and the Mann-Whitney test were used to compare the groups and considered significant when $P < 0.05$.

3.3 Results

3.3.1. The effect of old age and poloxamer 407 on pimonidazole staining

Pimonidazole staining was most often encountered in the pericentral region in livers from both young and old F344 rats (Fig. 3.1) and staining intensity increased manifold between periportal and pericentral region (Fig. 3.2A, 3.2B, 3.3A). This is consistent with the decline in sinusoidal oxygen tension as blood flows from the portal vein *via* zone 2 to the central vein. There were no effects of age on the intensity or distribution of pimonidazole staining. Furthermore, there was no effect of poloxamer 407 on pimonidazole staining in young Sprague Dawley rats, despite the induction of significant defenestration of the LSEC (Fig. 3.2C, 3.2D).

3.3.2. The effect of age on LSEC ATP levels

The ATP content of LSECs isolated from livers from old F344 rats (n = 4) was not significantly decreased compared to livers from young F344 rats (n = 4): young *versus* old: 3.6 ± 1.4 nmol *versus* 2.7 ± 1.8 nmol ATP per 10^6 cells.

3.3.3. The effect of age on VEGF expression

There was no difference in the expression of VEGF between livers from young (n = 4) and old (n = 6) F344 rats (Fig. 3.3B, 3.4A, 3.4B). Staining was more intense in the

pericentral regions than in the periportal regions and paralleled the distribution of staining seen for pimonidazole (Fig. 3.3B, 3.3A).

Figure 3.1. Zonal distribution of pimonidazole staining (hypoxic areas) in young and old rats

Zonal distribution of pimonidazole-adduct immunohistochemical staining in young and old rat livers. The distribution is depicted as the % of hypoxic liver zones ± SEM.

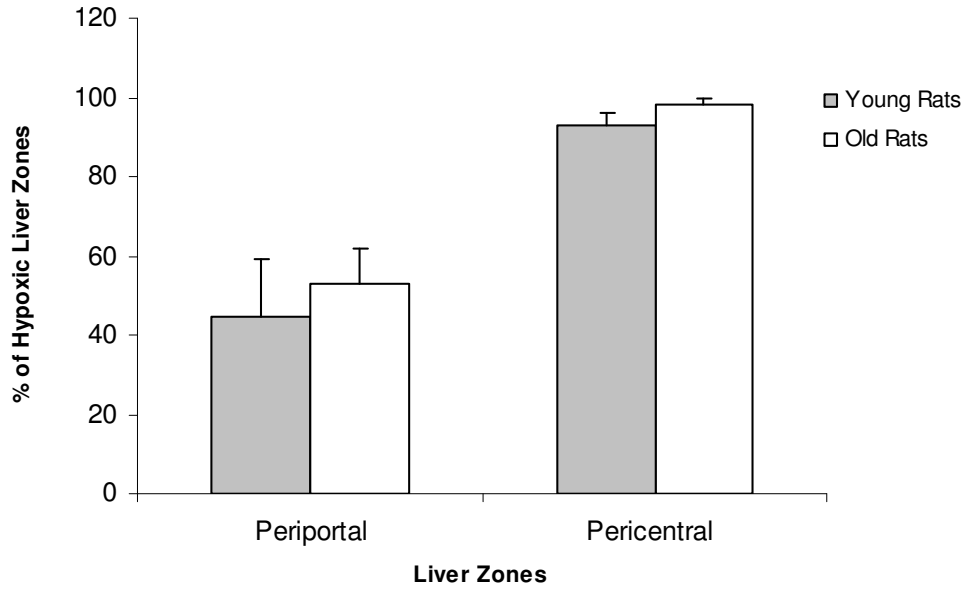

Figure 3.2. Pimonidazole immunohistochemistry of young and old rat livers

Pimonidazole immunohistochemistry (light microscopic sections 10×) in livers from: (A) Young F344 rat; (B) Old F344 rat; (C) Young Sprague Dawley rat; and (D) Young Sprague Dawley rat treated with poloxamer 407. There is zonal gradation of staining with increased intensity towards the pericentral regions, but no differential effect of ageing or poloxamer 407.

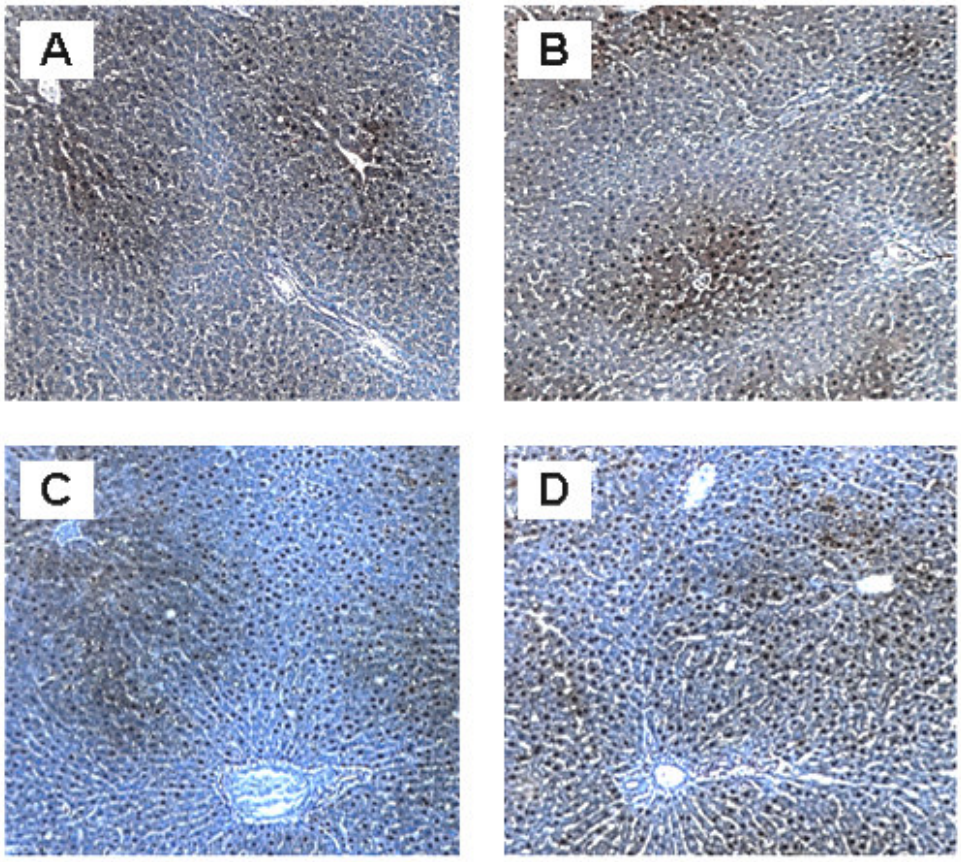

Figure 3.3. Quantification and comparison of pimonidazole and VEGF staining in livers from young and old rats

Quantification of pimonidazole (A) and VEGF (B) staining in livers from young and old rats shows a zonal gradient in intensity of staining from much less than + in the periportal region to about ++ (in a scale ranging over 0, +, ++, +++) in the pericentral zone. The intensity of pimonidazole and VEGF immunohistochemical staining in young and old rat livers are expressed in arbitrary units ± SEM. There was no statistically significant effect of age on the intensity of staining pimonidazole and VEGF.

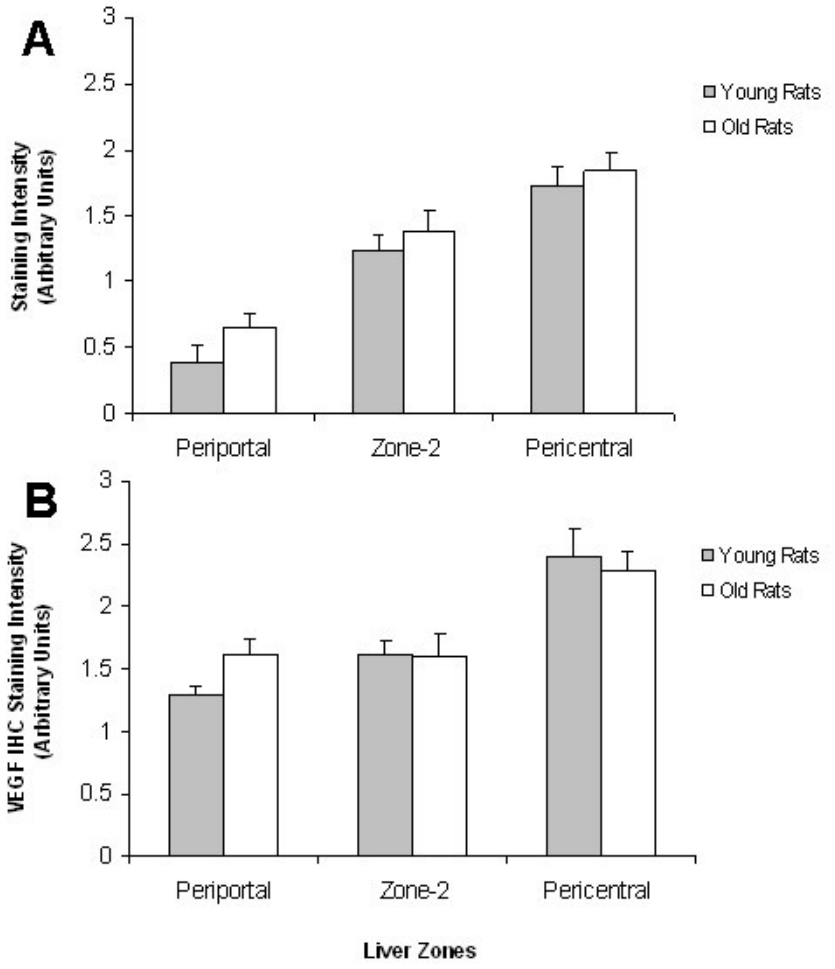

3.3.4. The effect of age on VEGFR2 expression

The intensity of sinusoidal and perisinusoidal staining for VEGFR2 was significantly increased ($P < 0.001$) in the livers from old F344 rats (2.5 ± 0.9; Fig. 3.4D, 3.4F; n = 6) when compared to livers from young F344 rats (1.1 ± 1.1; 3.4C, 3.4E; n = 4). On higher magnification (Fig 3.4E, 3.4F), it was observed that there is both increased diffuse staining in the LSECs and punctate expression along the sinusoids, possibly in LSECs or Kupffer cells or stellate cells.

3.3.5. Scanning electron microscopy

Total fenestration porosity was reduced in the old F344 rats (young 3.4 ± 1.2 %; n = 4 *versus* old 2.9 ± 1.5 %; n = 6), $P < 0.05$, as represented in Fig. 3.4A, 3.4B, with a trend towards reduction in fenestration diameter (young 75 ± 11 nm *versus* old 72 ± 11 nm, $P = 0.07$).

Poloxamer 407 reduced the porosity in Sprague Dawley rats (rats without poloxamer 407, 3.0 ± 1.7 %; n = 5 *versus* rats with poloxamer 407, 2.2 ± 1.0 %; n = 5), $P < 0.005$, as represented in Fig. 3.4C, 3.4D, with no statistically significant effect on diameter (80 ± 12 nm *versus* 77 ± 12 nm, $P = 0.2$).

Figure 3.4. Immunohistochemistry (light microscopic sections 10×) for VEGF and VEGFR2 in livers from young and old rats

Immunohistochemistry (light microscopic sections 10×) for VEGF in livers from young (A) and old (B) rats does not show any significant change. Immunohistochemistry for VEGFR2 shows in an increase in expression in old (D) *versus* young (C) livers. On higher magnification (40×), the increase in VEGFR2 expression appears to be related to an increase in staining in liver sinusoidal endothelial cells as well as punctate perisinusoidal staining in old (F) *versus* young (E) livers. The full arrow points to a stained sinusoid, the interrupted arrow to a stained stellate cell and the arrow-head to a cell displaying Kupffer cell morphology.

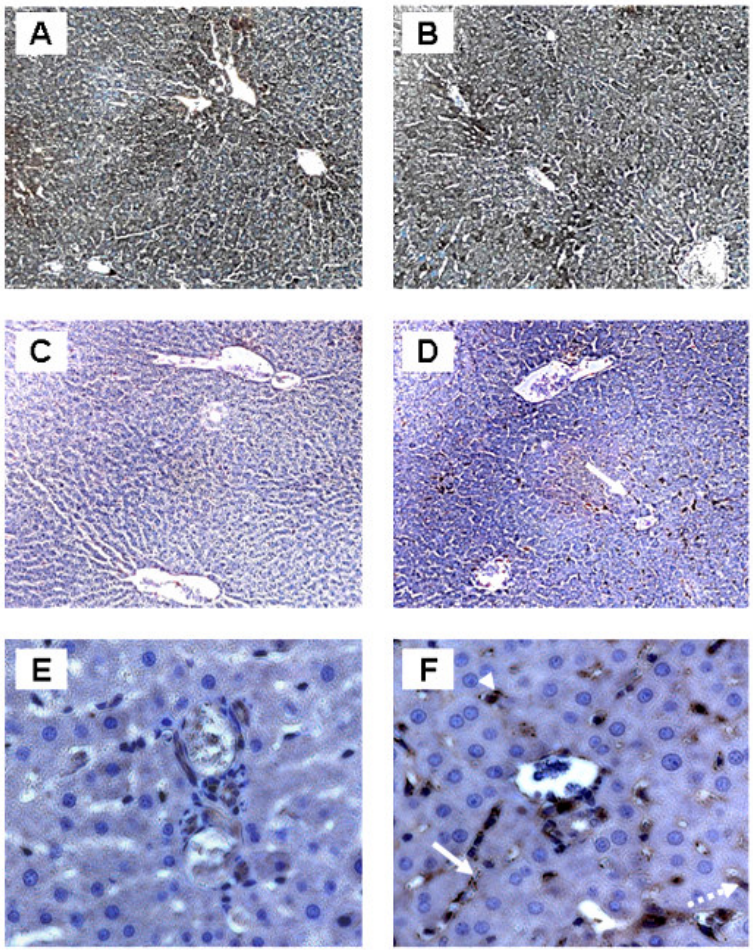

Figure 3.4. Scanning electron micrographs of sinusoids from livers from young and old rat livers as well as young rat livers untreated or treated with poloxamer 407

Scanning electron micrographs (25000×) of sinusoids from livers from young and old rat livers. There is a reduction in number of fenestrations (arrows) in young F344 rats (A) compared with old rats (B). Administration of poloxamer 407 reduced the number of fenestrations in young control Sprague Dawley rats: (C) Liver from control rat; (D) Liver from rat administered Poloxamer 407. The full arrow points at a sieve-plate circumscribing many fenestrations. The arrow-head indicates a single fenestration.

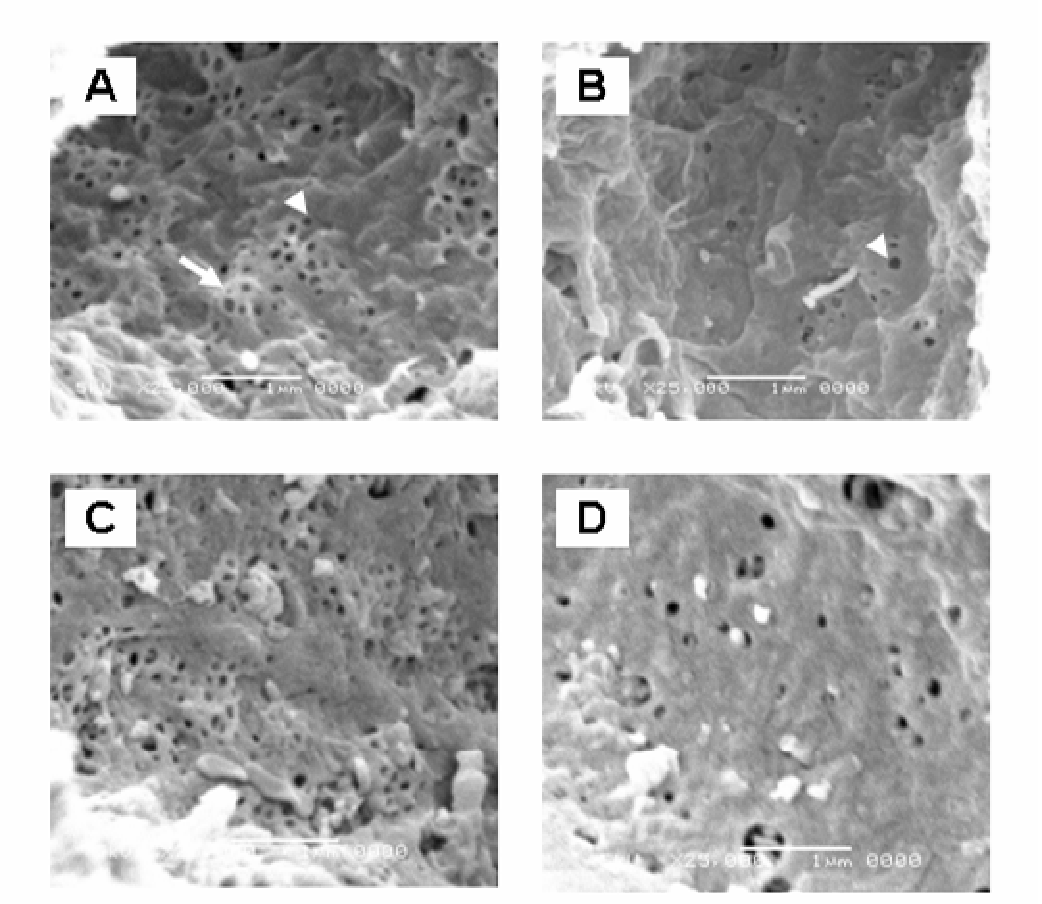

3.4. Discussion

The role of oxygen in ageing has been studied widely but primarily with respect to its role in free radical formation and oxidative stress. Tissue hypoxia secondary to vascular disease occurs with ageing (Katschinski, 2006). However there are also a few studies directly suggestive of impaired tissue oxygenation in old age. For example in the aged kidney, an increase in tissue hypoxia has been detected using pimonidazole staining (Tanaka et al, 2006). In the liver, indirect evidence for possible hypoxia comes from studies reporting lower levels of ATP measured in liver samples (Le Couteur et al, 2001; Selzner et al, 2007) and upregulation of hypoxia-responsive genes (Kang et al, 2005). It was suggested that age-related change in the in vivo activity of cytochrome P450 enzymes might be evidence of diminished hepatocyte oxygenation. Importantly it was hypothesized that age-related pseudocapillarization of the liver sinusoidal endothelium might impair oxygen diffusion from the blood to the hepatocytes (Le Couteur and McLean, 1998), somewhat similar to the oxygen limitation theory of cirrhosis of the liver (McLean and Morgan, 1991). However, in this study no evidence was found of intrahepatocytic hypoxia as assessed by pimonidazole immunohistochemistry. In addition the effects of the synthetic surfactant, poloxamer 407 which reduces fenestrations in the LSEC probably by coating the sinusoidal cell membrane (Cogger et al, 2006) was investigated. Although this induced a 30% reduction in fenestration porosity with poloxamer 407, it was not associated with any change in pimonidazole staining, indicating that convective flow of oxygen in plasma through fenestrations is not a rate-limiting step for hepatocyte oxygenation. These results do not support the concept of an oxygen diffusion barrier generated by age-related changes in the liver sinusoids or LSECs. Therefore, it can be

concluded that pseudocapillarization does not pose any significant barrier to oxygen uptake and that the age-related decline in ATP in the liver is most likely secondary to impaired mitochondrial function. The question arises as to alternate mechanisms for the age-related decrease in liver ATP levels. This is possibly attributable to decreased liver mass (Schmucker, 2001), mitochondrial oxidative stress (Sastre et al, 2003) or mitochondrial dysfunction (Sastre et al, 1996) in aged livers rather than intracellular hypoxia. The increased expression of HIF-1α and hypoxia-responsive genes observed earlier in the old rat liver (Kang et al, 2005) is unlikely to be secondary to hypoxia, and presumably is secondary to other age-related processes such as increased production of free radicals.

Pimonidazole has been used to assess hypoxia in many tissues including the liver (Arteel et al, 1997; Arteel et al, 1996; Arteel et al, 1995) and nitroimidazole staining becomes intense when cellular oxygen partial pressure falls below 10 mmHg (Gross et al, 1995). Most staining was in the pericentral region, with a clear gradient of intensity from the periportal to pericentral region. Most other studies in the normal liver have also shown staining confined to the pericentral region (Arteel et al, 1997; Arteel et al, 1995; Rosmorduc et al, 1999; Zhong et al, 2001), which is consistent with the loss of oxygen as blood flows down the hepatic sinusoid. Given that hypoxia is a potent stimulus for VEGF expression, it would be expected that there is a sinusoidal gradient in VEGF that corresponds with pimonidazole staining. Indeed increased VEGF expression was seen mostly in the pericentral hepatocytes, which are more hypoxic. There have been some similar reports (Corpechot et al, 2002; Maharaj et al, 2006; Turley et al, 1998), but also a few other reports that failed to find any such lobular gradient (Donahower et al, 2006; Ishikawa et al, 1999; Nyska et al, 2002). In

this study, the zonal gradation seen in VEGF expression (increasing from the periportal zone towards the pericentral zone *via* zone 2) is consistent with the zonal gradation in sinusoidal oxygenation evident in our pimonidazole immunohistochemical studies, as well as the metabolic zonal gradation observed in a number of previous studies (Jungermann and Kietzmann, 1996; Jungermann and Kietzmann, 2000).

The association between ageing and VEGF is of considerable interest because of the significant effects it has on new vessel growth. However, the effects of old age on VEGF expression are inconsistent, with reports in different tissues of both increased expression (Tanaka et al, 2006), and decreased expression (Di Giulio et al, 2005; Picciotti et al, 2004; Ryan et al, 2006). In the liver VEGF is especially important because of its effects on the LSEC and fenestrations. Hepatocytes produce VEGF and the LSECs express both VEGF receptors, VEGFR1 (Flt-1) and VEGFR2 (KDR/Flk-1) where VEGFR2 is the main receptor mediating permeability effects and is expressed only on endothelial cells (Ferrara, 2002; Funyu et al, 2001; LeCouter et al, 2003). Treatment of LSECs with VEGF increases fenestrations two- to fourfold (Funyu et al, 2001; Yokomori et al, 2003). On the other hand genetic downregulation of VEGFR2 causes a loss of endothelial lining (Gerber et al, 1999) and disrupted sinusoids with reduced numbers of fenestrations (Carpenter et al, 2005). Old age is associated with marked changes in the LSEC that have been called 'pseudocapillarization' (Le Couteur et al, 2001), including increased thickness of the LSEC, reduced fenestrations and altered expression of various endothelial antigens and stains (Cogger et al, 2003; Le Couteur et al, 2001; McLean et al, 2003). Therefore it was plausible that any age-related reduction in VEGF production by hepatocytes

might be important in the pathogenesis of pseudocapillarization. Using Western blotting and RT-PCR, it has been reported that VEGF expression is increased in old age in the rat (Kang et al, 2005). However, age-related changes in VEGF in the liver were not seen using immunohistochemistry. Whether VEGF is unchanged or increased in old age, age-related pseudocapillarization is not secondary to a reduction in VEGF production by hepatocytes in old age.

However, there was an increase in the sinusoidal expression of VEGFR2 in the old livers and almost no expression in the livers of young animals. The expression in the old livers was evident as diffuse staining along the sinusoids almost certainly within the LSECs and there was also some perisinusoidal punctate staining. VEGFR2 is found exclusively in endothelial cells (Quinn et al, 1993) and in the normal liver, VEGFR2 is expressed mostly in the larger vessels, however becomes expressed in the LSECs following partial hepatectomy. Recently stellate cells have been reported to express both VEGF receptors with upregulation of VEGFR1 following hypoxic stimuli (Ankoma-Sey et al, 2000). Our results indicate that old age is also associated with upregulation of VEGFR2 in the LSEC. The punctate staining might represent either karyomegalic endothelial cells (Nyska et al, 2002), or stellate cells which are increased and fat-engorged in old age (Tanuma and Ito, 1978; Vollmar et al, 2002; Warren et al, 2005; Yokoi et al, 1984), or Kupffer cells (Yamaguchi et al, 2000). The effects of age on VEGFR2 expression have rarely been reported. Expression was reported to be unchanged in the inner ear (Picciotti et al, 2004) and increased in the corpus cavernosum (Neves et al, 2006). In the liver, genetic downregulation of VEGFR2 is associated with defenestration (Carpenter et al, 2005) therefore it is unlikely that the age-related increase in VEGFR2 expression is involved in the

pathogenesis of pseudocapillarization where fenestrations are reduced in size and probably diameter (Le Couteur et al, 2001; McLean et al, 2001). On the other hand, it is possible that the increase in VEGFR2 is a compensatory response, perhaps attempting to increase fenestrations in response to pseudocapillarization.

Finally the effect of ageing on ATP levels in LSECs was determined. Previously a reduction of ATP in whole liver homogenates has been seen (Le Couteur et al, 2001). Furthermore, we also found that depletion of ATP by antimycin A caused a marked loss of fenestrations in isolated LSECs (Braet et al, 2003). Here we found that old age was not associated with any reduction in ATP levels in isolated LSECs. It should be noted that the isolation and culture of LSECs may have differential effects in old age and the measurement of ATP in isolated LSECs may not represent levels seen in vivo. Even so, our results suggest that mitochondrial function is reasonably well preserved in old age in this cell type and that ATP depletion is unlikely to be a contributory factor in the development of pseudocapillarization.

In conclusion, old age is not associated with hepatocyte hypoxia, LSEC ATP depletion or changes in VEGF expression. However, VEGFR2 expression along the sinusoids is increased. Therefore age-related reduction in liver ATP levels is more likely secondary to mitochondrial dysfunction rather than deficits in oxygen delivery. There are no changes in LSEC ATP and hepatocyte production of VEGF that would contribute to the pathogenesis of pseudocapillarization of the LSEC. The increase in VEGFR2 may reflect a response to age-related pseudocapillarization.

Table 3.1. Possible mechanisms and outcomes of age-related hepatic pseudocapillarization

Parameters altered with age Reviewed in (Le Couteur et al, 2008)	**Relevant citations**	**Possible mechanisms** Reviewed in (Le Couteur et al, 2006)	**Relevant citations**
Lipoprotein uptake and metabolism	(Hilmer et al, 2005)	Primary ageing	(Le Couteur et al, 2001)
Protein and drug uptake	(Brouwer et al, 1985; Ito et al, 2007)	Systemic vascular disease	(Lakatta, 2003)
Endocytosis	(Ito et al, 2007)	Mitochondrial parameters	(Sastre et al, 2000)
Immunotolerance	(Hilmer et al, 2007; Ito et al, 2007)	Dietary factors	(Clark et al, 1988; Fraser et al, 1995)
Normal adhesion molecule expression	(Ito et al, 2007; Le Couteur et al, 2001)	Age-related vascular inflammation	(Brod, 2000; Hager et al, 1994; Paolisso et al, 1998)
Normal hepatic perfusion	(Brouwer et al, 1985; Ito et al, 2007)	Gram-negative bacterial toxic and immune insult	This study , (Dobbs et al, 1994)
		Occult liver disease	

Chapter 4

Scanning electron microscopic analysis of two models of altered liver sinusoidal porosity: Diabetes mellitus 1 and Calorie-restriction

4. Scanning electron microscopic analysis of two models of liver sinusoidal porosity intervention: Diabetes mellitus 1 model and Calorie-restriction model

These two studies were led by Dr. Hamish Jamieson. My contribution to these studies was to process baboon and rat liver specimens, perform scanning electron microscopy on processed liver specimens, scanning electron micrograph morphometry and statistical analysis. These components were pivotal to the studies.

4.1. Scanning electron microscopic analysis of baboon livers: Diabetes mellitus 1 model

4.1.1. Introduction

Though diabetes mellitus is associated with extensive vascular pathology, little is known about its long-term effects on the liver sinusoidal endothelial cell (LSEC). Potential diabetic changes in the LSEC are important because of the role of fenestrations in the LSEC on the hepatic disposition of lipoproteins. The vascular complications of diabetes mellitus are well established and have major clinical significance (Singleton et al, 2003). However, little is known about the effects of diabetes mellitus on the hepatic microvasculature. In the introductory chapter of this thesis, the hepatic microvasculature was described to encompass innumerable porous web-like sinusoids that connect afferent portal triads to exiting central hepatic venules. These sinusoids form the rich capillary network of the liver, permitting the copious hepatic blood flow to flow slowly and intimately between the hepatocyte layers (Fraser et al, 1995; Le Couteur et al, 2005). In diabetes mellitus, LSEC fenestrations appear to act as conduits for the transfer of some lipoproteins, especially chylomicron remnants, between the blood and hepatocytes (Fraser et al, 1995; Le Couteur et al, 2002). In old age, there is a substantial loss of fenestrations in the LSEC (Cogger et al, 2003; Le Couteur et al, 2001; McLean et al, 2003; Warren et al, 2005), which impairs lipoprotein transfer to the hepatocyte (Hilmer et al, 2005). This provides a mechanism for age-related impairment in chylomicron remnant clearance and post-prandial hypertriglyceridemia, and thus might contribute to the enhanced vascular risk of older people (Le Couteur et al, 2002). As such, there are potential

parallels with dyslipidemia in diabetes mellitus (Adiels et al, 2006; Battula et al, 2000; Mamo et al, 1993). The paucity of research into the effects of diabetes mellitus on the LSEC probably reflects the considerable risk of liver biopsy in humans. Furthermore, many experimental animal models do not fully reflect the metabolic changes seen in humans with diabetes mellitus (Goldberg and Dansky, 2006; Heffernan et al, 1995). The Australian National Primate colony has a long established non-human primate colony (*Papio hamadryas*) in which type 1 diabetes mellitus was induced using streptozotocin administered at an average two years of age (Heffernan et al, 1995). Streptozotocin destroys the insulin secreting beta cells of the pancreas and creates a hypoinsulinemic, hyperglycaemic state that is similar to type 1 diabetes mellitus (Rees and Alcolado, 2005). In many animal models, streptozotocin-induced diabetes mellitus has been shown to closely resemble that seen in humans (Heffernan et al, 1995) and is generally considered to be an excellent model for the study of type 1 diabetes (Szkudelski, 2001). The hyperglycaemia in these baboons is partly controlled with once daily insulin injections to avoid weight loss and it has been possible to obtain a degree of control of type 1 diabetes similar to that in less well controlled humans with type 1 diabetes (Heffernan et al, 1995). The diabetic baboons have non-diabetic aged-matched controls. Previous data from this same baboon colony from the kidney and peripheral nerves has led the researchers to the conclusion that the structural and functional changes are similar to those seen in human diabetes and different from that of diabetic rats (Birrell et al, 2002; Heffernan et al, 1996). In this study, open liver biopsies from diabetic baboons and age-matched controls were obtained in order to study the effects of chronic, insulin-treated type 1 diabetes mellitus on the ultrastructure of the hepatic microvasculature. The key objective of this study was to determine whether diabetes mellitus influences fenestrations in the

LSEC because of potential mechanistic implications for diabetic dyslipidemia. Surgical liver biopsies for electron microscopy were obtained from baboons with long-standing streptozotocin-induced and insulin-treated diabetes mellitus and compared with age-matched controls using scanning electron microscopy.

4.1.2. Materials and methods

4.1.2.1. Animal protocols and specimen collection

Baboons (*Papio hamadryas*) were recruited from the National Baboon Colony, Sydney, Australia. The animals are members of a breeding colony of *P. hamadryas*. Streptozotocin (60mg/kg, intravenous) had been injected into the baboons at an average two years of age to create a diabetic state (Birrell et al, 2002; Heffernan et al, 1996; Heffernan et al, 1995). Capillary blood glucose levels are measured second daily in the diabetic baboons and subcutaneous insulin (human regular and ultralente, approximately a total of 4 units) is administered daily according to the trend of glucose levels and the glycated hemoglobin (HbA1c) level. The overall target levels are a random plasma glucose level of 15 to 30 mmol/L and HbA1c level from 8.0 to 10.0%, reflecting sub-optimally controlled human type 1 diabetes. All animals are housed in family groups and are fed a standard diet and are under the supervision of experienced veterinarians. Ethics approval for this procedure was obtained from the Central Sydney Area Health Service Animal Welfare Ethics Committee and in accordance with the Principles of Laboratory Animal Care (NIH Publication 85-23, revised 1985). Four diabetic baboons aged ten to fifteen years, with diabetes duration of approximately 10 yrs, were randomly chosen from the colony. Four non-diabetic control animals were matched with the diabetic baboons based on age and body weight. They were fasted on the night before the procedure. Intramuscular ketamine was used to induce general anaesthesia. A 1 cm^3 open liver biopsy was taken by an experienced human and primate surgeon. Approximately one third of the liver biopsy was fixed in 4% phosphate buffered paraformaldehyde. The remaining liver was

perfusion-fixed for electron microscopy as previously published (Cogger et al, 2003). An aliquot (1-2 ml) of fixative (2% glutaraldehyde and 3% paraformaldehyde in 0.1 M sodium cacodylate buffer 0.1 M sucrose, 2 mM $CaCl_2$) was injected slowly into the liver sample using a 25G needle until the tissue hardened.

4.1.2.2. Scanning electron microscopy

Fixed liver tissue was treated with 1% osmium, dehydrated in an ethanol gradient to and incubated for ten minutes in hexamethyldisilazane (Sigma, St Louis, MO). Samples were mounted, and then splutter-coasted with gold. Specimens were visualized using a Joel JSM 6380 scanning electron microscope. Twelve random sinusoids, at 25000 times magnification, were photographed from each liver. All scanning electron micrographs were analysed using ImageJ (http://rsb.info.nih.gov/ij/) to determine endothelial porosity, average fenestration diameter and fenestration density.

4.1.2.3. Statistics

Results are expressed as mean ± standard error of the mean. Comparisons of the blood results and electron microscopy data were performed using either the Students t-test or Mann-Whitney rank sum test for nonparametric data. Differences were considered significant when $P < 0.05$.

4.1.3. Results

4.1.3.1. Age, weights and blood results

Diabetic and control animals were well matched for body weight and age (Table. 4.1). Fasting bloods showed significantly elevated HbA1c and glucose in the diabetic group. Plasma triglyceride levels were increased substantially ($P < 0.05$).

Table 4.1. Age, weight and blood tests for control and diabetic baboons

	Controls	**Diabetics**	***P* Value**
Age (years)	12.8 ± 2.21	12.8 ± 2.0	ns
Weight (kilograms)	22.3 ± 1.2	21.2 ± 2.7	ns
Glycated haemoglobin (%)	3.6 ± 0.25	7.8 ± 0.7	P < 0.05
Random plasma glucose (mmol/L)	9.2 ± 2.2	31 ± 6.2	P < 0.05
Cholesterol (mmol/L)	2.3 ± 0.4	2.8 ± 0.2	P < 0.05
Triglycerides (mmol/L)	0.3 ± 0.1	2.3 ± 0.65	P < 0.05

Fasting bloods showed statistically significantly elevation of HbA1c, glucose and triglyceride.

4.1.3.2. Scanning electron microscopy

The porosity of the LSECs was significantly reduced to nearly one half in the diabetic livers (1.4 ± 0.1% *versus* 2.6 ± 0.2%, P < 0.01, Table. 4.2, Fig. 4.1). This was secondary to both a reduction in fenestration diameter and frequency.

Table 4.2. Ultrastructural sinusoidal changes in control *versus* diabetic baboons

	Controls	**Diabetics**	***P* Value**
Porosity (%)	2.6 ± 0.2	1.4 ± 0.1	< 0.01
Fenestration diameter (nm)	50 ± 1	43 ± 1	< 0.01
Fenestration frequency (per μm^2)	12.1 ± 0.8	7.8 ± 0.8	< 0.01

Figure 4.1. Scanning electron microscope images of liver sinusoids of diabetic and age-matched control baboons

Scanning electron microscope images (20000×) of liver sinusoids in diabetic baboon (A) and age-matched control (B). There are fewer fenestrations (→) in the diabetic livers.

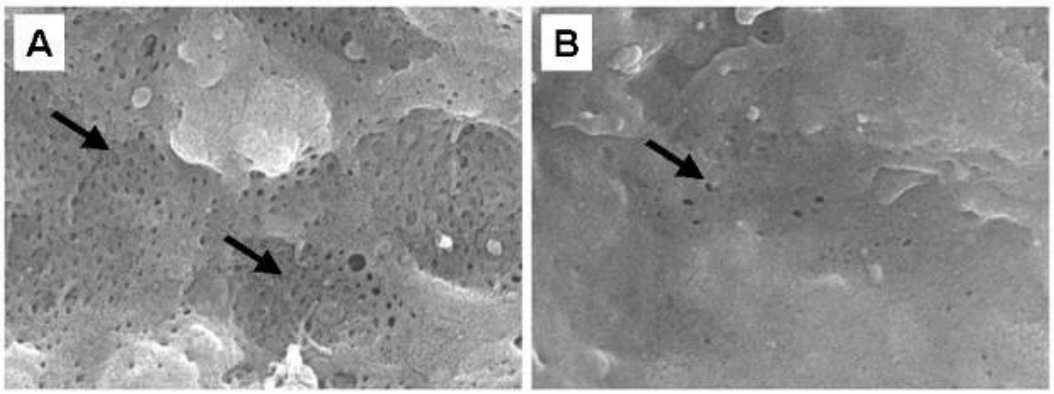

Sinusoidal porosity in diabetic rat livers was reduced to nearly 50% of the age- and weight- matched controls ($P < 0.01$). This was secondary to both a reduction in fenestration diameter and frequency.

4.1.4. Discussion

The streptozotocin-induced diabetic *Papio hamadryas* baboon colony has proven to be a very useful animal model for the study of type 1 diabetes mellitus (Birrell et al, 2002; Heffernan et al, 1996; Heffernan et al, 1995). In this study, data are presented from middle-aged baboons (approximately 13 yrs of age compared with maximum life expectancy of 25-30 yrs) that have been treated with insulin for over a decade. Blood results revealed the expected features of diabetes mellitus such as elevated glucose, HbA1c and markedly elevated triglycerides.

This study focused on the effects of diabetes on the LSEC because recent reports indicate an association between pathological changes in the LSEC and dyslipidemia (Fraser et al, 1995; Hilmer et al, 2005; Le Couteur et al, 2002). In the diabetic livers, the porosity of fenestrations was reduced by about 50%. These are substantial changes and are of a similar magnitude to those reported in old age (Cogger et al, 2003; Le Couteur et al, 2001; McLean et al, 2003; Warren et al, 2005). The ultrastructural changes noted confirm that diabetes mellitus is associated with significant changes in the hepatic sinusoid and LSEC.

Although the microvascular complications of diabetes mellitus are well established (Singleton et al, 2003), there have been few previous reports of the effects of diabetes mellitus on the hepatic microvasculature or that have specifically studied LSEC fenestrations. Berneau and colleagues (Bernuau et al, 1982) studied liver biopsies of 12 insulin-dependent diabetic patients aged 23-56 years. Moderate increases in collagen and basal lamina deposition in the space of Disse were reported compared

with slightly younger subjects with unconjugated hyperbilirubinemia (aged 31-42 yrs). Perisinusoidal deposition of collagen was noted, both in the diabetic and non-diabetic BB rats (Bernuau et al, 1985). In both these reports, the endothelial cells were stated to be unaffected. On the other hand, a pilot scanning electron microscopy study of rats 8 months after administration of streptozotocin found a small but significant increase in fenestration diameter and a reduction in fenestration frequency (Jamieson et al, 2001).

This study demonstrates that diabetes mellitus is associated with liver sinusoidal defenestration. This has potential implications for liver function, particularly the hepatic clearance of lipoproteins such as chylomicron remnants (Fraser et al, 1995). One of the initial steps in the metabolism of lipoproteins is that chylomicron remnants pass through fenestrations into the Space of Disse for receptor-mediated uptake and subsequent processing in hepatocytes. This study demonstrated the strong association between loss of porosity and loss of fenestrations with impaired lipoprotein transfer across the liver sinusoidal endothelium. Lipoproteins of an average diameter of 56 nm freely cross the liver endothelium in young rats. However defenestration associated with old age (Hilmer et al, 2005) and treatment with a surfactant, poloxamer 407 (Cogger et al, 2006) is associated with impaired transfer of lipoproteins and hypertriglyceridemia. Delayed chylomicron remnant clearance and subsequent postprandial hypertriglyceridemia are features of type I diabetes (Adiels et al, 2006; Battula et al, 2000; Mamo et al, 1993). It is thus possible that the substantial loss of fenestrations may contribute to this dyslipidemia. A possible explanation as to the cause of these changes involves oxidative stress, which is increased in diabetes

(Ceriello, 2006), also has marked effects on the structure of the LSEC (Cogger et al, 2001; Cogger et al, 2004).

In conclusion, there are significant diabetes-related hepatic microvascular changes, namely defenestration of the liver sinusoidal endothelium. Such changes are likely to have a significant effect on liver function and the clearance of many components of the blood, including lipoproteins. This could contribute to the pathogenesis of systemic macrovascular disease associated with diabetes mellitus.

4.2. Scanning electron microscopic analysis of rat livers: Calorie-restriction model

4.2.1. Introduction

The implications of age-related impairment in liver function are well recognized (Le Couteur et al, 2005; Schmucker, 2005). One mechanism for this change is age-related alterations in the ultrastructure of the liver sinusoidal endothelium (Le Couteur et al, 2005). The liver sinusoidal endothelium of young adults is very thin and perforated by fenestrations. In old age, there is a 30-50% reduction in the area of the endothelium perforated by fenestrations ('porosity'). This is associated with increased endothelial thickness and extracellular matrix in the space of Disse, including collagen and basal lamina (Cogger et al, 2003; Le Couteur et al, 2001; McLean et al, 2003; Warren et al, 2005). All of these age-related changes have been termed age-related pseudocapillarization, reflecting the shift to a typical capillary morphology. The thickened endothelium and defenestration are likely to reduce the transfer of many substrates between the sinusoid and hepatocytes (Le Couteur et al, 2005), particularly lipoproteins (Hilmer et al, 2005; Le Couteur et al, 2002). It was recently shown that the loss of fenestrations in old age impedes the transfer of some lipoproteins from the blood to the hepatocytes, which provides a mechanism for age-related postprandial hypertriglyceridemia and impaired chylomicron remnant clearance (Hilmer et al, 2005; Huet and Villeneuve, 2005). Therefore it is of therapeutic interest to determine whether pseudocapillarization is preventable through the effects of caloric restriction (CR).

CR increases longevity and those physiological and pathological changes delayed by CR are generally considered to be an integral part of the ageing process (Ingram et al, 2004; Masoro, 2005; Sinclair, 2005). Reducing caloric intake delays the onset of age-related diseases and increase maximum lifespan by between 20% and 40% in many species (Everitt et al, 2005). CR influences lipoprotein profiles and the onset of vascular disease in animal models (Zhu et al, 2004) and similar effects have replicated in short term studies in humans (Heilbronn et al, 2006).

One mechanism for the effects of CR on lipoprotein metabolism and susceptibility to vascular disease might be related to its effects on the liver sinusoidal endothelium (Le Couteur et al, 2001). The liver sinusoidal endothelium is exquisitely sensitive to oxidative stress (Cogger et al, 2001; Cogger et al, 2004) and other toxic insults (McCuskey, 2006). Thus, it is plausible that the structure of the liver sinusoidal endothelium may be profoundly influenced by the quantity of the dietary load, with its concomitant oxidants and toxins delivered to it *via* the portal vein. The study described here assessed whether CR reduces age-related pseudocapillarization of the liver sinusoidal endothelium.

Since age-related hepatic pseudocapillarization may contribute to the pathogenesis of dyslipidemia and since CR is a powerful model for the study of ageing as it extends lifespan; assessment of the effects of CR on the hepatic sinusoid was done to determine whether pseudocapillarization is preventable. This may unravel a possible novel target for the prevention of age-related dyslipidemia.

4.2.2. Materials and methods

4.2.2.1. Animal protocols and specimen collection

Young (6 months) and old (24 month) CR and AL Fisher F344 rats were obtained from the National Institute on Aging (Baltimore, Maryland) derived from stock from the National Institutes of Health and Harlan Sprague Dawley Inc. The rats were specific pathogen free. They were barrier maintained with a 12-hour light/dark cycle and fed sterilized NIH 31 rat chow. CR was started at weaning and increased at 10% per week. Forty percent CR was reached at 2.5 months. The CR rats were then maintained on a 40% CR diet. The research had the ethical approval of the Animal Care and Users Committee of the National Institute on Aging.

The liver samples were obtained from these rats under anesthesia with pentobarbital (60 mg/kg, I.P.). Segments of the liver were perfused for 10 min with electron microscope fixative solution (3% glutaraldehyde, 2% paraformaldehyde, 2 mM calcium chloride, 1% sucrose in 0.1 M sodium cacodylate buffer). Following fixation, 1 mm^3 samples were taken, post-fixed, washed and then stored in 0.1M sodium cacodylate buffer at 4°C.

4.2.2.2. Scanning electron microscopy

Preparations of samples for scanning electron microscopy was performed as previously described (Cogger et al, 2003; Le Couteur et al, 2001; Warren et al, 2005). Fixed tissue was treated with 1% osmium tetroxide in 0.1 M sodium cacodylate buffer

for two hours, dehydrated in an ethanol gradient and treated for 10 minutes in hexamethyldisilazane (Sigma, St Louis, MO). Six random samples from each liver were sputter-coated with gold. Samples were examined using a Joel JSM 6380 Scanning electron microscope. Ten random sinusoids (magnification × 25000) were photographed from each liver. Analysis of porosity, fenestration diameter and fenestration frequency was made using the ImageJ image analysis program obtained from NIH (http://rsb.info.nih.gov/ij/). The total numbers of fenestrations counted in the scanning electron microscopic study were 2777 for young AL, 6291 young CR, 6290 for old AL and 5114 for old CR rats.

4.1.2.3. Statistics

Results of the image analysis are presented as the mean of the values for each field analyzed ± standard error of the mean. The P values reported are those derived from the Student-Newman-Keuls method if one-way ANOVA showed a significant difference ($P<0.05$) between the observations in the four groups. Two-way ANOVA was used to analyse the interaction between age and response to caloric restriction. Statistical calculations were performed using Sigmastat version 2.03 (SPSS Inc, CA).

4.2.3. Results

4.2.3.1. Animal particulars

The liver and body weights are shown in Table. 4.3. Liver weight was significantly lower in the CR rats both at 6 and 24 months of age. Five out of eleven old AL rats and one out of five old CR rat were excluded from all analyses because of the presence of an extensive myeloproliferative infiltrate in the liver and spleen with substantial splenomegaly that has been reported to occur very frequently in old F344 rats (Sass et al, 1975).

Table 4.3. Liver and body weights for the young and old, CR and AL F344 rats

Parameter	**Young AL (n=5)**	**Young CR (n=5)**	**Old AL (n=6)**	**Old CR (n=4)**
Body weight (g)	368 ± 12	214 ± 4	396 ± 21	291 ± 11
Liver weight (g)	10.9 ± 1.1	5.1 ± 0.4	13.1 ± 0.9	6.9 ± 0.6
Liver weight (% of body weight)	3.0 ± 0.2	2.4 ± 0.2	3.3 ± 0.1	2.4 ± 0.1

4.2.3.2. Scanning electron microscopy

The results of the image analysis of the electron microscopy are shown in Table 4.4 and representative micrographs are shown in Fig. 4.2. Old age was associated with reduced fenestration porosity in AL rats. CR rats had greater porosity than AL rats at both 6 and 24 months of age. Two-way ANOVA showed there was a significant difference between the four groups ($P<0.001$); both age and CR influenced porosity ($P<0.001$ for both); and age did not influence the response to CR (ns). The changes in fenestration porosity appeared to be mediated mostly by changes in the frequency of the fenestrations rather than their diameters (Table. 4.4).

Table 4.4. Scanning electron micrograph analysis of the effects of ageing and CR on the liver sinusoidal endothelium

Parameter	Young AL	Young CR	Old AL	Old CR
Porosity (%)	3.4 ± 0.3	4.3 ± 0.2	2.4 ± 0.1	3.9 ± 0.3
No. of Fenestrations/ μm^2	8.0 ± 0.6	10.8 ± 0.8	6.3 ± 0.4	10.9 ± 0.6
Fenestration Diameter (nm)	68 ± 1	67 ± 1	66 ± 2	62 ± 1

Old AL was significantly less than young AL ($P < 0.001$) and old CR ($P < 0.001$). Young CR was significantly greater than young AL ($P < 0.001$).

Figure 4.2. Scanning electron microscope images of sinusoids of young CR (YCR), young AL (YAL), old CR (OCR) and old AL (OAL) rats

Scanning electron micrographs (25000×) of livers from young CR (YCR), young AL (YAL), old CR (OCR) and old AL (OAL) rats. Old age was associated with reduced fenestration porosity in AL rats. CR rats had greater porosity than AL rats at both 6 and 24 months of age.

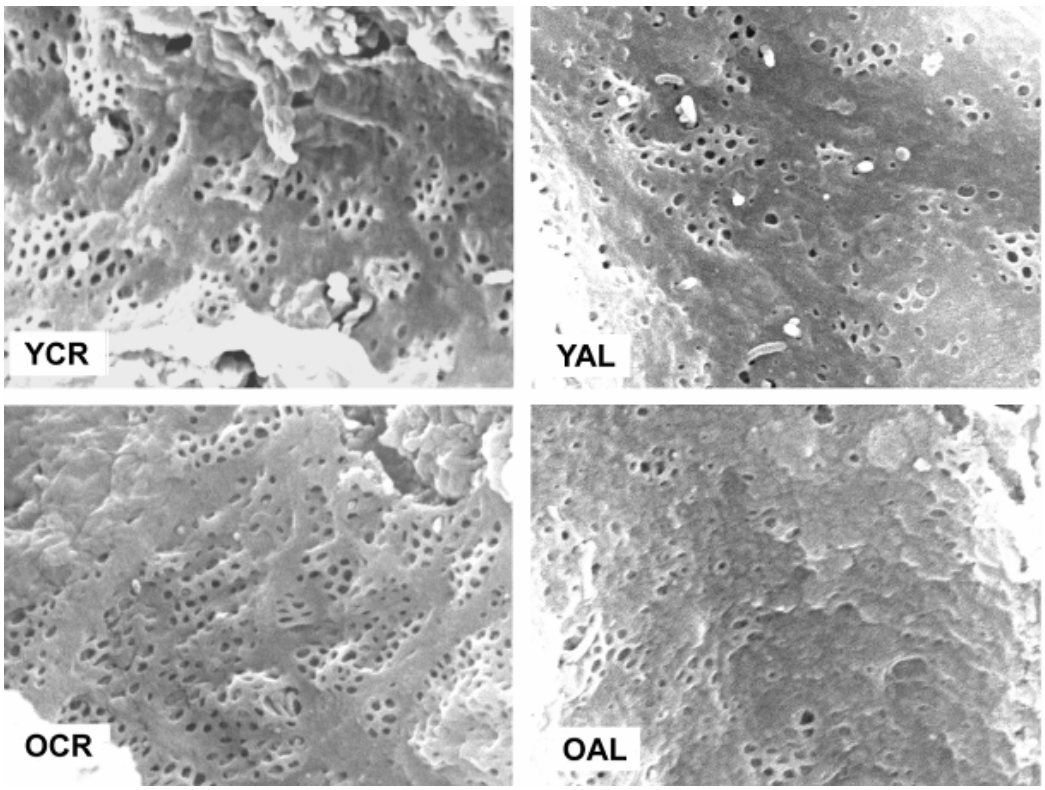

4.2.4. Discussion

The major findings of this study are: (1) confirmation of the presence of significant liver sinusoidal changes in old age in rats; (2) CR delays such changes at least until the age of 24 months; and (3) the effects of CR on the liver sinusoidal endothelial cell are apparent early in life.

Previous reports showing age-related changes ultrastructural changes in liver sinusoidal endothelium in rats (Le Couteur et al, 2001), non-human primates (Cogger et al, 2003), mice (Ito et al, 2005; Warren et al, 2005) and humans (McLean et al, 2003) were confirmed in this study. This study revealed that CR rats had a higher porosity at 24 months of age ($3.9 \pm 0.1\%$) compared to AL rats ($2.4 \pm 0.1\%$, $P<0.01$) implying that CR had a dramatic preserving effect on the morphological characteristics of young liver sinusoidal endothelium in terms of endothelial porosity. This provides a crucial mechanism for the effects of CR on lipids and vascular disease. One of the most important functions of fenestrations appears to be related to the transfer of chylomicrons remnants across the endothelium for subsequent hepatic metabolism (Fraser et al, 1986). This transfer of lipoproteins is very impaired in old age (Hilmer et al, 2005). The preservation of fenestrations by CR will presumptively be associated with improved hepatic clearance of chylomicron remnants and hence, less risk of developing systemic vascular disease.

The effects of CR on fenestration porosity were seen relatively early in the lifespan. At six months of age, fenestration porosity was significantly increased in the CR rats ($4.3 \pm 1.4\%$) compared to the AL rats ($3.4 \pm 1.5\%$, $P<0.01$).

In conclusion, ageing is associated with significant ultramicroscopic morphological changes in liver and CR prevents the age-related decreases in fenestration porosity indicating that these changes are intrinsically part of the ageing process. Intriguingly, CR resulted in a higher porosity than AL fed animals apparent even at 6 months, which suggests that the liver sinusoidal endothelium may contribute to the beneficial effects of CR in later life. Furthermore, the prevention of age-related pseudocapillarization by CR shows that it is a plausible therapeutic target for the amelioration or prevention of age-related dyslipidemia.

Chapter 5

Conclusions

5. Conclusions

The studies presented in this thesis underscore the pivotal role of the liver sinusoidal endothelium and fenestrations in the pathophysiology of bacterial toxin-induced injury as well as septicaemia-related, ageing-related and post-prandial hyperlipidemias. In addition the results suggest novel therapeutic strategies for these conditions.

In chapter 2, it was shown that pyocyanin treatment over a wide range of concentrations is associated with a substantial loss of LSEC porosity. Pyocyanin also induces significant acute changes in the *in vivo* liver sinusoidal endothelium without any morphological hepatocellular alterations including mitochondrial morphology and frequency or any other signs of hepatocyte injury or oxidative stress. These LSEC changes were not accompanied by evidence of structural, biochemical hepatocellular changes or changes in the fenestration constituent protein, caveolin-1. In addition, a decrease in endothelial thickness with pyocyanin was noted, a change that has not been reported with any other toxic injury to the LSEC. These findings indicate that the LSEC is initial site of injury induced by pyocyanin, and indeed may even have a role in protecting hepatocytes from endo- and xenobiotics. Damage to the liver sinusoids and LSECs induced by pyocyanin could impact graft outcome and prognosis following pseudomonal sepsis. The results also support the concept that hyperlipidemia associated with sepsis might in part be a result of LSEC defenestration.

In chapter 3, the hypothesis that age-related pseudocapillarization of the liver sinusoidal endothelium might impair oxygen diffusion from the blood to the hepatocytes was examined to account for the decreased phase 1 metabolism, decrease in ATP levels and increased expression of hypoxia-responsive genes in aged human and animal livers. Using pimonidazole immunohistochemistry for *in vivo* detection of tissue hypoxia, it was shown that age-related liver sinusoidal pseudocapillarization does not pose any significant barrier to oxygen uptake and that the age-related decline in ATP in the liver is most likely secondary to impaired mitochondrial function. In this study, the zonal gradation seen in VEGF expression was consistent with the zonal gradation of hepatic hypoxia. However, there was an increase in the sinusoidal expression of VEGFR2 in the old livers and almost no expression in the livers of young animals. It is possible that the increase in VEGFR2 is a compensatory response, perhaps attempting to increase fenestrations in response to pseudocapillarization.

In chapter 4, using a baboon model it was demonsrated that type 1 diabetes mellitus was associated with liver sinusoidal defenestration and therefore of significance for liver function, particularly the hepatic clearance of lipoproteins. Since delayed lipoprotein clearance and subsequent postprandial hypertriglyceridemia are features of type I diabetes, it is possible that the sinusoidal defenestration in diabetes mellitus may be an important mechanism. Such changes are likely to have a significant effect on liver function, blood lipoprotein clearance and the pathogenesis of systemic macrovascular disease in type 1 diabetes mellitus.

In chapter 4, using a CR rat model, it was shown CR prevents age-related decreases in fenestration porosity. CR also resulted in a higher porosity than AL fed animals very early on, which suggests that the liver sinusoidal endothelium may contribute to the beneficial effects of CR in later life. The prevention of age-related pseudocapillarization by CR shows that CR could be a plausible therapeutic target for the prevention or amelioration of dyslipidemia associated with ageing.

These studies examine the crucial role of the liver sinusoids and LSECs in pathogenesis of disease in bacterial infections and ageing. Future studies should aspire to evaluate LSEC fenestration biology and pathophysiological mechanisms for changes in fenestrations in disease and ageing. The ensuing data may permit development of potential therapeutic targets and agents that may prevent or alter LSEC fenestration morphology and pathology in various disease states, including sepsis, transplantation, diabetes mellitus and ageing.

References

1. Adiels, M., Olofsson, S.O., Taskinen, M.R., Boren, J., 2006. Diabetic dyslipidaemia. Curr Opin Lipidol 17, 238-46.

2. Aduen, J.F., Hellinger, W.C., Kramer, D.J., Stapelfeldt, W.H., Bonatti, H., Crook, J.E., Steers, J.L., Burger, C.D., 2005. Spectrum of pneumonia in the current era of liver transplantation and its effect on survival. Mayo Clin Proc 80, 1303-1306.

3. Ankoma-Sey, V., Wang, Y., Dai, Z., 2000. Hypoxic stimulation of vascular endothelial growth factor expression in activated rat hepatic stellate cells. Hepatology 31, 141-148.

4. Arias, I.M., 1990. The biology of hepatic endothelial cell fenestrae. Prog Liver Dis 9, 11-26.

5. Arteel, G.E., Iimuro, Y., Yin, M., Raleigh, J.A., Thurman, R.G., 1997. Chronic enteral ethanol treatment causes hypoxia in rat liver tissue in vivo. Hepatology 25, 920-6.

6. Arteel, G.E., Raleigh, J.A., Bradford, B.U., Thurman, R.G., 1996. Acute alcohol produces hypoxia directly in rat liver tissue in vivo: role of Kupffer cells. Am J Physiol 271, G494-500.

7. Arteel, G.E., Thurman, R.G., Raleigh, J.A., 1998. Reductive metabolism of the hypoxia marker pimonidazole is regulated by oxygen tension independent of the pyridine nucleotide redox state. Eur J Biochem 253, 743-50.

8. Arteel, G.E., Thurman, R.G., Yates, J.M., Raleigh, J.A., 1995. Evidence that hypoxia markers detect oxygen gradients in liver: pimonidazole and retrograde perfusion of rat liver. Brit J Cancer 72, 889-95.

9. Bannerman, D.D., Goldblum, S.E., 1999. Direct effects of endotoxin on the endothelium: barrier function and injury. Lab Invest 79, 1181-99.

10. Battula, S.B., Fitzsimons, O., Moreno, S., Owens, D., Collins, P., Johnson, A., Tomkin, G.H., 2000. Postprandial apolipoprotein B48-and B100-containing lipoproteins in type 2 diabetes: do statins have a specific effect on triglyceride metabolism? Metabolism 49, 1049-54.

11. Bernuau, D., Guillot, R., Durand, A.M., Raoux, N., Gabreau, T., Passa, P., Feldmann, G., 1982. Ultrastructural aspects of the liver perisinusoidal space in diabetic patients with and without microangiopathy. Diabetes 31, 1061-7.

12. Bernuau, D., Guillot, R., Durand-Schneider, A.M., Poussier, P., Moreau, A., Feldmann, G., 1985. Liver perisinusoidal fibrosis in BB rats with or without overt diabetes. Am J Pathol 120, 38-45.

13. Birrell, A.M., Heffernan, S.J., Kirwan, P., McLennan, S., Gillin, A.G., Yue, D.K., 2002. The effects of aminoguanidine on renal changes in a baboon model of Type 1 diabetes. J Diabetes Complications 16, 301-9.

14. Bouwens, L., 1988. Proliferation and phenotypic expression of non-parenchymal liver cells. Scand J Gastroenterol Suppl 151, 46-51.

15. Bouwens, L., 1988. Structural and functional aspects of Kupffer cells. Revis Biol Celular 16, 69-94.

16. Bouwens, L., De Bleser, P., Vanderkerken, K., Geerts, B., Wisse, E., 1992. Liver cell heterogeneity: functions of non-parenchymal cells. Enzyme 46, 155-68.

17. Bouwens, L., Marinelli, A., Kuppen, P.J., Eggermont, A.M., van de Velde, C.J., Wisse, E., 1990. Electron microscopic observations on the accumulation of large granular lymphocytes (pit cells) and Kupffer cells in the liver of rats treated with continuous infusion of interleukin-2. Hepatology 12, 1365-70.

18. Braet, F., De Zanger, R., Jans, D., Spector, I., Wisse, E., 1996. Microfilament-disrupting agent latrunculin A induces and increased number of fenestrae in rat liver sinusoidal endothelial cells: comparison with cytochalasin B. Hepatology 24, 627-35.

19. Braet, F., De Zanger, R., Sasaoki, T., Baekeland, M., Janssens, P., Smedsrod, B., Wisse, E., 1994. Assessment of a method of isolation, purification, and cultivation of rat liver sinusoidal endothelial cells. Lab Invest 70, 944-52.

20. Braet, F., Muller, M., Vekemans, K., Wisse, E., Le Couteur, D.G., 2003. Antimycin A-induced defenestration in rat hepatic sinusoidal endothelial cells. Hepatology 38, 394-402.

21. Braet, F., Spector, I., De Zanger, R., Wisse, E., 1998. A novel structure involved in the formation of liver endothelial cell fenestrae revealed by using the actin inhibitor misakinolide. Proc Natl Acad Sci U S A 95, 13635-40.

22. Braet, F., Spector, I., Shochet, N., Crews, P., Higa, T., Menu, E., de Zanger, R., Wisse, E., 2002. The new anti-actin agent dihydrohalichondramide reveals fenestrae-forming centers in hepatic endothelial cells. BMC Cell Biol 3, 7.

23. Braet, F., Wisse, E., 2002. Structural and functional aspects of liver sinusoidal endothelial cell fenestrae: a review. Compar Hepatol 1, 1-17.

24. Braet(a), F., De Zanger, R., Baekeland, M., Crabbe, E., Van Der Smissen, P., Wisse, E., 1995. Structure and dynamics of the fenestrae-associated cytoskeleton of rat liver sinusoidal endothelial cells. Hepatology 21, 180-189.

25. Braet(b), F., De Zanger, R., Crabbe, E., Wisse, E., 1995. New observations on cytoskeleton and fenestrae in isolated rat liver sinusoidal endothelial cells. J Gastroenterol Hepatol 10 Suppl 1, S3-7.

26. Britigan, B.E., Rasmussen, G.T., Cox, C.D., 1997. Augmentation of oxidant injury to human pulmonary epithelial cells by the Pseudomonas aeruginosa siderophore pyochelin. Infect Immun 65, 1071-1076.

27. Britigan, B.E., Roeder, T.L., Rasmussen, G.T., Shasby, D.M., McCormick, M.L., Cox, C.D., 1992. Interaction of the Pseudomonas aeruginosa secretory products pyocyanin and pyochelin generates hydroxyl radical and causes synergistic damage to endothelial cells. Implications for Pseudomonas-associated tissue injury. J Clin Invest 90, 2187-2196.

28. Brod, S.A., 2000. Unregulated inflammation shortens human functional longevity. Inflamm Res 49, 561-70.

29. Brouwer, A., Barelds, R.J., Knook, D.L., 1985. Age-related changes in the endocytic capacity of rat liver Kupffer and endothelial cells. Hepatology 5, 362-6.

30. Brown, A.P., Schultze, A.E., Holdan, W.L., Buchweitz, J.P., Roth, R.A., Ganey, P.E., 1996. Lipopolysaccharide-induced hepatic injury is enhanced by polychlorinated biphenyls. Environ Health Perspect 104, 634-40.

31. Carpenter, B., Lin, Y., Stoll, S., Raffai, R.L., McCuskey, R., Wang, R., 2005. VEGF is crucial for the hepatic vascular development required for lipoprotein uptake. Development 132, 3293-3303.

32. Ceriello, A., 2006. Controlling oxidative stress as a novel molecular approach to protecting the vascular wall in diabetes. Curr Opin Lipidol 17, 510-8.

33. Charels, K., De Zanger, R.B., Van Bossuyt, H., Van Ver Smissen, P., Wisse, W., 1986. Influence of acute alcohol administration on endothelial fenestrae of rat livers. Cells of the Hepatic Sinusoid 1, 497-502.

34. Chen, J., Braet, F., Brodsky, S., Weinstein, T., Romanov, V., Noiri, E., Goligorsky, M.S., 2002. VEGF-induced mobilization of caveolae and increase in permeability of endothelial cells. Am J Physiol 282, C1053-63.

35. Cho, C.S., McLean, A.J., Rivory, L.P., Gatenby, P.A., Hardman, D.T., Le Couteur, D.G., 2001. Carbon monoxide wash-in method to determine gas transfer in vascular beds: application to rat hind limb. Am J Physiol 280, H1802-1806.

36. Clark, S.A., Angus, H.B., Cook, H.B., George, P.M., Oxner, R.B., Fraser, R., 1988. Defenestration of hepatic sinusoids as a cause of hyperlipoproteinaemia in alcoholics. Lancet 2, 1225-7.

37. Cogger, V.C., Hilmer, S.N., Sullivan, D., Muller, M., Fraser, R., Le Couteur, D.G., 2006. Hyperlipidemia and surfactants: the liver sieve is a link. Atherosclerosis 189, 273-281.

38. Cogger, V.C., Le Couteur, D.G., 2008. Fenestrations. The Liver: Biology and Pathobiology 5.

39. Cogger, V.C., Mross, P.E., Hosie, M.J., Ansselin, A.D., McLean, A.J., Le Couteur, D.G., 2001. The effect of acute oxidative stress on the ultrastructure of the perfused rat liver. Pharmacology & Toxicology 89, 306-311.

40. Cogger, V.C., Muller, M., Fraser, R., McLean, A.J., Khan, J., Le Couteur, D.G., 2004. The effects of oxidative stress on the liver sieve. Journal of Hepatology 41, 370-376.

41. Cogger, V.C., Warren, A., Fraser, R., Ngu, M., McLean, A.J., Le Couteur, D.G., 2003. Hepatic sinusoidal pseudocapillarization with aging in the non-human primate. Experimental Gerontology 38, 1101-1107.

42. Copple, B.L., Moulin, F., Hanumegowda, U.M., Ganey, P.E., Roth, R.A., 2003. Thrombin and protease-activated receptor-1 agonists promote

lipopolysaccharide-induced hepatocellular injury in perfused livers. J Pharmacol Exp Ther 305, 417-25.

43. Corpechot, C., Barbu, V., Wendum, D., Kinnman, N., Rey, C., Poupon, R., Housset, C., Rosmorduc, O., 2002. Hypoxia-induced VEGF and collagen I expressions are associated with angiogenesis and fibrogenesis in experimental cirrhosis. Hepatology 35, 1010-21.

44. Couetil, J.P., Houssin, D.P., Soubrane, O., Chevalier, P.G., Dousset, B.E., Loulmet, D., Achkar, A., Tolan, M.J., Amrein, C.I., Guinvarch, A., et al., 1995. Combined lung and liver transplantation in patients with cystic fibrosis. A 4 1/2-year experience. J Thorac Cardiovasc Surg 110, 1415-22; discussion 1422-3.

45. Cuervas-Mons, V., Julio Martinez, A., Dekker, A., Starzl, T.E., Van Thiel, D.H., 1986. Adult liver transplantation: an analysis of the early causes of death in 40 consecutive cases. Hepatology 6, 495-501.

46. Deaciuc, I.V., Spitzer, J.A., 1987. Calcium content in liver and heart and its intracellular distribution in liver during endotoxicosis and sepsis in rats. Cell Calcium 8, 365-76.

47. Deleve, L.D., 2007. Hepatic microvasculature in liver injury. Semin Liver Dis 27, 390-400.

48. Di Giulio, C., Bianchi, G., Cacchio, M., Artese, L., Rapino, C., Macri, M.A., Di Ilio, C., 2005. Oxygen and life span: chronic hypoxia as a model for studying HIF-1alpha, VEGF and NOS during aging. Respir Physiol Neurobiol 147, 31-8.

49. Dobbs, B.R., Rogers, G.W., Xing, H.Y., Fraser, R., 1994. Endotoxin-induced defenestration of the hepatic sinusoidal endothelium: a factor in the pathogenesis of cirrhosis? Liver 14, 230-233.

50. Donahower, B., McCullough, S.S., Kurten, R., Lamps, L.W., Simpson, P., Hinson, J.A., James, L.P., 2006. Vascular endothelial growth factor and hepatocyte regeneration in acetaminophen toxicity. Am J Physiol Gastrointest Liver Physiol 291, G102-9.

51. Doria, C., Marino, I.R., 2005. Bacteremia using the molecular adsorbent recirculating system in patients bridged to liver transplantation. Exp Clin Transplant 3, 289-92.

52. Enomoto, N., Ikejima, K., Bradford, B.U., Rivera, C.A., Kono, H., Goto, M., Yamashina, S., Schemmer, P., Kitamura, T., Oide, H., Takei, Y., Hirose, M., Shimizu, H., Miyazaki, A., Brenner, D.A., Sato, N., Thurman, R.G., 2000. Role of Kupffer cells and gut-derived endotoxins in alcoholic liver injury. J Gastroenterol Hepatol 15 Suppl, D20-5.

53. Enomoto, N., Schemmer, P., Ikejima, K., Takei, Y., Sato, N., Brenner, D.A., Thurman, R.G., 2001. Long-term alcohol exposure changes sensitivity of rat Kupffer cells to lipopolysaccharide. Alcohol Clin Exp Res 25, 1360-7.

54. Enomoto, N., Takei, Y., Hirose, M., Kitamura, T., Ikejima, K., Sato, N., 2003. Protective effect of thalidomide on endotoxin-induced liver injury. Alcohol Clin Exp Res 27, 2S-6S.

55. Enomoto, N., Takei, Y., Yamashina, S., Fukuda, T., Suzuki, S., Ikejima, K., Kitamura, T., Sato, N., 2004. Burn injury sensitizes rat Kupffer cells via mechanisms dependent on gut-derived endotoxin. J Gastroenterol 39, 1175-81.

56. Esser, S., Wolburg, K., Wolburg, H., Breier, G., Kurzchalia, T., Risau, W., 1998. Vascular endothelial growth factor induces endothelial fenestrations in vitro. J Cell Biol 140, 947-59.

57. Everitt, A., Roth, G.S., Le Couteur, D.G., Hilmer, S.N., 2005. Calorie restriction versus drug therapy to delay the onset of aging diseases and extend life. Age 27, 1-10.

58. Ferrara, N., 2002. Role of vascular endothelial growth factor in physiologic and pathologic angiogenesis: therapeutic implications. Semin Oncol 29, 10-4.

59. Ferrara, N., 2004. Vascular endothelial growth factor: basic science and clinical progress. Endocr Rev 25, 581-611.

60. Ferrara, N., Gerber, H.P., LeCouter, J., 2003. The biology of VEGF and its receptors. Nat Med 9, 669-76.

61. Fetzer, A.E., Werner, A.S., Hagstrom, J.W., 1967. Pathologic features of pseudomonal pneumonia. Am Rev Respir Dis 96, 1121-1130.

62. Fraser, R., Bosanquet, A.G., Day, W.A., 1978. Filtration of chylomicrons by the liver may influence cholesterol metabolism and atherosclerosis. Atherosclerosis 29, 113-123.

63. Fraser, R., Bowler, L.M., Day, W.A., 1980. Damage of rat liver sinusoidal endothelium by ethanol. Pathology 12, 371-376.

64. Fraser, R., Bowler, L.M., Day, W.A., Dobbs, B., Johnson, H.D., Lee, D., 1980. High perfusion pressure damages the sieving ability of sinusoidal endothelium in rat livers. Br J Exp Pathol 61, 222-228.

65. Fraser, R., Clark, S.A., Bowler, L.M., Murray, F.E., Wakasugi, J., Ishihara, M., Tomikawa, M. The opposite effects of nicotine and pantethine on the porosity of the liver sieve and lipoprotein metabolism. In: Wisse E, Knook DL, Decker K, editors. Cells of the Hepatic Sinusoid. Rijswijk: Kupffer Cell Foundation; 1989. p. 335-338.

66. Fraser, R., Clark, S.A., Day, W.A., Murray, F.E., 1988. Nicotine decreases the porosity of the rat liver sieve: a possible mechanism for hypercholesterolaemia. Br J Exp Pathol 69, 345-50.

67. Fraser, R., Day, W.A., Fernando, N.S. Atherosclerosis and the liver sieve. In: Kirn A, Knook DL, Wisse E, editors. Cells of the Hepatic Sinusoid. Rijswijk: The Kupffer Cell Foundation; 1986. p. 317-322.

68. Fraser, R., Day, W.A., Fernando, N.S., 1986. The liver sinusoidal cells. Their role in disorders of the liver, lipoprotein metabolism and atherogenesis. Pathology 18, 5-11.

69. Fraser, R., Dobbs, B.R., Rogers, G.W., 1995. Lipoproteins and the liver sieve: the role of the fenestrated sinusoidal endothelium in lipoprotein metabolism, atherosclerosis, and cirrhosis. Hepatology 21, 863-874.

70. Fraser, R., Heslop, V.R., Murray, F.E., Day, W.A., 1986. Ultrastructural studies of the portal transport of fat in chickens. Br J Exp Pathol 67, 783-791.

71. Fraser, R., Rogers, G.W.T., Sutton, L.E., Dobbs, B.R. Single dose models of defenestration: tools to explore mechanisms, modulation and measurement of hepatic sinusoidal porosity. In: Wisse E, Knook DL, Wake K, editors. Cells of the hepatic Sinusoids. Leiden: Kupffer Cell Foundation; 1995. p. 263-266.

72. Froomes, P.R., Sachinidis, J., Ghabrial, H., Tochon-Danguy, H., Scott, A., Ching, M.S., Morgan, D.J., Angus, P.W., 2003. A novel method for determining hepatic sinusoidal oxygen permeability in the isolated perfused rat liver using [15O]O2. Nucl Med Biol 30, 93-100.

73. Funyu, J., Mochida, S., Inao, M., Matsui, A., Fujiwara, K., 2001. VEGF can act as vascular permeability factor in the hepatic sinusoids through upregulation of porosity of endothelial cells. Biochem Biophys Res Commun 280, 481-5.

74. Gaeta, G.B., Wisse, E., 1983. Endotoxin effect on the isolated perfused rat liver: functional and ultrastructural observations. J Submicrosc Cytol 15, 705-12.

75. Gao, W., Bentley, R.C., Madden, J.F., Clavien, P.A., 1998. Apoptosis of sinusoidal endothelial cells is a critical mechanism of preservation injury in rat liver transplantation. Hepatology 27, 1652-60.

76. Gatmaitan, Z., Varticovski, L., Ling, L., Mikkelsen, R., Steffan, A.M., Arias, I.M., 1996. Studies on fenestral contraction in rat liver endothelial cells in culture. Am J Pathol 148, 2027-41.

77. Gerber, H.P., Hillan, K.J., Ryan, A.M., Kowalski, J., Keller, G.A., Rangell, L., Wright, B.D., Radtke, F., Aguet, M., Ferrara, N., 1999. VEGF is required for growth and survival in neonatal mice. Development 126, 1149-59.

78. Goldberg, I.J., Dansky, H.M., 2006. Diabetic vascular disease: an experimental objective. Arterioscler Thromb Vasc Biol 26, 1693-701.

79. Gong, J.P., Dai, L.L., Liu, C.A., Wu, C.X., Shi, Y.J., Li, S.W., Li, X.H., 2002. Expression of CD14 protein and its gene in liver sinusoidal endothelial cells during endotoxemia. World J Gastroenterol 8, 551-4.

80. Gorgen, I., Hartung, T., Leist, M., Niehorster, M., Tiegs, G., Uhlig, S., Weitzel, F., Wendel, A., 1992. Granulocyte colony-stimulating factor treatment protects rodents against lipopolysaccharide-induced toxicity via suppression of systemic tumor necrosis factor-alpha. J Immunol 149, 918-24.

81. Gouvea, E.F., Branco, R.C., Monteiro, R.C., Halpern, M., Ribeiro-Filho, J., Silveira, V.G., Tavares, G.C., Rodrigues, M.S., Coelho, H.S., Basto, S.T., Santoro-Lopes, G., 2004. Outcome of infections caused by multiple drug-resistant bacteria in liver transplant recipients. Transplant Proc 36, 958-60.

82. Griffith, O.W., 1980. Determination of glutathione and glutathione disulfide using glutathione reductase and 2-vinylpyridine. Anal Biochem 106, 207-12.

83. Gross, M.W., Karbach, U., Groebe, K., Franko, A.J., Mueller-Klieser, W., 1995. Calibration of misonidazole labeling by simultaneous measurement of oxygen tension and labeling density in multicellular spheroids. Int J Cancer 61, 567-73.

84. Hager, K., Machein, U., Krieger, S., Platt, D., Seefried, G., Bauer, J., 1994. Interleukin-6 and selected plasma proteins in healthy persons of different ages. Neurobiol Aging 15, 771-772.

85. Harman, J.W., Macbrinn, M.C., 1963. The Effect of Phenazine Methosulphate, Pyocyanine and Edta on Mitochondrial Succinic Dehydrogenase. Biochem Pharmacol 12, 1265-1278.

86. Harris, H.W., Gosnell, J.E., Kumwenda, Z.L., 2000. The lipemia of sepsis: triglyceride-rich lipoproteins as agents of innate immunity. J Endotoxin Res 6, 421-430.

87. Hart, D.W., Chinkes, D.L., Gore, D.C., 2003. Increased tissue oxygen extraction and acidosis with progressive severity of sepsis. J Surg Res 112, 49-58.

88. Hart, D.W., Gore, D.C., Rinehart, A.J., Asimakis, G.K., Chinkes, D.L., 2003. Sepsis-induced failure of hepatic energy metabolism. J Surg Res 115, 139-47.

89. Hassan, H.M., Fridovich, I., 1980. Mechanism of the antibiotic action of pyocyanine. J Bacteriol 141, 156-63.

90. Hassett, D.J., Charniga, L., Bean, K., Ohman, D.E., Cohen, M.S., 1992. Response of Pseudomonas aeruginosa to pyocyanin: mechanisms of resistance, antioxidant defenses, and demonstration of a manganese-cofactored superoxide dismutase. Infect Immun 60, 328-36.

91. Heffelfinger, S.C., Hawkins, H.H., Barrish, J., Taylor, L., Darlington, G.J., 1992. SK HEP-1: a human cell line of endothelial origin. In Vitro Cell Dev Biol 28A, 136-142.

92. Heffernan, S., James, V., Zilkens, R., Kirwan, P., Birrell, A., McLennan, S., Hennessy, A., Gillin, A., Horvath, J., Tiller, D., Yue, D., Turtle, J., 1996. Changes of extracellular matrix in a baboon (Papio hamadryas) model of insulin dependent diabetes: studies using electron microscopy and X-ray diffraction techniques. Diabetes Res Clin Pract 34, 65-72.

93. Heffernan, S., Phippard, A., Sinclair, A., McLennan, S., Hennessy, A., Gillin, A., Horvath, J., Tiller, D., Yue, D., Turtle, J., 1995. A baboon (Papio hamadryas) model of insulin-dependent diabetes. J Med Primatol 24, 29-34.

94. Heilbronn, L.K., de Jonge, L., Frisard, M.I., DeLany, J.P., Larson-Meyer, D.E., Rood, J., Nguyen, T., Martin, C.K., Volaufova, J., Most, M.M., Greenway, F.L., Smith, S.R., Deutsch, W.A., Williamson, D.A., Ravussin, E., 2006. Effect of 6-month calorie restriction on biomarkers of longevity, metabolic adaptation, and oxidative stress in overweight individuals: a randomized controlled trial. Jama 295, 1539-48.

95. Henriksen, J.H., Horn, T., Christoffersen, P., 1984. The blood-lymph barrier in the liver. A review based on morphological and functional concepts of normal and cirrhotic liver. Liver 4, 221-32.

96. Herrlinger, C., Klotz, U., 2001. Drug metabolism and drug interactions in the elderly. Best Pract Res Clin Gastroenterol 15, 897-918.

97. Hewett, J.A., Roth, R.A., 1995. The coagulation system, but not circulating fibrinogen, contributes to liver injury in rats exposed to lipopolysaccharide from gram-negative bacteria. J Pharmacol Exp Ther 272, 53-62.

98. Hilmer, S.N., Cogger, V.C., Fraser, R., McLean, A.J., Sullivan, D., Le Couteur, D.G., 2005. Age-related changes in the hepatic sinusoidal endothelium impede lipoprotein transfer in the rat. Hepatology 42, 1349-1354.

99. Hilmer, S.N., Cogger, V.C., Le Couteur, D.G., 2007. Basal activity of Kupffer cells increases with old age. J Gerontol A Biol Sci Med Sci 62, 973-8.

100. Horn, T., Christoffersen, P., Henriksen, J.H., 1987. Alcoholic liver injury: defenestration in noncirrhotic livers--a scanning electron microscopic study. Hepatology 7, 77-82.

101. Horn, T., Henriksen, J.H., Christoffersen, P., 1986. The sinusoidal lining cells in "normal" human liver. A scanning electron microscopic investigation. Liver 6, 98-110.

102. Huet, P.M., Nagaoka, M.R., Desbiens, G., Tarrab, E., Brault, A., Bralet, M.P., Bilodeau, M., 2004. Sinusoidal endothelial cell and hepatocyte death following cold ischemia-warm reperfusion of the rat liver. Hepatology 39, 1110-9.

103. Huet, P.M., Villeneuve, J.P., 2005. Microcirculation of the aging liver: is getting old like having cirrhosis? Hepatology 42, 1248-51.

104. Hussain, A.S., Bozinovski, J., Maurice, D.H., McLaughlin, B.E., Marks, G.S., Brien, J.F., Nakatsu, K., 1997. Inhibition of the action of nitric oxide prodrugs by pyocyanin: mechanistic studies. Can J Physiol Pharmacol 75, 398-406.

105. Iinuma, Y., Senda, K., Fujihara, N., Saito, T., Takakura, S., Kudo, T., Kiuchi, T., Tanaka, K., Ichiyama, S., 2004. Surgical site infection in living-donor liver transplant recipients: a prospective study. Transplantation 78, 704-9.

106. Ingram, D.K., Anson, R.M., de Cabo, R., Mamczarz, J., Zhu, M., Mattison, J., Lane, M.A., Roth, G.S., 2004. Development of calorie restriction mimetics as a prolongevity strategy. Ann N Y Acad Sci 1019, 412-23.

107. Ishikawa, K., Mochida, S., Mashiba, S., Inao, M., Matsui, A., Ikeda, H., Ohno, A., Shibuya, M., Fujiwara, K., 1999. Expressions of vascular endothelial growth factor in nonparenchymal as well as parenchymal cells in rat liver after necrosis. Biochem Biophys Res Commun 254, 587-93.

108. Ito, Y., McCuskey, M.K., Sorensen, K.K., Smedsrod, B., McCuskey, R.S., 2005. Age-related hepatic microvascular dysfunction in mice. Hepatology 42 (S1), 446A (Abstract).

109. Ito, Y., Sorensen, K.K., Bethea, N.W., Svistounov, D., McCuskey, M.K., Smedsrod, B.H., McCuskey, R.S., 2007. Age-related changes in the hepatic microcirculation in mice. Exp Gerontol 42, 789-97.

110. Jacob, A.I., Goldberg, P.K., Bloom, N., Degenshein, G.A., Kozinn, P.J., 1977. Endotoxin and bacteria in portal blood. Gastroenterology 72, 1268-70.

111. Jaeschke, H., 1997. Cellular adhesion molecules: regulation and functional significance in the pathogenesis of liver diseases. Am J Physiol 273, G602-11.

112. Jaeschke, H., 1992. Enhanced sinusoidal glutathione efflux during endotoxin-induced oxidant stress in vivo. Am J Physiol 263, G60-8.

113. Jaeschke, H., 2002. Neutrophil-mediated tissue injury in alcoholic hepatitis. Alcohol 27, 23-7.

114. Jaeschke, H., Farhood, A., 1991. Neutrophil and Kupffer cell-induced oxidant stress and ischemia-reperfusion injury in rat liver. Am J Physiol 260, G355-62.

115. Jaeschke, H., Farhood, A., Fisher, M.A., Smith, C.W., 1996. Sequestration of neutrophils in the hepatic vasculature during endotoxemia is independent of beta 2 integrins and intercellular adhesion molecule-1. Shock 6, 351-6.

116. Jaeschke, H., Farhood, A., Smith, C.W., 1990. Neutrophils contribute to ischemia/reperfusion injury in rat liver in vivo. FASEB J 4, 3355-9.

117. Jaeschke, H., Gores, G.J., Cederbaum, A.I., Hinson, J.A., Pessayre, D., Lemasters, J.J., 2002. Mechanisms of hepatotoxicity. Toxicol Sci 65, 166-76.

118. Jaeschke, H., Smith, C.W., Clemens, M.G., Ganey, P.E., Roth, R.A., 1996. Mechanisms of inflammatory liver injury: adhesion molecules and cytotoxicity of neutrophils. Toxicol Appl Pharmacol 139, 213-26.

119. Jamieson, H., Dobbs, B.R., Day, W.A., Rogers, G.W.T., Fraser, R., 2001. The liver sieve in diabetes: are the ultrastructural changes similar to those seen in alcoholism? Cells of the hepatic sinusoid In: Wisse E, Knook DL, De Zanger R, Arthur MJP (eds) , vol 8. Proceedings of the 10th international symposium on cells of the hepatic sinusoid. Kupffer Cell Foundation, Leiden, pp 8, 123–124.

120. Jamieson, H.A., Cogger, V.C., Twigg, S.M., McLennan, S.V., Warren, A., Cheluvappa, R., Hilmer, S.N., Fraser, R., de Cabo, R., Le Couteur, D.G., 2007. Alterations in liver sinusoidal endothelium in a baboon model of type 1 diabetes. Diabetologia 50, 1969-1976.

121. Jamieson, H.A., Cogger, V.C., Twigg, S.M., McLennan, S.V., Warren, A., Cheluvappa, R., Hilmer, S.N., Fraser, R., de Cabo, R., Le Couteur, D.G., 2007. Alterations in liver sinusoidal endothelium in a baboon model of type 1 diabetes. Diabetologia 50, 1969-76.

122. Jia, J.B., Han, D.W., Xu, R.L., Gao, F., Zhao, L.F., Zhao, Y.C., Yan, J.P., Ma, X.H., 1998. Effect of endotoxin on fibronectin synthesis of rat primary cultured hepatocytes. World J Gastroenterol 4, 329-331.

123. Jungermann, K., Kietzmann, T., 2000. Oxygen: modulator of metabolic zonation and disease of the liver. Hepatology 31, 255-60.

124. Jungermann, K., Kietzmann, T., 1996. Zonation of parenchymal and nonparenchymal metabolism in liver. Annu Rev Nutr 16, 179-203.

125. Kamoun, W.S., Karaa, A., Kresge, N., Merkel, S.M., Korneszczuk, K., Clemens, M.G., 2006. LPS inhibits endothelin-1-induced endothelial NOS activation in hepatic sinusoidal cells through a negative feedback involving caveolin-1. Hepatology 43, 182-90.

126. Kamoun, W.S., Karaa, A., Kresge, N., Merkel, S.M., Korneszczuk, K., Clemens, M.G., 2006. LPS inhibits endothelin-1-induced endothelial NOS activation in hepatic sinusoidal cells through a negative feedback involving caveolin-1. Hepatology 43, 182-190.

127. Kang, M.J., Kim, H.J., Kim, H.K., Lee, J.Y., Kim, D.H., Jung, K.J., Kim, K.W., Baik, H.S., Yoo, M.A., Yu, B.P., Chung, H.Y., 2005. The effect of age and calorie restriction on HIF-1-responsive genes in aged liver. Biogerontology 6, 27-37.

128. Kassissia, I., Rose, C.P., Goresky, C.A., Schwab, A.J., Bach, G.G., Guirguis, S., 1992. Flow-limited tracer oxygen distribution in the isolated perfused rat liver: effects of temperature and hematocrit. Hepatology 16, 763-775.

129. Katschinski, D.M., 2006. Is there a molecular connection between hypoxia and aging? Exp Gerontol 41, 482-4.

130. Kinirons, M.T., O'Mahony, M.S., 2004. Drug metabolism and ageing. Br J Clin Pharmacol 57, 540-4.

131. Kitano, H., Fukui, H., Okamoto, Y., Kikuchi, E., Matsumoto, M., Kikukawa, M., Morimura, M., Tsujita, S., Nagamoto, I., Hoppo, K., Nakatani, Y., Nakatani, T., Tsujii, T., 1996. Protective mechanism of high-density lipoprotein against endotoxemia in chronic alcohol ingestion. Alcohol Clin Exp Res 20, 356A-359A.

132. Kitano, H., Fukui, H., Okamoto, Y., Kikuchi, E., Matsumoto, M., Kikukawa, M., Morimura, M., Tsujita, S., Nagamoto, I., Nakatani, T., Takaya, A., Tsujii, T.,

1996. Role of albumin and high-density lipoprotein as endotoxin-binding proteins in rats with acute and chronic alcohol loading. Alcohol Clin Exp Res 20, 73A-76A.

133. Klugewitz, K., Blumenthal-Barby, F., Schrage, A., Knolle, P.A., Hamann, A., Crispe, I.N., 2002. Immunomodulatory effects of the liver: deletion of activated CD4+ effector cells and suppression of IFN-gamma-producing cells after intravenous protein immunization. J Immunol 169, 2407-13.

134. Kmiec, Z., 2001. Cooperation of liver cells in health and disease. Adv Anat Embryol Cell Biol 161, III-XIII, 1-151.

135. Knight, M., Hartman, P.E., Hartman, Z., Young, V.M., 1979. A new method of preparation of pyocyanin and demonstration of an unusual bacterial sensitivity. Anal Biochem 95, 19-23.

136. Knolle, P.A., Gerken, G., 2000. Local control of the immune response in the liver. Immunol Rev 174, 21-34.

137. Knolle, P.A., Germann, T., Treichel, U., Uhrig, A., Schmitt, E., Hegenbarth, S., Lohse, A.W., Gerken, G., 1999. Endotoxin down-regulates T cell activation by antigen-presenting liver sinusoidal endothelial cells. J Immunol 162, 1401-7.

138. Knolle, P.A., Limmer, A., 2003. Control of immune responses by savenger liver endothelial cells. Swiss Med Wkly 133, 501-6.

139. Knolle, P.A., Schmitt, E., Jin, S., Germann, T., Duchmann, R., Hegenbarth, S., Gerken, G., Lohse, A.W., 1999. Induction of cytokine production in naive CD4(+) T cells by antigen-presenting murine liver sinusoidal endothelial cells but failure to induce differentiation toward Th1 cells. Gastroenterology 116, 1428-40.

140. Knolle, P.A., Uhrig, A., Hegenbarth, S., Loser, E., Schmitt, E., Gerken, G., Lohse, A.W., 1998. IL-10 down-regulates T cell activation by antigen-presenting liver sinusoidal endothelial cells through decreased antigen uptake via the mannose

receptor and lowered surface expression of accessory molecules. Clin Exp Immunol 114, 427-33.

141. Korvick, J.A., Marsh, J.W., Starzl, T.E., Yu, V.L., 1991. Pseudomonas aeruginosa bacteremia in patients undergoing liver transplantation: an emerging problem. Surgery 109, 62-8.

142. Krasinski, S.D., Cohn, J.S., Schaefer, E.J., Russell, R.M., 1990. Postprandial plasma retinyl ester response is greater in older subjects compared with younger subjects. Evidence for delayed plasma clearance of intestinal lipoproteins. J Clin Invest 85, 883-892.

143. Kumar, P., Clark, M., 2005. Kumar & Clark: Clinical Medicine, Sixth Edition. Elsevier Limited Liver, biliary tract and pancreatic disease, 348.

144. Kume, M., Hayashi, T., Yuasa, H., Tanaka, H., Nishioka, J., Ido, M., Gabazza, E.C., Kawarada, Y., Suzuki, K., 2003. Bacterial lipopolysaccharide decreases thrombomodulin expression in the sinusoidal endothelial cells of rats -- a possible mechanism of intrasinusoidal microthrombus formation and liver dysfunction. J Hepatol 38, 9-17.

145. Kumwenda, Z.L., Wong, C.B., Johnson, J.A., Gosnell, J.E., Welch, W.J., Harris, H.W., 2002. Chylomicron-bound endotoxin selectively inhibits NF-kappaB activation in rat hepatocytes. Shock 18, 182-8.

146. Lakatta, E.G., 2003. Arterial and cardiac aging: major shareholders in cardiovascular disease enterprises: Part III: cellular and molecular clues to heart and arterial aging. Circulation 107, 490-7.

147. Lalor, P.F., Adams, D.H., 1999. Adhesion of lymphocytes to hepatic endothelium. Mol Pathol 52, 214-9.

148. Lalor, P.F., Shields, P., Grant, A., Adams, D.H., 2002. Recruitment of lymphocytes to the human liver. Immunol Cell Biol 80, 52-64.

149. Landau, B.R., Hastings, A.B., Zottu, S., 1963. Pyocyanin and Metabolic Pathways in Liver Slices in Vitro. Biochim Biophys Acta 74, 629-34.

150. Lang, C.H., Pollard, V., Fan, J., Traber, L.D., Traber, D.L., Frost, R.A., Gelato, M.C., Prough, D.S., 1997. Acute alterations in growth hormone-insulin-like growth factor axis in humans injected with endotoxin. Am J Physiol 273, R371-8.

151. Lau, G.W., Ran, H., Kong, F., Hassett, D.J., Mavrodi, D., 2004. Pseudomonas aeruginosa pyocyanin is critical for lung infection in mice. Infect Immun 72, 4275-4278.

152. Le Couteur, D.G., Cogger, V.C., Hilmer, S.N., Muller, M., Harris, M., Sullivan, D., McLean, A.J., Fraser, R. Aging, atherosclerosis and the liver sieve. In: Clark LV, editor. New Research in Atherosclerosis. NY: Nova Science; 2006. p. 19-44.

153. Le Couteur, D.G., Cogger, V.C., Markus, A.M., Harvey, P.J., Yin, Z.L., Ansselin, A.D., McLean, A.J., 2001. Pseudocapillarization and associated energy limitation in the aged rat liver. Hepatology 33, 537-43.

154. Le Couteur, D.G., Cogger, V.C., McCuskey, R.S., R, D.E.C., Smedsrod, B., Sorensen, K.K., Warren, A., Fraser, R., 2007. Age-related changes in the liver sinusoidal endothelium: a mechanism for dyslipidemia. Ann N Y Acad Sci 1114, 79-87.

155. Le Couteur, D.G., Fraser, R., Cogger, V.C., McLean, A.J., 2002. Hepatic pseudocapillarisation and atherosclerosis in ageing. Lancet 359, 1612-1615.

156. Le Couteur, D.G., Fraser, R., Hilmer, S., Rivory, L.P., McLean, A.J., 2005. The hepatic sinusoid in aging and cirrhosis: effects on hepatic substrate disposition and drug clearance. Clin Pharmacokinet 44, 187-200.

157. Le Couteur, D.G., McLean, A.J., 1998. The aging liver. Drug clearance and an oxygen diffusion barrier hypothesis. Clin Pharmacokinet 34, 359-73.

158. Le Couteur, D.G., McLean, A.J., 1998. The influence of age on oxygen uptake by the liver - The hepatic oxygen barrier hypothesis. Clinical Pharmacology & Therapeutics 63, 223-223.

159. Le Couteur, D.G., Muller, M., Yang, M.C., Mellick, G.D., McLean, A.J., 2002. Age-environment and gene-environment interactions in the pathogenesis of Parkinson's disease. Rev Environ Health 17, 51-65.

160. Le Couteur, D.G., Warren, A., Cogger, V.C., Smedsrod, B., Sorensen, K.K., De Cabo, R., Fraser, R., McCuskey, R.S., 2008. Old age and the hepatic sinusoid. Anat Rec (Hoboken) 291, 672-683.

161. Le Couteur, D.G., Yin, Z.L., Rivory, L.P., McLean, A.J., 1999. Carbon monoxide disposition in the perfused rat liver. Am J Physiol 277, G725-G730.

162. LeCouter, J., Moritz, D.R., Li, B., Phillips, G.L., Liang, X.H., Gerber, H.P., Hillan, K.J., Ferrara, N., 2003. Angiogenesis-independent endothelial protection of liver: role of VEGFR-1. Science 299, 890-3.

163. Lee, H.B., Blaufox, M.D., 1985. Blood volume in the rat. J Nucl Med 26, 72-76.

164. Leidal, K.G., Munson, K.L., Denning, G.M., 2001. Small molecular weight secretory factors from Pseudomonas aeruginosa have opposite effects on IL-8 and RANTES expression by human airway epithelial cells. Am J Respir Cell Mol Biol 25, 186-195.

165. Limmer, A., Knolle, P.A., 2001. Liver sinusoidal endothelial cells: a new type of organ-resident antigen-presenting cell. Arch Immunol Ther Exp (Warsz) 49 Suppl 1, S7-11.

166. Limmer, A., Ohl, J., Wingender, G., Berg, M., Jungerkes, F., Schumak, B., Djandji, D., Scholz, K., Klevenz, A., Hegenbarth, S., Momburg, F., Hammerling, G.J., Arnold, B., Knolle, P.A., 2005. Cross-presentation of oral antigens by liver sinusoidal endothelial cells leads to CD8 T cell tolerance. Eur J Immunol 35, 2970-81.

167. Liu, P., Fisher, M.A., Farhood, A., Smith, C.W., Jaeschke, H., 1994. Beneficial effects of extracellular glutathione against endotoxin-induced liver injury during ischemia and reperfusion. Circ Shock 43, 64-70.

168. Liu, P., McGuire, G.M., Fisher, M.A., Farhood, A., Smith, C.W., Jaeschke, H., 1995. Activation of Kupffer cells and neutrophils for reactive oxygen formation is responsible for endotoxin-enhanced liver injury after hepatic ischemia. Shock 3, 56-62.

169. Lohse, A.W., Knolle, P.A., Bilo, K., Uhrig, A., Waldmann, C., Ibe, M., Schmitt, E., Gerken, G., Meyer Zum Buschenfelde, K.H., 1996. Antigen-presenting function and B7 expression of murine sinusoidal endothelial cells and Kupffer cells. Gastroenterology 110, 1175-81.

170. Lumsden, A.B., Henderson, J.M., Kutner, M.H., 1988. Endotoxin levels measured by a chromogenic assay in portal, hepatic and peripheral venous blood in patients with cirrhosis. Hepatology 8, 232-6.

171. Luo, D.Z., Vermijlen, D., Ahishali, B., Triantis, V., Plakoutsi, G., Braet, F., Vanderkerken, K., Wisse, E., 2000. On the cell biology of pit cells, the liver-specific NK cells. World J Gastroenterol 6, 1-11.

172. Luyendyk, J.P., Copple, B.L., Barton, C.C., Ganey, P.E., Roth, R.A., 2003. Augmentation of aflatoxin B1 hepatotoxicity by endotoxin: involvement of endothelium and the coagulation system. Toxicol Sci 72, 171-81.

173. Luyendyk, J.P., Maddox, J.F., Green, C.D., Ganey, P.E., Roth, R.A., 2004. Role of hepatic fibrin in idiosyncrasy-like liver injury from lipopolysaccharide-ranitidine coexposure in rats. Hepatology 40, 1342-51.

174. Luyendyk, J.P., Mattes, W.B., Burgoon, L.D., Zacharewski, T.R., Maddox, J.F., Cosma, G.N., Ganey, P.E., Roth, R.A., 2004. Gene expression analysis points to hemostasis in livers of rats cotreated with lipopolysaccharide and ranitidine. Toxicol Sci 80, 203-13.

175. Ma, Y.K., Yan, L.N., Li, B., Lu, S.C., Huang, A.H., Wen, T.F., Zeng, Y., Cheng, N.S., 2005. Diagnosis and treatment of bacterial pneumonia in liver transplantation recipients: report of 33 cases. Chin Med J (Engl) 118, 1879-85.

176. Madarame, T., Nagaoka, T., Inomata, M., Suzuki, K., Sato, S., Kanno, S., Yoshida, Y., Sakuma, T., Satodate, R. Basement membrane-like structure may play a role in the alteration of endothelial fenestration. In: Wisse E, Knook DL, McCuskey RS, editors. Cells of the Hepatic Sinusoid. Leiden: Kupffer Cell Foundation; 1991. p. 98-101.

177. Magnusson, S., Berg, T., 1989. Extremely rapid endocytosis mediated by the mannose receptor of sinusoidal endothelial rat liver cells. Biochem J 257, 651-6.

178. Mahajan-Miklos, S., Tan, M.W., Rahme, L.G., Ausubel, F.M., 1999. Molecular mechanisms of bacterial virulence elucidated using a Pseudomonas aeruginosa-Caenorhabditis elegans pathogenesis model. Cell 96, 47-56.

179. Maharaj, A.S., Saint-Geniez, M., Maldonado, A.E., D'Amore, P.A., 2006. Vascular endothelial growth factor localization in the adult. Am J Pathol 168, 639-48.

180. Mak, K.M., Lieber, C.S., 1984. Alterations in endothelial fenestrations in liver sinusoids of baboons fed alcohol: a scanning electron microscopic study. Hepatology 4, 386-91.

181. Mamo, J.C., Elsegood, C.L., Umeda, Y., Hirano, T., Redgrave, T.G., 1993. Effect of probucol on plasma clearance and organ uptake of chylomicrons and VLDLs in normal and diabetic rats. Arterioscler Thromb 13, 231-9.

182. Masoro, E.J., 2005. Overview of caloric restriction and ageing. Mech Ageing Dev 126, 913-22.

183. McCuskey, P.A., McCuskey, R.S., Hinton, D.E. Electron microscopy of the cells of the hepatic sinsusoids in rainbow trout. In: Kirn A, Knook DL, Wisse E, editors. Cells of the Hepatic Sinusoid. Rijswijk: The Kupffer Cell Foundation; 1986. p. 489-494.

184. McCuskey, R.S., 2006. Sinusoidal endothelial cells as an early target for hepatic toxicants. Clin Hemorheol Microcirc 34, 5-10.

185. McCuskey, R.S., McCuskey, P.A., Mitchell, D.B., Dezanger, R.B., Wisse, E. Ultrastructure of the canine hepatic sinusoid. In: Kirn A, Knook DL, Wisse E, editors. Cells of the Hepatic Sinusoid. Rijswijk: The Kupffer Cell Foundation; 1986. p. 509-510.

186. McLean, A.J., Cogger, V.C., Chong, G.C., Warren, A., Markus, A.M., Dahlstrom, J.E., Le Couteur, D.G., 2003. Age-related pseudocapillarization of the human liver. J Pathol 200, 112-7.

187. McLean, A.J., Cogger, V.C., Harvey, P.J., Yin, Z.L., Ansselin, A.D., Le Couteur, D.G., 2001. Pseudocapillarization of the aged liver. Clinical Pharmacology & Therapeutics 69, P15-P15.

188. McLean, A.J., Morgan, D.J., 1991. Clinical pharmacokinetics in patients with liver disease. Clin Pharmacokinet 21, 42-69.

189. Miller, R.A., Rasmussen, G.T., Cox, C.D., Britigan, B.E., 1996. Protease cleavage of iron-transferrin augments pyocyanin-mediated endothelial cell injury via promotion of hydroxyl radical formation. Infect Immun 64, 182-188.

190. Molina, P.E., Lang, C.H., Bagby, G.J., D'Souza, N.B., Spitzer, J.J., 1989. Ethanol administration diminishes the endotoxin-induced increase in glucose metabolism. Alcohol Clin Exp Res 13, 407-12.

191. Moreno, A., Mensa, J., Almela, M., Vilardell, J., Navasa, M., Claramonte, J., Cruceta, A., Serrano, R., Garcia-Valdecasas, J.C., Soriano, E., et al., 1994. [138 episodes of bacteremia or fungemia in patients with solid organ (renal or hepatic) transplantation]. Med Clin (Barc) 103, 161-4.

192. Mori, T., Okanoue, T., Sawa, Y., 1991. Effect of ethanol on the sinusoidal endothelial fenestrations of rat liver- in vivo and in vitro study. Cells of the Hepatic Sinusoid 3, 469-471.

193. Moulin, F., Pearson, J.M., Schultze, A.E., Scott, M.A., Schwartz, K.A., Davis, J.M., Ganey, P.E., Roth, R.A., 1996. Thrombin is a distal mediator of lipopolysaccharide-induced liver injury in the rat. J Surg Res 65, 149-58.

194. Muhlen, K.A., Schumann, J., Wittke, F., Stenger, S., Van Rooijen, N., Van Kaer, L., Tiegs, G., 2004. NK cells, but not NKT cells, are involved in Pseudomonas aeruginosa exotoxin A-induced hepatotoxicity in mice. J Immunol 172, 3034-41.

195. Muhlradt, P.F., Tsai, H., Conradt, P., 1986. Effects of pyocyanine, a blue pigment from Pseudomonas aeruginosa, on separate steps of T cell activation: interleukin 2 (IL 2) production, IL 2 receptor formation, proliferation and induction of cytolytic activity. Eur J Immunol 16, 434-40.

196. Muller, M., 2006. Premature cellular senescence induced by pyocyanin, a redox-active Pseudomonas aeruginosa toxin. Free Radic Biol Med 41, 1670-1677.

197. Muller, M., 2002. Pyocyanin induces oxidative stress in human endothelial cells and modulates the glutathione redox cycle. Free Rad Biol Med 33, 1527-1533.

198. Muller, M., Sorrell, T.C., 1992. Leukotriene B4 omega-oxidation by human polymorphonuclear leukocytes is inhibited by pyocyanin, a phenazine derivative produced by Pseudomonas aeruginosa. Infect Immun 60, 2536-2540.

199. Muller, M., Sorrell, T.C., 1997. Oxidative stress and the mobilisation of arachidonic acid in stimulated human platelets: Role of hydroxyl radical. Prostaglandins 54, 493-509.

200. Muller, P.K., Krohn, K., Muhlradt, P.F., 1989. Effects of pyocyanine, a phenazine dye from Pseudomonas aeruginosa, on oxidative burst and bacterial killing in human neutrophils. Infect Immun 57, 2591-2596.

201. Munford, R.S., Andersen, J.M., Dietschy, J.M., 1981. Sites of tissue binding and uptake in vivo of bacterial lipopolysaccharide-high density lipoprotein complexes: studies in the rat and squirrel monkey. J Clin Invest 68, 1503-13.

202. Munford, R.S., Dietschy, J.M., 1985. Effects of specific antibodies, hormones, and lipoproteins on bacterial lipopolysaccharides injected into the rat. J Infect Dis 152, 177-84.

203. Munford, R.S., Hall, C.L., Dietschy, J.M., 1981. Binding of Salmonella typhimurium lipopolysaccharides to rat high-density lipoproteins. Infect Immun 34, 835-43.

204. Mustafa, S.B., Olson, M.S., 1999. Effects of calcium channel antagonists on LPS-induced hepatic iNOS expression. Am J Physiol 277, G351-60.

205. Naito, M., Wisse, E., 1978. Filtration effect of endothelial fenestrations on chylomicron transport in neonatal rat liver sinusoids. Cell Tissue Res 190, 371-82.

206. Neves, D., Santos, J., Tomada, N., Almeida, H., Vendeira, P., 2006. Aging and orchidectomy modulate expression of VEGF receptors (Flt-1 and Flk-1) on corpus cavernosum of the rat. Ann N Y Acad Sci 1067, 164-72.

207. Nopanitaya, W., Carson, J.L., Grisham, J.W., Aghajanian, J.G., 1979. New observations on the fine structure of the liver in goldfish (Carassius auratus). Cell Tissue Res 196, 249-61.

208. Nopanitaya, W., Grisham, J.W., Carson, J.L., Dotson, M.M., 1976. Surface features of cirrhotic liver. Virchows Arch A Pathol Anat Histol 372, 97-108.

209. Nopanitaya, W., Lamb, J.C., Grisham, J.W., Carson, J.L., 1976. Effect of hepatic venous outflow obstruction on pores and fenestration in sinusoidal endothelium. Br J Exp Pathol 57, 604-9.

210. Nyska, A., Moomaw, C.R., Foley, J.F., Maronpot, R.R., Malarkey, D.E., Cummings, C.A., Peddada, S., Moyer, C.F., Allen, D.G., Travlos, G., Chan, P.C., 2002. The hepatic endothelial carcinogen riddelliine induces endothelial apoptosis, mitosis, S phase, and p53 and hepatocytic vascular endothelial growth factor expression after short-term exposure. Toxicol Appl Pharmacol 184, 153-64.

211. Oda, M., Kamegaya, Y., Yokomori, H., Han, J.Y., Akiba, Y., Nakumura, M., Ishii, H., Tsuchiya, M. Roles of plasma membrane Ca-ATPase in the relaxation and contraction of hepatic sinusoidal endothelial fenestrae - effects of prostaglandin E1 and endothelin 1. In: Wisse E, Knook DL, Balabaud C, editors. Cells of the Hepatic Sinusoid. Leiden: Kupffer Cell Foundation; 1997. p. 313-317.

212. Oda, M., Kazemoto, S., Kaneko, H., al., e., 1993. Involvement of Ca++-calmodulin-actomyosin system in contractility of hepatic sinusoidal endothelial fenestrae. Cells of the hepatic sinusoid 4, 174-178.

213. Ogi, M., Yokomori, H., Oda, M., Yoshimura, K., Nomura, M., Ohshima, S., Akita, M., Toda, K., Ishii, H., 2003. Distribution and localization of caveolin-1 in sinusoidal cells in rat liver. Med Electron Microsc 36, 33-40.

214. Ogle, C.K., Guo, X., Wu, J.Z., Ogle, J.D., Fischer, J.E., 1995. Effect of hepatocytes from normal or endotoxin treated animals on the production of tumour necrosis factor, interleukin-6, and prostaglandin-E2 by macrophages incubated in vitro with various fatty acids. Eur J Surg 161, 123-7.

215. O'Malley, Y.Q., Reszka, K.J., Spitz, D.R., Denning, G.M., Britigan, B.E., 2004. Pseudomonas aeruginosa pyocyanin directly oxidizes glutathione and decreases its levels in airway epithelial cells. Am J Physiol Lung Cell Mol Physiol 287, L94-103.

216. Paolisso, G., Rizzo, M., Mazziotti, G., Tagliamonte, M., Gambardella, A., Rotondi, M., Carella, C., Giugliano, D., Varricchio, M., D'onofrio, F., 1998. Advancing Age And Insulin Resistance: Role Of Plasma Tumor Necrosis Factor-A. Am. J. Physiol. 275, E294-E299.

217. Pearson, J.M., Schultze, A.E., Jean, P.A., Roth, R.A., 1995. Platelet participation in liver injury from gram-negative bacterial lipopolysaccharide in the rat. Shock 4, 178-86.

218. Pedersen, P.V., Warner, B.W., Bjornson, H.S., Hiyama, D.T., Li, S., Rigel, D.F., Hasselgren, P.O., Fischer, J.E., 1989. Hemodynamic and metabolic alterations during experimental sepsis in young and adult rats. Surg Gynecol Obstet 168, 148-56.

219. Picciotti, P., Torsello, A., Wolf, F.I., Paludetti, G., Gaetani, E., Pola, R., 2004. Age-dependent modifications of expression level of VEGF and its receptors in the inner ear. Exp Gerontol 39, 1253-8.

220. Pitt, T.L., 1986. Biology of Pseudomonas aeruginosa in relation to pulmonary infection in cystic fibrosis. J R Soc Med 79 Suppl 12, 13-8.

221. Quinn, T.P., Peters, K.G., De Vries, C., Ferrara, N., Williams, L.T., 1993. Fetal liver kinase 1 is a receptor for vascular endothelial growth factor and is selectively expressed in vascular endothelium. Proc Natl Acad Sci U S A 90, 7533-7.

222. Ran, H., Hassett, D.J., Lau, G.W., 2003. Human targets of Pseudomonas aeruginosa pyocyanin. Proc Natl Acad Sci U S A 100, 14315-20.

223. Read, T.E., Grunfeld, C., Kumwenda, Z.L., Calhoun, M.C., Kane, J.P., Feingold, K.R., Rapp, J.H., 1995. Triglyceride-rich lipoproteins prevent septic death in rats. J Exp Med 182, 267-72.

224. Rees, D.A., Alcolado, J.C., 2005. Animal models of diabetes mellitus. Diabet Med 22, 359-70.

225. Roberts, W.G., Palade, G.E., 1997. Neovasculature induced by vascular endothelial growth factor is fenestrated. Cancer Res 57, 765-72.

226. Rockey, D., 1997. The cellular pathogenesis of portal hypertension: stellate cell contractility, endothelin, and nitric oxide. Hepatology 25, 2-5.

227. Rose, C.P., Goresky, C.A., 1985. Limitations of tracer oxygen uptake in the canine coronary circulation. Circ Res 56, 57-71.

228. Rose, S., Baumann, H., Jahreis, G.P., Sayeed, M.M., 1994. Diltiazem and superoxide dismutase modulate hepatic acute phase response in gram-negative sepsis. Shock 1, 87-93.

229. Rosmorduc, O., Wendum, D., Corpechot, C., Galy, B., Sebbagh, N., Raleigh, J., Housset, C., Poupon, R., 1999. Hepatocellular hypoxia-induced vascular endothelial growth factor expression and angiogenesis in experimental biliary cirrhosis. Am J Pathol 155, 1065-73.

230. Roth, R.A., Harkema, J.R., Pestka, J.P., Ganey, P.E., 1997. Is exposure to bacterial endotoxin a determinant of susceptibility to intoxication from xenobiotic agents? Toxicol Appl Pharmacol 147, 300-11.

231. Ryan, N.A., Zwetsloot, K.A., Westerkamp, L.M., Hickner, R.C., Pofahl, W.E., Gavin, T.P., 2006. Lower skeletal muscle capillarization and VEGF expression in aged vs. young men. J Appl Physiol 100, 178-85.

232. Sakamoto, S., Okanoue, T., Itoh, Y., Nakagawa, Y., Nakamura, H., Morita, A., Daimon, Y., Sakamoto, K., Yoshida, N., Yoshikawa, T., Kashima, K., 2002. Involvement of Kupffer cells in the interaction between neutrophils and sinusoidal endothelial cells in rats. Shock 18, 152-7.

233. Salgia, R., Becker, J.H., Sayeed, M.M., 1993. Altered membrane fluidity in rat hepatocytes during endotoxic shock. Mol Cell Biochem 121, 143-8.

234. Sarphie, G., D'Souza, N.B., Van Thiel, D.H., Hill, D., McClain, C.J., Deaciuc, I.V., 1997. Dose- and time-dependent effects of ethanol on functional and structural aspects of the liver sinusoid in the mouse. Alcohol Clin Exp Res 21, 1128-36.

235. Sarphie, T.G., D'Souza, N.B., Deaciuc, I.V., 1996. Kupffer cell inactivation prevents lipopolysaccharide-induced structural changes in the rat liver sinusoid: an electron-microscopic study. Hepatology 23, 788-96.

236. Sass, B., Rabstein, L.S., Madison, R., Nims, R.M., Peters, R.L., Kelloff, G.J., 1975. Incidence of spontaneous neoplasms in F344 rats throughout the natural life-span. J Natl Cancer Inst 54, 1449-56.

237. Sastre, J., Pallardo, F.V., Pla, R., Pellin, A., Juan, G., O'Connor, J.E., Estrela, J.M., Miquel, J., Vina, J., 1996. Aging of the liver: age-associated mitochondrial damage in intact hepatocytes. Hepatology 24, 1199-1205.

238. Sastre, J., Pallardo, F.V., Vina, J., 2000. Mitochondrial oxidative stress plays a key role in aging and apoptosis. IUBMB Life 49, 427-35.

239. Sastre, J., Pallardo, F.V., Vina, J., 2003. The role of mitochondrial oxidative stress in aging. Free Radic Biol Med 35, 1-8.

240. Sayeed, M.M., Maitra, S.R., 1987. Effect of diltiazem on altered cellular calcium regulation during endotoxic shock. Am J Physiol 253, R549-54.

241. Schaber, J.A., Triffo, W.J., Suh, S.J., Oliver, J.W., Hastert, M.C., Griswold, J.A., Auer, M., Hamood, A.N., Rumbaugh, K.P., 2007. Pseudomonas aeruginosa forms biofilms in acute infection independent of cell-to-cell signaling. Infect Immun 75, 3715-3721.

242. Schmucker, D.L., 2005. Age-related changes in liver structure and function: implications for disease? Experimental Gerontology 40, 650-659.

243. Schmucker, D.L., 2001. Liver function and phase I drug metabolism in the elderly: a paradox. Drugs Aging 18, 837-851.

244. Scholl, R.A., Lang, C.H., Bagby, G.J., 1984. Hypertriglyceridemia and its relation to tissue lipoprotein lipase activity in endotoxemic, Escherichia coli bacteremic, and polymicrobial septic rats. J Surg Res 37, 394-401.

245. Schumann, J., Angermuller, S., Bang, R., Lohoff, M., Tiegs, G., 1998. Acute hepatotoxicity of Pseudomonas aeruginosa exotoxin A in mice depends on T cells and TNF. J Immunol 161, 5745-54.

246. Schumann, J., Bluethmann, H., Tiegs, G., 2000. Synergism of Pseudomonas aeruginosa exotoxin A with endotoxin, superantigen, or TNF results in TNFR1- and TNFR2-dependent liver toxicity in mice. Immunol Lett 74, 165-72.

247. Schumann, J., Wolf, D., Pahl, A., Brune, K., Papadopoulos, T., van Rooijen, N., Tiegs, G., 2000. Importance of Kupffer cells for T-cell-dependent liver injury in mice. Am J Pathol 157, 1671-83.

248. Scoazec, J.Y., Feldmann, G., 1990. Both macrophages and endothelial cells of the human hepatic sinusoid express the CD4 molecule, a receptor for the human immunodeficiency virus. Hepatology 12, 505-10.

249. Scoazec, J.Y., Feldmann, G., 1991. In situ immunophenotyping study of endothelial cells of the human hepatic sinusoid: results and functional implications. Hepatology 14, 789-97.

250. Selzner, M., Selzner, N., Jochum, W., Graf, R., Clavien, P.A., 2007. Increased ischemic injury in old mouse liver: An ATP-dependent mechanism. Liver Transpl 13, 382-90.

251. Seto, S., Kaido, T., Yamaoka, S., Yoshikawa, A., Arii, S., Nakamura, T., Niwano, M., Imamura, M., 1998. Hepatocyte growth factor prevents lipopolysaccharide-induced hepatic sinusoidal endothelial cell injury and intrasinusoidal fibrin deposition in rats. J Surg Res 80, 194-199.

252. Shimizu, H., Miyazaki, M., Ito, H., Nakagawa, K., Ambiru, S., Kato, A., Nukui, Y., Nozawa, S., Nakajima, N., 2001. Mechanism of cold ischemia-reperfusion-induced graft injury after orthotopic liver transplantation in rats. Hepatogastroenterology 48, 216-219.

253. Shnyra, A., Hultenby, K., Lindberg, A.A., 1993. Role of the physical state of Salmonella lipopolysaccharide in expression of biological and endotoxic properties. Infect Immun 61, 5351-60.

254. Shnyra, A., Lindberg, A.A., 1995. Scavenger receptor pathway for lipopolysaccharide binding to Kupffer and endothelial liver cells in vitro. Infect Immun 63, 865-73.

255. Sinclair, D.A., 2005. Toward a unified theory of caloric restriction and longevity regulation. Mech Ageing Dev 126, 987-1002.

256. Singh, N., Gayowski, T., Rihs, J.D., Wagener, M.M., Marino, I.R., 2001. Evolving trends in multiple-antibiotic-resistant bacteria in liver transplant recipients: a longitudinal study of antimicrobial susceptibility patterns. Liver Transpl 7, 22-6.

257. Singh, N., Gayowski, T., Wagener, M.M., Marino, I.R., 1999. Pulmonary infiltrates in liver transplant recipients in the intensive care unit. Transplantation 67, 1138-44.

258. Singh, N., Wagener, M.M., Obman, A., Cacciarelli, T.V., de Vera, M.E., Gayowski, T., 2004. Bacteremias in liver transplant recipients: shift toward gram-negative bacteria as predominant pathogens. Liver Transpl 10, 844-849.

259. Singleton, J.R., Smith, A.G., Russell, J.W., Feldman, E.L., 2003. Microvascular complications of impaired glucose tolerance. Diabetes 52, 2867-73.

260. Smedsrod, B., Pertoft, H., Eggertsen, G., Sundstrom, C., 1985. Functional and morphological characterization of cultures of Kupffer cells and liver endothelial cells prepared by means of density separation in Percoll, and selective substrate adherence. Cell Tissue Res 241, 639-49.

261. Smedsrod, B., Pertoft, H., Gustafson, S., Laurent, T.C., 1990. Scavenger functions of the liver endothelial cell. Biochem J 266, 313-27.

262. Soave, R., Murray, H.W., Litrenta, M.M., 1978. Bacterial invasion of pulmonary vessels. Pseudomonas bacteremia mimicking pulmonary thromboembolism with infarction. Am J Med 65, 864-867.

263. Spector, I., Braet, F., Shochet, N.R., Bubb, M.R., 1999. New anti-actin drugs in the study of the organization and function of the actin cytoskeleton. Microsc Res Tech 47, 18-37.

264. Spitzer, J.J., Bagby, G.J., Hargrove, D.M., Lang, C.H., Meszaros, K., 1989. Alterations in the metabolic control of carbohydrates in sepsis. Prog Clin Biol Res 308, 545-61.

265. Spitzer, J.J., Bagby, G.J., Meszaros, K., Lang, C.H., 1988. Alterations in lipid and carbohydrate metabolism in sepsis. JPEN J Parenter Enteral Nutr 12, 53S-58S.

266. Spolarics, Z., 1998. Endotoxemia, pentose cycle, and the oxidant/antioxidant balance in the hepatic sinusoid. J Leuk Biol 63, 534-541.

267. Spolarics, Z., 1996. Endotoxin stimulates gene expression of ROS-eliminating pathways in rat hepatic endothelial and Kupffer cells. Am J Physiol 270, G660-6.

268. Spolarics, Z., Navarro, L., 1994. Endotoxin stimulates the expression of glucose-6-phosphate dehydrogenase in Kupffer and hepatic endothelial cells. J Leukoc Biol 56, 453-7.

269. Spolarics, Z., Stein, D.S., Garcia, Z.C., 1996. Endotoxin stimulates hydrogen peroxide detoxifying activity in rat hepatic endothelial cells. Hepatology 24, 691-6.

270. Steffan, A.M., Gendrault, J.L., Kirn, A., 1987. Increase in the number of fenestrae in mouse endothelial liver cells by altering the cytoskeleton with cytochalasin B. Hepatology 7, 1230-8.

271. Stewart-Tull, D.E., Armstrong, A.V., 1972. The effect of 1-hydroxyphenazine and pyocyanin from Pseudomonas aeruginosa on mammalian cell respiration. J Med Microbiol 5, 67-73.

272. Sumitran-Holgersson, S., Ge, X., Karrar, A., Xu, B., Nava, S., Broome, U., Nowak, G., Ericzon, B.G., 2004. A novel mechanism of liver allograft rejection facilitated by antibodies to liver sinusoidal endothelial cells. Hepatology 40, 1211-1221.

273. Sun, X., Kimura, T., Kobayashi, T., Noriki, S., Imamura, Y., Fukuda, M., Yamaguchi, A., 2001. Viability of liver grafts from fasted donor rats: relationship to sinusoidal endothelial cell apoptosis. J Hepatobiliary Pancreat Surg 8, 268-273.

274. Svistounov, D., Smedsrod, B., 2004. Hepatic clearance of advanced glycation end products (AGEs)--myth or truth? J Hepatol 41, 1038-40.

275. Szkudelski, T., 2001. The mechanism of alloxan and streptozotocin action in B cells of the rat pancreas. Physiol Res 50, 537-46.

276. Takahashi, K., Sawasaki, Y., Hata, J., Mukai, K., Goto, T., 1990. Spontaneous transformation and immortalization of human endothelial cells. In Vitro Cell Dev Biol 26, 265-74.

277. Takei, Y., Kawano, S., Nishimura, Y., Goto, M., Nagai, H., Chen, S.S., Omae, A., Fusamoto, H., Kamada, T., Ikeda, K., et al., 1995. Apoptosis: a new mechanism of endothelial and Kupffer cell killing. J Gastroenterol Hepatol 10 Suppl 1, S65-7.

278. Takeuchi, M., Nakashima, Y., Miura, Y., Nakagawa, K., Uragoh, K., Iwanaga, S., Hori, Y., Sueishi, K., 1994. The localization of lipopolysaccharide in an endotoxemic rat liver and its relation to sinusoidal thrombogenesis: light and electron microscopic studies. Pathol Res Pract 190, 1123-33.

279. Tanaka, T., Kato, H., Kojima, I., Ohse, T., Son, D., Tawakami, T., Yatagawa, T., Inagi, R., Fujita, T., Nangaku, M., 2006. Hypoxia and expression of hypoxia-inducible factor in the aging kidney. J Gerontol A Biol Sci Med Sci 61, 795-805.

280. Tanuma, Y., Ito, T., 1978. Electron microscope study on the hepatic sinusoidal wall and fat-storing cells in the bat. Arch Histol Jpn 41, 1-39.

281. Tiao, G., Noguchi, Y., Lieberman, M.A., Fischer, J.E., Hasselgren, P.O., 1995. Sepsis stimulates polyamine biosynthesis in the liver and increases tissue levels of ornithine decarboxylase mRNA. Shock 4, 403-10.

282. Tiegs, G., Wendel, A., 1988. Leukotriene-mediated liver injury. Biochem Pharmacol 37, 2569-73.

283. Tiegs, G., Wolter, M., Wendel, A., 1989. Tumor necrosis factor is a terminal mediator in galactosamine/endotoxin-induced hepatitis in mice. Biochem Pharmacol 38, 627-31.

284. Tsukada, N., Oda, M., Yonei, M., 1986. Alterations of the hepatic sinusoidal fenestrae in response to vasoactive substances in the rat- in vivo and in vitro studies. Cells of the Hepatic Sinusoid Vol 1, 515-516.

285. Turley, H., Scott, P.A., Watts, V.M., Bicknell, R., Harris, A.L., Gatter, K.C., 1998. Expression of VEGF in routinely fixed material using a new monoclonal antibody VG1. J Pathol 186, 313-8.

286. Ueno, M., 1990. [Endotoxemia and its compensatory mechanisms in experimental liver cirrhosis]. Nippon Shokakibyo Gakkai Zasshi 87, 1692-700.

287. Usher, L.R., Lawson, R.A., Geary, I., Taylor, C.J., Bingle, C.D., Taylor, G.W., Whyte, M.K., 2002. Induction of neutrophil apoptosis by the Pseudomonas aeruginosa exotoxin pyocyanin: a potential mechanism of persistent infection. J Immunol 168, 1861-1868.

288. Valente, E., Assis, M.C., Alvim, I.M., Pereira, G.M., Plotkowski, M.C., 2000. Pseudomonas aeruginosa induces apoptosis in human endothelial cells. Microb Pathog 29, 345-356.

289. Vidal-Vanaclocha, F., Barbera-Guillem, E., 1985. Fenestration patterns in endothelial cells of rat liver sinusoids. J Ultrastruct Res 90, 115-23.

290. Vollmar, B., Pradarutti, S., Richter, S., Menger, M.D., 2002. In vivo quantification of ageing changes in the rat liver from early juvenile to senescent life. Liver 22, 330-41.

291. Wade, J., Rolando, N., Williams, R., 1998. The significance of aerobic gram-negative bacilli in clinical specimens following orthotopic liver transplantation. Liver Transpl Surg 4, 51-7.

292. Wagener, M.M., Yu, V.L., 1992. Bacteremia in transplant recipients: a prospective study of demographics, etiologic agents, risk factors, and outcomes. Am J Infect Control 20, 239-247.

293. Wake, K., Decker, K., Kirn, A., Knook, D.L., McCuskey, R.S., Bouwens, L., Wisse, E., 1989. Cell biology and kinetics of Kupffer cells in the liver. Int Rev Cytol 118, 173-229.

294. Walker, R.M., Racz, W.J., McElligott, T.F., 1983. Scanning electron microscopic examination of acetaminophen-induced hepatotoxicity and congestion in mice. Am J Pathol 113, 321-30.

295. Warren, A., Bertolino, P., Cogger, V.C., McLean, A.J., Fraser, R., Couteur, D.G., 2005. Hepatic pseudocapillarization in aged mice. Exp Gerontol 40, 807-12.

296. Warren, A., Le Couteur, D.G., Fraser, R., Bowen, D.G., McCaughan, G.W., Bertolino, P., 2006. T lymphocytes interact with hepatocytes through fenestrations in murine liver sinusoidal endothelial cells. Hepatology 44, 1182-90.

297. Warren, J.B., Loi, R., Rendell, N.B., Taylor, G.W., 1990. Nitric oxide is inactivated by the bacterial pigment pyocyanin. Biochem J 266, 921-3.

298. Watanabe, N., Takashimizu, S., Nishizaki, Y., Kojima, S., Kagawa, T., Matsuzaki, S., 2007. An endothelin A receptor antagonist induces dilatation of sinusoidal endothelial fenestrae: implications for endothelin-1 in hepatic microcirculation. J Gastroenterol 42, 775-82.

299. Watson, D., MacDermot, J., Wilson, R., Cole, P.J., Taylor, G.W., 1986. Purification and structural analysis of pyocyanin and 1-hydroxyphenazine. Eur J Biochem 159, 309-313.

300. Weintraub, M.S., Grosskopf, I., Rassin, T., Miller, H., Charach, G., Rotmensch, H.H., Liron, M., Rubinstein, A., Iaina, A., 1996. Clearance of chylomicron remnants in normolipidaemic patients with coronary heart disease: case control study over three years. BMJ 312, 935-939.

301. Wilson, R., Pitt, T., Taylor, G., Watson, D., MacDermot, J., Sykes, D., Roberts, D., Cole, P., 1987. Pyocyanin and 1-hydroxyphenazine produced by Pseudomonas aeruginosa inhibit the beating of human respiratory cilia in vitro. J Clin Invest 79, 221-229.

302. Wilson, R., Sykes, D.A., Watson, D., Rutman, A., Taylor, G.W., Cole, P.J., 1988. Measurement of Pseudomonas aeruginosa phenazine pigments in sputum and assessment of their contribution to sputum sol toxicity for respiratory epithelium. Infect Immun 56, 2515-2517.

303. Wisse, E., 1970. An electron microscopic study of the fenestrated endothelial lining of rat liver sinusoids. J Ultrastruct Res 31, 125-150.

304. Wisse, E., Braet, F., Luo, D., De Zanger, R., Jans, D., Crabbe, E., Vermoesen, A., 1996. Structure and function of sinusoidal lining cells in the liver. Toxicol Pathol 24, 100-11.

305. Wisse, E., De Zanger, R., Fraser, R., McCuskey, R.S., 1980. On the role of liver endothelial filter in the transport of particulate fat (chylomicrons and their remnants) to parenchymal cells and the influence of certain hormones on the endothelial fenestrae. Communications of liver cells MTP Press, Lancaster., 195-200.

306. Wisse, E., De Zanger, R.B., Jacobs, R., McCuskey, R.S., 1983. Scanning electron microscope observations on the structure of portal veins, sinusoids and central veins in rat liver. Scan Electron Microsc 1441-52.

307. Wisse, W., De Zanger, R.B., Charels, K., Van Der Smissen, P., McCuskey, R.S., 1985. The liver sieve: considerations concerning the structure and function of endothelial fenestrae, the sinusoidal wall and the space of Disse. Hepatology 5, 683-692.

308. Wojnar, M.M., Hawkins, W.G., Lang, C.H., 1995. Nutritional support of the septic patient. Crit Care Clin 11, 717-33.

309. Wright, P.L., Smith, K.F., Day, W.A., Fraser, R., 1983. Hepatic sinusoidal endothelium in sheep: an ultrastructural reinvestigation. Anat Rec 206, 385-90.

310. Yamaguchi, R., Yano, H., Nakashima, Y., Ogasawara, S., Higaki, K., Akiba, J., Hicklin, D.J., Kojiro, M., 2000. Expression and localization of vascular endothelial growth factor receptors in human hepatocellular carcinoma and non-HCC tissues. Oncol Rep 7, 725-9.

311. Yamamoto, Y., Sezai, S., Sakurabayashi, S., Hirano, M., Kamisaka, K., Oka, H., 1994. A study of endotoxaemia in patients with primary biliary cirrhosis. J Int Med Res 22, 95-9.

312. Yee, S.B., Hanumegowda, U.M., Copple, B.L., Shibuya, M., Ganey, P.E., Roth, R.A., 2003. Endothelial cell injury and coagulation system activation during synergistic hepatotoxicity from monocrotaline and bacterial lipopolysaccharide coexposure. Toxicol Sci 74, 203-14.

313. Yokoi, Y., Namihisa, T., Kuroda, H., Komatsu, I., Miyazaki, A., Watanabe, S., Usui, K., 1984. Immunocytochemical detection of desmin in fat-storing cells (Ito cells). Hepatology 4, 709-14.

314. Yokomori, H., Oda, M., Yoshimura, K., Nagai, T., Ogi, M., Nomura, M., Ishii, H., 2003. Vascular endothelial growth factor increases fenestral permeability in hepatic sinusoidal endothelial cells. Liver Int 23, 467-475.

315. Yokoyama, H., Mizukami, T., Kamegaya, Y., Fukuda, M., Okamura, Y., Matsumoto, M., Kato, S., Ishii, H., 1998. Formation of superoxide anion in the hepatic sinusoid after lipopolysaccharide challenge. Alcohol Clin Exp Res 22, 133S-136S.

316. Zhong, Z., Li, X., Yamashina, S., von Frankenberg, M., Enomoto, N., Ikejima, K., Kolinsky, M., Raleigh, J.A., Thurman, R.G., 2001. Cyclosporin A causes a hypermetabolic state and hypoxia in the liver: prevention by dietary glycine. J Pharmacol Exp Ther 299, 858-65.

317. Zhu, J., Dong, J.H., Chen, P., Yang, S.Z., Zhang, Y.J., 2006. [Relationship between sinusoidal endothelial cell apoptosis and hepatocyte injury after their transplantation into rats]. Zhonghua Gan Zang Bing Za Zhi 14, 114-7.

318. Zhu, M., Miura, J., Lu, L.X., Bernier, M., DeCabo, R., Lane, M.A., Roth, G.S., Ingram, D.K., 2004. Circulating adiponectin levels increase in rats on caloric restriction: the potential for insulin sensitization. Exp Gerontol 39, 1049-59.

Protocol- and criteria-sheets involving my innovations and modifications

6. Protocols and criteria-sheets involving my innovations and modifications

6.1. Chemical synthesis of pyocyanin

1. 100 ml of 10 mM TRIS HCl prepared
    a. MW of TRIS HCl= 158
    b. 1 M TRIS HCl= 158 g/1000ml= 0.158 g/ml
    c. 10 mM TRIS HCl= 0.00158 g/ml= 0.158 g/100ml
2. 100 mg PMS added to 100 ml of 10 mM TRIS HCl in a 100 ml capacity thin stemmed round bottomed glass flask
3. PH to 7.4
4. The reaction mixture kept adjacent to a daylight fluorescent tube light for 2.5 hours. The following specific brand details of the tube light was preferred
    a. Phillips TLD 18 W/54
    b. Thailand
    c. TIS.958-2533
    d. TIS.236-2533
5. Chloroform added to the reaction mixture in a separation funnel kept in a fume hood (adjusting the ratios or number of sequences)
6. The lower chloroform (organic) phase with pyocyanin transferred to a pear-shaped flask
7. Nitrogen bubbled through the contents of the pear-shaped flask till a blue pyocyanin sludge remains after all the chloroform has been evaporated

8. Blue pyocyanin sludge resuspended in 50 ml chloroform
9. 0.1 M (that is, 0.1 N) HCl prepared
    a. 6.25 ml of 16 M stock HCl solution mixed with 93.75 ml of Millipore water to give a 1 M HCl solution
    b. 0.1 M HCl solution prepared by adding 10 ml of 1 M HCl solution to 90 ml of Millipore water
10. Pyocyanin chloroform solution acidified with 50 ml of 0.1 M HCl
11. 50 ml of chloroform added
12. 0.5 M (that is 0.5 N) NaOH prepared
    a. 1 M NaOH consists of 40 g in 1000 ml of water
    b. 20 ml of 0.5 M NaOH prepared by adding 0.4 g of NaOH (2 NaOH pellets) to 20 ml of Millipore water
13. Few drops of 500 mM NaOH added
14. Chloroform extraction done twice with 50 ml chloroform
15. Pyocyanin chloroform solution kept at –20°C freezer overnight
16. Chloroform evaporated
17. Pyocyanin resuspended in small amounts of more chloroform
18. Pyocyanin chloroform (concentrated) solution transferred to a vertical Pyrex glass tube
19. Chloroform evaporated
20. Hexane wash done by adding hexane (pyocyanin is insoluble in hexane), swirling the tube, and aspirating the hexane out
21. Chloroform (SMALL volume) added to pyocyanin
22. Hexane (large volume) added SLOWLY, DROP by DROP to the pyocyanin chloroform solution

23. 10 minutes waiting period mandated
24. Pyocyanin crystallized automatically
25. Pyocyanin in hexane and chloroform is centrifuged at 5000 rpm in 50 ml polypropylene tubes
26. Supernatant pipetted out from the 50 ml tubes and discarded
27. Lower phase with the pyocyanin crystals transferred to a polypropylene syringe (without a piston) with its tip compactly fitted into a the top nozzle of a filter apparatus containing a type EH 0.5 μ filter
28. Pyocyanin crystals trapped by filter
29. Methanol elution into a screw-capped glass bottle done
30. Methanol evaporated by nitrogen bubbling
31. Small amount of methanol used to dissolve the pyocyanin
32. Pyocyanin methanol solution kept at –20°C freezer overnight
33. Methanol evaporated by nitrogen bubbling
34. Pyocyanin reconstituted in a small amount of chloroform
35. Silica glass TLC plate activated
    a. TLC plates from Merck (HPTLC Pre-coated Silica Gel 60 Plates) used
    b. Excess silica from 3 edges scraped out
    c. TLC plate kept vertically in 10 ml methanol in a glass cage without paper lining. The most jagged/ damaged edge placed inferior and in contact with methanol in the glass cage. Glass plate used to cover the glass cage
    d. TLC plate is taken out of the methanol (and the glass cage) as soon as the solvent (methanol) front reaches 2 cm from the top edge (of the TLC plate)
    e. TLC plate kept outside the glass cage, inside the hood, for 10 minutes

f. TLC plate kept on a folded A4 size paper and heated with silica side up in a microwave at power setting 2 for 5 minutes
g. TLC plate heated in the microwave at power setting 3 for 10 more minutes
h. TLC plate kept in the dark or inside a desiccator till use

36. Sample applicator (Camag Nanomat) fitted with a applicator syringe fitted with a 1 µl (preferably) or a 5 µl glass tip, utilized to apply pyocyanin chloroform solution to the silica part of the silica glass TLC plate
37. TLC plate with loaded pyocyanin kept in chloroform methanol mixture (12.5 ml: 12.5ml) inside a glass cage with a paper lining
38. TLC plate removed from the glass cage when the solvent front reaches 2 cm from the top edge
39. TLC plate computer-scanned and image saved
40. Silica layer with the pyocyanin carefully scraped from the glass part of the TLC plate
41. Scraped silica with pyocyanin dissolved in 2 cm methanol in a screw capped glass bottle
42. Silica pyocyanin methanol solution transferred to small glass tubes (compatible in the slots of the centrifuge to be described soon)
43. Glass tubes centrifuged twice in the centrifuge available inside the walk-in refrigerator (the sealing lid is not shut, only the topmost trap lid is shut)
44. Shimadzu Spectrophotometer Precautions
    a. Remember that only the proximal slot is for the test sample(s) and the distal slot is for the blank

b. While calibrating and taking absorption measurements Blanking (or Baselining) should be done with blanks at both the proximal slot and the distal slot prior to taking the test sample(s) reading

c. A Deuterium Lamp emits UV light with wavelength ranging from 200-350 nm. A Halogen Lamp emits visible range light with wavelength ranging from 350-800 nm. Adjustments of the wavelengths should be made such that no absorbance peak occurs at the junction of the UV light spectra and the visible range light spectra

d. Only quartz cuvettes are to be used. The Normal (1 ml) cuvette is preferred to the Small or Semimicro cuvettes

45. Shimadzu Spectrophotometer Preparations

a. Check the spectrophotometer slots to see if they are empty first

b. Switch the spectrophotometer on (Switch on the left flank)

c. Click F4 on the spectrophotometer (This connects it to the computer)

46. Computer Manipulation of Spectrophotometer Functioning

a. Programs

b. Shimadzu

c. UV120 IPC

d. Acquire Mode

e. Spectrum: The calibrations should be as follows:

i.	Measuring Mode:	Abs
ii.	Recording Range:	Low 0.0 to High 0.5
iii.	Wavelength Range (nm):	800 to 200 nm
iv.	Scan Speed:	Fast
v.	Sampling Interval nm:	1

47. Spectrophotometric Estimation of Pyocyanin Concentration

a. Only quartz cuvettes are to be used. The Normal (1 ml) cuvette is preferred to the Small or Semimicro cuvettes
b. Use 2 cuvettes filled with methanol in each to blank (baseline). Place cuvette 1 in the proximal slot and cuvette 2 in the distal slot of the spectrophotometer
c. Blanking (baselining) is done by clicking Baseline
d. To check whether the blanking was done properly, click Start. The absorbance value should be 0
e. Dilute pyocyanin in methanol to 1: 100 dilution (10µl: 990µl) in cuvette 1 (from proximal slot in the spectrophotometer). This is the sample cuvette. Place the sample cuvette in the proximal slot in the spectrophotometer
f. Click Start
g. Pyocyanin typically peaks at 718 nm, 318 nm and 239 nm. The absorption values at these spectra are noted

48. Calculation of Molar Concentration using Spectrophotometer Absorption Data

a. Adjust the concentration of pyocyanin (by drying the methanol using nitrogen surface insufflation in a Fume Hood and/ or by adding more methanol) till a 1 mM concentration is obtained. The millimolar concentration of pyocyanin solution in methanol can be determined as follows
b. Please note that extinction coefficients depend on the solvent used and the specific wavelength of absorption spectra
    i. Different solvents have different Extinction Coefficients

ii. Different Absorption wavelengths have different Extinction Coefficients

c. Absorbance = Molar Concentration × Light path × Extinction Coefficient

d. $A = E \times L \times C = E \times 1\ Cm \times C = EC$

e. Therefore the Molar Concentration C = A / E × Dilution Factor = A / E × 100

f. The absorption values obtained were as follows:

Wavelength (nm)	Absorption
718	
318	
239	

g. The typically used absorption wavelength of pyocyanin for calculation of Molar concentration is at 318 nm, because that is where the highest peak is seen

h. The Extinction Coefficient E of pyocyanin in methanol at 318 nm is 30199.5

i. Therefore the millimolar concentration of pyocyanin is 1 mM

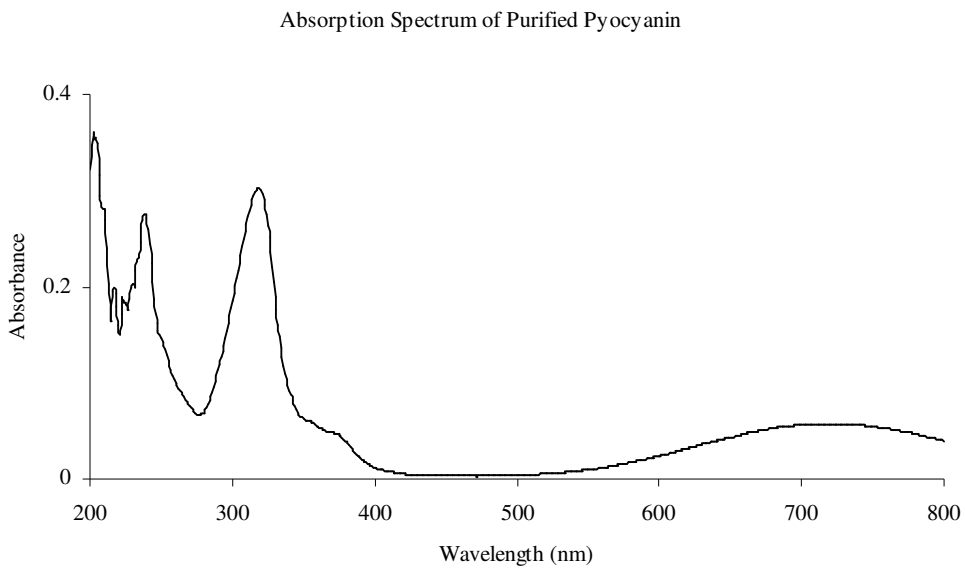
Absorption Spectrum of Purified Pyocyanin
0.4
0.2
0
Absorbance
200
300
400
500
600
700
800
Wavelength (nm)

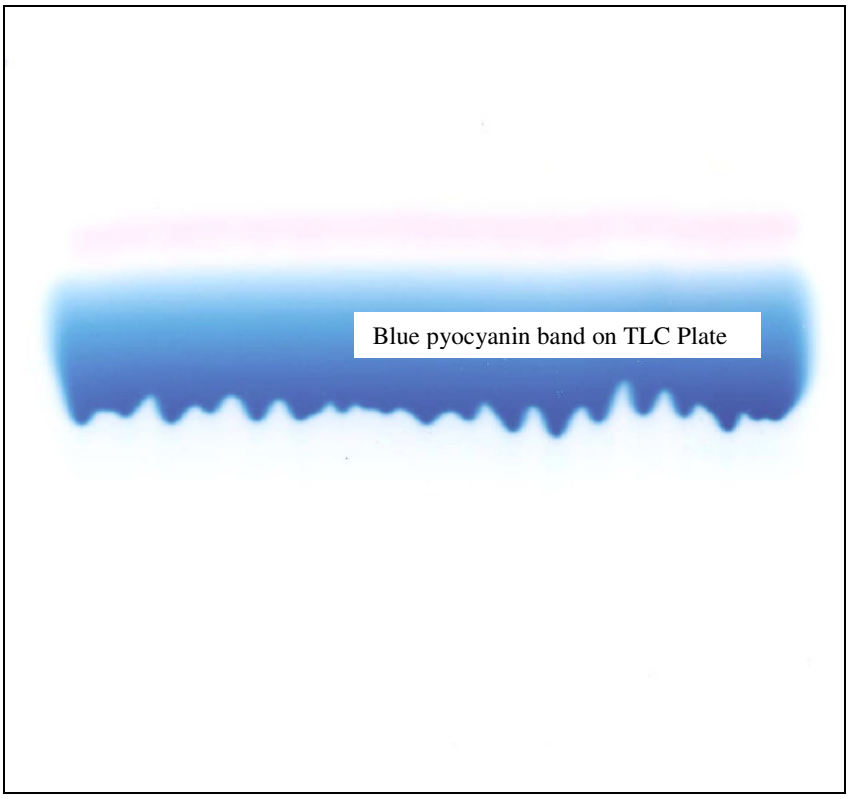
Blue pyocyanin band on TLC Plate

6.2. Image analysis using ImageJ

METHOD FOR IMAGE ANALYSIS- PRELIMINARY STEPS

1. Open image J program
2. Open a Tiff Image first
3. To set scale click on ANALYZE then SET SCALE
    a. Set scale depending on magnification picture was taken at

Magnification	SEM Scale
6,000	0.6 pixels/nm
15,000	0.15 pixels/nm
25,000	0.25 pixels/nm

Magnification	TEM Scale
4,600	0.069 pixels/nm
19,000	0.269 pixels/nm

    b. Select global on the set scale page
4. On image J select the "love heart shape"
    a. On the image, pick the area that is SINUSOIDAL ENDOTHELIUM WITHOUT ANY RIPS
    b. Hold the left button on the mouse down while you encircle the appropriate area on the image
    c. When finished lift the button on the mouse up.
5. Select EDIT then CLEAR IMAGE

6. Select ANALYSIS and MEASURE to measure area.
7. Cut the AREA measurement out and paste it into EXCEL.

MEASURING THE FENESTRATIONS (Best done in quadrants)

8. Enlarge the image to 100% by selecting the magnifying glass on the tool bar and then left clicking twice on the image. At the top of the image you will not see any magnification size on the image (you can alter the image size and increase it by left clicks on the mouse and decrease it by right clicks).
9. Use the scroll icon and move one quadrant into the screen only.
10. Select the line icon. AFTER YOU DO THIS YOU NEED TO CLICK ON A LINE OUTSIDE THE AREA OF THE IMAGE
11. Scroll down each fenestrations along its maximum diameter. After each diameter has a line down it, push the "M" key to measure it.
12. Careful to measure each fenestrations once and only once
13. When you have completed a quadrant, move to the next quadrant and measure the fenestrations. To move to the next quadrant select the scroll icon then left click on the image and move it. When the next quadrant is in view select the line icon and scroll down the length of each fenestrations then click "M"

COLLATING DATA

14. When all the fenestrations have been measured go to RESULTS page; then click EDIT; and then click SELECT ALL. Cut all the results out and paste them into EXCEL. Remember the first number on each line is the number of fenestrations and the last number is the diameter.
15. To Convert diameter to area apply the formula:
    a. Eg to convert a diameter in e2 and give the result in f2 then in f2 put =(0.5 × e2 × 0.5 × e2 × 3.14 × 0.5)
    b. Copy this for all the diameters

STATISTICS: CALCULATING AVERAGES

1. Calculate average fenestration diameter (in nm)
2. Calculate porosity of the endothelium (in %). To do this:
    a. Calculate the TOTAL AREAS of all fenestrations
    b. Porosity is AREA OF ALL FENESTRATIONS/ AREA OF ENDOTHELIUM × 100
3. Calculate the number of fenestrations per square micrometer.
    a. This is number of fenestrations / area of sinusoid (in nm) × 1,000,000
    b. Note this is conventionally expressed fenestration s/ μm^2, not fenestrations / nm^2 so the results needs to be multiplied by 1,000,000.

6.3. Preparation of isolated rat LSECs

LSEC PREPARATION- MATERIALS

1. Sterile Bag 1: 2 Straight Forceps
2. Sterile Bag 2: 5 Mosquito Artery Forceps, 1 Broad-end Scissors, 1 Sharp-end Scissors, 2 Forceps
3. HBSS for initial rat liver perfusion
    - HBSS Should NOT have Ca^{2+}
4. Collagenase solution (A) – make up 100 ml of 0.05 % collagenase (50 mg) in HBSS (with Ca^{2+}), neutralize the non-specific proteases with 5% FCS
    - Should be prepared just before experiment
    - HBSS SHOULD have Ca^{2+}
5. Collagenase solution (B) – Make up 50 ml of 0.05% collagenase (25 mg) and 0.001% DN'ase [DN'ase added as a "pinch" just before use] and 2.7 ml FCS in HBSS (with Ca^{2+})
    - Should be prepared just before experiment
    - HBSS SHOULD have Ca^{2+}
6. Stock Percoll – Prepare stock Percoll solution (SPS) by mixing 10 ml of 10-fold concentrated (10 X) Dulbecco's PBS (no Ca^{2+}) with 90 ml Percoll
    - Can be prepared 1 day before experiment
    - 10 X Dulbecco's PBS should NOT have Ca^{2+}
    - Prepare 30 ml of SPS (3 ml 10X Dulbecco's PBS 3 ml + 27 ml Percoll)
7. Percoll gradient prepared just before experiment – Do duplicates
    - Dulbecco's PBS should NOT have Ca^{2+}

- EACH Percoll gradient consists of:
    i. Upper layer 20 ml 25% Percoll: Obtained by mixing 5 ml SPS and 15 ml PBS
    ii. Lower layer 15 ml 50% Percoll: Obtained by mixing 7.5 ml SPS and 7.5 ml PBS
- Therefore, prepare a total (for duplicates) of:
    i. 40 ml of 25% Percoll: Obtained by mixing 10 ml SPS and 30 ml PBS
    ii. 30 ml of 50% Percoll: Obtained by mixing 15 ml SPS and 15 ml PBS

8. Complete RPMI-1640 with Glutamine (0.02 g/100ml), 2% FCS (heat-inactivated), antibiotics (1 ml/ 100 ml) (100 U/ml penicillin, 100 µg/ml streptomycin)
9. Collagen solution for wells and coverslips. Use Collagen-S solution as substrate for the culture of LSECs by equally distributing it on the plastic surface of the wells or coverslips. After 18 hours at 4°C, rinse the coverslips with RPMI-1640 leaving behind a thin film of collagen.

LSEC PREPARATION- METHODS

1. Anaesthetize a rat (Male Sprague- Dawley, 250-350 g) intraperitoneally with 0 .5 ml [1 ml/ kg weight of rat] out of a total of 1ml in an insulin syringe that consists of:
    a. 40mg (0.6ml on 100mg/ml) Ketamine
    b. 4mg (0.06ml of 100mg/ml) Xylazil
    c. 0.34 ml saline

2. Administer heparin (150 U-a pinch with 0.3 ml normal saline) into inferior mesenteric vein
3. After laparotomy, insert and secure a 18G catheter into the portal vein
4. Cut the inferior vena cava beneath the liver immediately cut and start perfusion with 39°C HBSS (no Ca^{2+})
5. Flush 200 ml HBSS (no Ca^{2+}) through the liver at a flow rate of 10 ml/min. - 200 ml can also be 150, 100 ml, or even 75 ml; from the moment the liver is completely discolored (from red/purple to brown/ochre)
6. Perfuse liver with HBSS (with Ca^{2+}, 100 ml) collagenase solution at a flow rate of 5 ml/min
7. Remove liver after 20-25 minutes
8. Discard Glisson's capsule along with the vessels with the aid of forceps
9. Disrupt the paste-like liver substance further disrupted by mincing it between forceps
10. Shake the forceps-minced paste-like liver substance (gently) in 10 ml of fresh Collagenase B solution [HBSS (with Ca^{2+}) containing 0.05% collagenase, 0.001% DN'ase (added as a “pinch” just before use), and FCS] for approximately 10 min at 39°C. Repeat 4 times, each time filtering using the following step (9):
    a. Each time, the cell suspension is filtered through nylon gauze (mesh 100) to remove undigested tissue
    b. Don’t exceed a total incubation time of 30 minutes, including RT AND Incubator steps
11. Centrifuge cell suspension at 100 g for 5 min at 20° (break low) to remove most hepatocytes
12. Centrifuge supernatant (enriched in sinusoidal cells) for 10 min. at 350 g

13. Resuspend cell pellet in 50 ml PBS and centrifuge again for 10 min at 350 g
14. Resuspend the resulting cell pellet in 20 ml PBS
15. Layer 10 ml of the cell suspension on top of each of the two-step Percoll gradient
16. Centrifuge gradients immediately at 900 g for 20 min (break off)
17. Discard top layer (45 ml to 25 ml) FIRST, and use a sterile Pasteur pipette to collect the intermediate zone (25 ml to 10 ml layer; between the two density layers; especially around the 15 cm mark), which is enriched in LSECs
18. Dilute these enriched LSECs with an equal volume of PBS & centrifuge at 900 g for 10 min
19. Resuspend the resulting cell pellet in 10 ml culture medium. Pipette the resulting cell suspension into FOUR 5 cm diameter tissue grade petridishes without any coating
20. Incubate the petridishes for 7-8 min ONLY (NOT MORE than 10 min) at 37°C in a humidified incubator under 5% CO_2 in air, to allow the selective attachment of the Kupffer cells
21. Collect LSECs by REALLY firmly (NOT too firmly!) washing the wells; otherwise ↓ yield;
22. LSEC count calculation:
    a. 50 µl cell suspension + 450 µl Trypan blue (Dilution is *10) and mix well
    b. Add sufficient quantity (less than 50 µl) to Improved Neubauer chamber with cover slip already in place. Before loading, add a drop of water to each side groove of Neubauer Chamber to enhance cover-slip grip (to the Neubauer chamber)
    c. Count the LSECs in all the 4 corners of the grid (n)
    d. Total Cell Count= n/4* 10 * 10^4 per ml

e. 1 ml (STRICTLY:- no more volume, no less volume!) at $0.80x10^6$ LSECs/ml (semi-confluent) or $1.60x10^6$ LSEC/ml (confluent) is seeded on collagen-coated cover slips

f. If cell-suspension is to be concentrated to bring to the appropriate cell density for seeding the wells with cover-slips, centrifuge at 250 g for 10 minutes, and resuspend cell pellet in apt volume of media

23. Do a media change 2-4 hours after plating to wash the culture (gently) and further changes occurred at 24-hour intervals subsequently

24. Cells are preferably used ASAP (6-12 hours post inoculation)

6.4. Processing of LSECs for scanning electron microscopy

1. Fix cells with 4% EM grade Glutaraldehyde in 0.2 M Na-Cacodylate buffer with 0.1M sucrose (IMPORTANT!)
    a. 1 ml for each cover slip
    b. 5 ml for 5 coverslips
    c. 5 ml contains 0.8 ml 25% glutaraldehyde, 2.5 ml 0.2 M Na-Cacodylate buffer, 1.7 ml of Millipore water, and 0.17 g sucrose
        i. Stock glutaraldehyde= 25%
        ii. 1% glutaraldehyde= 4 ml in 100 ml
        iii. 4% glutaraldehyde= 16 ml in 100 ml
        iv. 4% glutaraldehyde= 16/20 in 5 ml= 0.8 ml in 5 ml
2. Allow to fix for about 4hours in the fridge or 1hr at room temperature
3. [Carry on with the following steps if time is available. If not, keep cells in 0.1M Na-Cacodylate buffer in fridge ovenight and on the next day, do 2 washes in 0.1M Na-Cacodylate buffer, not 3, as in the case of the regular protocol]
4. Wash 3 x 5 minutes in 0.1M Na-Cacodylate buffer
5. Post fix in 1% tannic acid in 0.15 M Na-Cacodylate buffer (PH= 7.4) for 1 hour
    a. Adequate volume of tannic acid must be paper filtered before use
6. Wash 3 x 2 minutes in 0.1M Na-Cacodylate buffer
7. Post fix in 1 % OsO_4 in 0.1M Na Cacodylate buffer for 1 hour
    b. Done in pathology lab (S35?)
    c. See that the fume hood has boost air-flow switched on
    d. Handle osmium very carefully
    e. Small skull and crossbones metallic container contains unused osmium,

and big skull and crossbones metallic container is for osmium discard

f. Keep plastic pipette which made contact with fresh osmium in the sink to use again for osmium waste aspiration, and discard it after thorough rinsing

8. Wash 3 x 2 minutes in 0.1M Na-Cacodylate buffer
9. Dehydrate:
    a. 50 % Ethanol 4 times, each 2 mins
    b. 70 % Ethanol 4 times, each 2 mins
    c. 95 % Ethanol 4 times, each 2 mins
    d. 100 % Ethanol 2 times, each 5 mins
    e. 100 % Molecular sieve ethanol 2 times, each 5 mins
10. Drying in Hexamethyldisilazane 3 mins
    a. After 100% molecular sieve ethanol treatment, leave the molecular sieve ethanol in the respective wells
    b. Bring the Hexamethyldisilazane can from the fridge into the fume hood
    c. Remove the Hexamethyldisilazane bottle from its can and remove the parafilm around the neck and cap
    d. Transfer 1 ml of Hexamethyldisilazane per well into dry wells corresponding with wells with cell-coated cover-slips and immediately transfer into a desiccator and close the lid
    e. Wrap parafilm over the neck and cap of Hexamethyldisilazane bottle, place the bottle in its can, and take it back into the fridge
    f. Transfer cover-slips from the wells with molecular sieve ethanol to the corresponding wells with 1 ml Hexamethyldisilazane and keep for 3 minutes; all steps done inside the desiccator kept inside the fume hood

g. After 3 minutes, transfer the coverslips from the wells with 1 ml Hexamethyldisilazane into corresponding dry wells

h. Aspirate all molecular sieve ethanol and Hexamethyldisilazane from all wells and discard into plastic container and let evaporate inside the fume hood

i. Keep the tray with (coverslips in dry wells) without closing the tray lid inside the desiccator and move desiccator outside the fume hood onto the work table

11. Place in desiccator overnight

12. Mount

a. Marinate "Grooved SEM Type Slug Mounts" in 100% ethanol for 10 minutes

b. Always lift slug mounts with dull-tipped forceps

c. Always handle coverslips and sticky carbon strips with sharp-tipped forceps

d. Air dry slug mounts on absorbent paper on table with the side with concentric circles facing upwards

e. Label plain side of the slug mounts with appropriate name for permanent records

f. Stick a (double sharp sided shaving blade cut) 2-sided sticky carbon strip from a roll of the same on the side with the concentric circles

g. Lift coverslips from the tray in the desiccator to visualize the cell-layered side of the coverslip

h. Paste coverslips on the sticky carbon strip with the cell-layer side facing upwards (away from the sticky carbon adhesive strip)

i. Press firmly on the middle of the coverslip with the tip of the sharp-tipped forceps to ensure proper adhesion to the sticky carbon strip placed on the slug mounts

j. Using a tip of a toothpick coated with carbon-graphite paint (placed in a plastic bottle with a tapering nozzle), paint the non-cellular side of the coverslips especially at the junction of the slug mount and the coverslip circumferentially

k. Place a rolled 2-sided adhesive tape on the 24-well-plate cover

l. Stick the plain side of the slug mounts on the rolled adhesive tape so that they will face the wells of the 24-well plate when the 24- well plate is placed on the 24-well plate cover

m. Invert 24-well plate over the firmly stuck slug mounts and place the whole set-up in the desiccator with the 24-well plate cover at the bottom and the 24-well plate bottom facing the top

13. Coat with gold film

14. LOOK

6.5. Processing of rat liver specimens for scanning electron microscopy

Liver Fixative for SEM/ TEM

(Paraformaldehyde & Glutaraldehyde EM Fixative)

1. Composition:
    a. 25 % EM Grade Glutaraldehyde 12 ml
    b. Paraformaldehyde 2 g
    c. 1 M $CaCl_2$ 2 ml
    d. Sucrose 2 g
    e. 0.2 M Na Cacodylate Buffer 50 ml
    f. Distilled water 10 ml (or enough to make up to 100 ml totally)
    g. Strong NaOH and HCl for pH adjustment
    h. Total Osmolality: 440 milliosmoles
2. Final Concentrations of Constituents:
    a. 25 % EM Grade Glutaraldehyde 3 %
    b. Paraformaldehyde 2-2.5 %
    c. 1 M $CaCl_2$ 2 mmol/ liter
    d. Sucrose 2 %
    e. 0.2 M Na Cacodylate Buffer 0.1 mol/ liter
    f. Distilled water 100 ml
    g. Strong NaOH and HCl for pH adjustment
3. Preparation Method:
    a. Always prepare fresh (within 24 hours of use)

b. Mixture 1 (Glutaraldehyde, Na- Cacodylate, Sucrose)
    i. Add 12 ml Glutaraldehyde, 50 ml of 0.2 M Na Cacodylate buffer, and 2 g of sucrose
c. Mixture 1 (8-10 % Paraformaldehyde)
    i. Weigh out paraformaldehyde wearing gloves in a fume hood and avoid inhalation of powder
    ii. Add 2 g of Paraformaldehyde powder to 25 ml of distilled water in a beaker
    iii. Heat to 60°C stirring constantly using magnetic stirring bar
    iv. Solution will turn milky
    v. Allow to heat for 2 min
    vi. Cool to 40°C
    vii. Add 1 M NaOH drop-wise, until clear
    viii. Cool to RT
d. Final mixture (Mixture 1 + Mixture 2)
    i. Add Mixture 1 (Glutaraldehyde, Na- Cacodylate, Sucrose) to Mixture 2 (8-10 % Paraformaldehyde, when cool)
    ii. Add 2 ml of 1 M $CaCl_2$

<u>Procedure for Fixing Liver Specimens for SEM/ TEM</u>

1. Perfuse liver with pre-perfusion buffer (Normal Saline) using insulin syringe under low pressure: 2 Min
2. Perfuse liver (In Fume Hood) with Paraformaldehyde & Glutaraldehyde EM Fixative using insulin syringe under low pressure UNTIL liver is hard: APPROXIMATELY 5 Min

3. Cut liver into an appropriate number of 1 mm^3 bits
4. Post-fix in Paraformaldehyde & Glutaraldehyde EM Fixative: 4-24 hours (overnight)
5. Rinse 3 times with 0.1 M Na-Cacodylate, holding liver bits with forceps
6. Store in 0.1 M Na-Cacodylate till used
7. Transfer liver bits into appropriately labeled plastic mesh rack layers (WHERE IT STAYS FOR THE REST OF THE STEPS) in the specimen holder and place it in a polypropylene tube (0.1 M Na-Cacodylate) with a tight cap
8. THE LIVER BITS STAY IN THIS APPARATUS FOR THE REST OF THE STEPS
9. Post fix in 1 % OsO_4 (pathology lab) in 0.1M Na Cacodylate buffer for 2 hours
10. Wash 2 x 5 minutes in 0.1M Na-Cacodylate buffer
11. Dehydrate:
    a. 50 % Ethanol 2 times, each 5 mins
    b. 70 % Ethanol 2 times, each 5 mins
    c. 95 % Ethanol 3 times, each 5 mins
    d. 100 % Ethanol 2 times, each 10 mins
    e. 100 % Molecular sieve ethanol 2 times, each 10 mins
12. Dry with Hexamethyldisilazane in desiccator for 10 mins
13. Place frame in desiccator overnight
14. Mount
    a. Marinate "Grooved SEM Type Slug Mounts" in 100% ethanol for 10 minutes
    b. Always lift slug mounts with dull-tipped forceps
    c. Always handle coverslips and sticky carbon strips with sharp-tipped

forceps

d. Air dry slug mounts on absorbent paper on table with the side with concentric circles facing upwards
e. Label plain side of the slug mounts with appropriate name for permanent records
f. Stick a (double sharp sided shaving blade cut) 2-sided sticky carbon strip from a roll of the same on the side with the concentric circles
g. Place 6 small liver bits (with the even surface facing upwards) on the sticky carbon strip of each slog mount
h. Using a tip of a toothpick coated with carbon-graphite paint, paint bands extending from each live bit to the edge of the circular surface of the slug mount
i. Place a rolled 2-sided adhesive tape on a 24-well-plate cover
j. Stick the plain side of the slug mounts on the rolled adhesive tape so that they will face the wells of the 24-well plate when the 24- well plate is placed on the 24-well plate cover
k. Invert 24-well plate over the firmly stuck slug mounts and place the whole set-up in the desiccator with the 24-well plate cover at the bottom and the 24-well plate bottom facing the top

15. Coat with gold film
16. Look with SEM: SEM fields should preferably include at least 10 fields/ rat encompassing:
    a. At least 2 representative fields/ liver block
    b. At least 5 liver blocks/ rat

6.6. Preparation of 4% phosphate buffered paraformaldehyde (paraformaldehyde buffered saline) for immunohistochemistry

4% Phosphate-buffered Paraformaldehyde

1. Composition:

i. Paraformaldehyde	8g
ii. Distilled water	200 ml
iii. $NaH_2PO_4.2H_2O$	0.41 g
iv. Na_2HPO_4	2.47 g
v. NaCl	1 g
vi. 1 N NaOH	"Small Amount"

2. Preparation:
   i. Weigh out paraformaldehyde wearing gloves in a fume hood and avoid inhalation of powder
   ii. In fume cupboard, combine paraformaldehyde and distilled water and heat to 60°C
   iii. Add a few drops of 1 N NaOH until solution clears
   iv. Cool the mixture
   v. Add the 3 remaining ingredients and stir until dissolved
   vi. Filter and check pH
3. Fixation time:
   i. Fixation time prior to immunohistochemistry should be for the shortest possible time to achieve good morphology but prevent antigen masking due to excessive cross-linking of proteins

ii. For blocks of tissue 2 cm square by 3-4 mm thick, 6-24 hours fixation is recommended

iii. For smaller blocks, adequate fixation will be achieved in several hours

6.7. Criteria for assessment of pictures obtained for immunohistochemistry for pimonidazole and VEGF

Pimonidazole and VEGF IHC Rating Criteria

Rat ID: _____

	PERICENTRAL STAINING			**PERIPORTAL STAINING**			**OVERALL STAINING**					
Photo No:	PC No. Counted	CP Stain	Nu Stain	PP No. Counted	CP Stain	Nu Stain	PC	PP	Z2	**Sinusoid Stain?**	**Bile Ductule Stain?**	**"PT" Bundles**
1												
2												
3												
4												
5												
6												
7												
8												
9												
10												

6.8. Criteria for assessment of pictures obtained for immunohistochemistry for VEGFR2

VEGFR2 IHC Intensity (0,1,2,3) Rating Criteria

Rat ID: _____

PHOTO NO	PORTAL AREA INTENSITY					Z2 AREA INTENSITY			CENTRAL AREA INTENSITY					Overall	KCs	Stellate C	Bil Ep St
	PT No	PT Endo	PP Sinusd Endo (Z-1)	PP Stain Cm	PP Stain Nu	Z-2 Sinusd Endo (Z-2)	Z-2 Stain Cm	Z-2 Stain Nu	CV No	CV End	PC Sinusd Endo (Z-3)	PC Stain Cm	PC Stain Nu				
1																	
2																	
3																	
4																	
5																	
6																	
7																	